FINAL REPORT

STUDY AND DEVELOPMENT OF A CRYOGENIC HEAT EXCHANGER FOR LIFE SUPPORT SYSTEMS

73-9117
March 23, 1973

Prepared for

George C. Marshall Space Flight Center Office
National Aeronautics and Space Administration

Contract Number NAS 8-28099

AIRESEARCH MANUFACTURING COMPANY
Torrance, California

FINAL REPORT

STUDY AND DEVELOPMENT OF A CRYOGENIC HEAT EXCHANGER FOR LIFE SUPPORT SYSTEMS

73-9117
March 23, 1973

Prepared for

George C. Marshall Space Flight Center Office
National Aeronautics and Space Administration
Contract Number NAS 8-28099

AIRESEARCH MANUFACTURING COMPANY
Torrance, California

AIRESEARCH MANUFACTURING COMPANY
Torrance, California

STUDY AND DEVELOPMENT OF A CRYOGENIC HEAT EXCHANGER FOR LIFE SUPPORT SYSTEMS FINAL REPORT

This Report was prepared by AiResearch Manufacturing Company under Contract NAS 8-28099 for the George C. Marshall Space Flight Center of the National Aeronautics and Space Administration

Report No. 73-9117 March 23, 1973

Prepared by: M. M. Soliman
Principal Investigator
Preliminary Design Department

Approved by: G. G. Stockwell
G. G. Stockwell
Program Manager
Heat Transfer and Cryogenic Systems

W. J. O'Reilly
Chief Engineer
Heat Transfer and Cryogenic Systems

CONTENTS

Section		Page
1	SUMMARY	1-1
2	INTRODUCTION	2-1
3	HEAT TRANSFER AND FLUID FLOW CONSIDERATIONS	3-1
	Performance Predictions of the Cryogen Side	3-1
	Performance Predictions of the Warm Fluid Side	3-15
4	INTERFACE DEFINITION	4-1
5	WARM FLUID SELECTION	5-1
	Warm Fluid Survey	5-1
	Warm Fluid Final Selection	5-3
6	HEAT EXCHANGER TRADEOFF STUDY	6-1
	General Approach	6-1
	Candidate Heat Exchanger Designs	6-2
	Tradeoff Study for Plate-Fin, Cross-Counterflow Heat Exchanger	6-6
	Tradeoff Study for Tubular, Cross-Counterflow Heat Exchanger	6-11
	Tradeoff Study for Cross-Parallel Flow Heat Exchanger	6-16
	Summary of the Tradeoff Study	6-19
7	CONTROL SYSTEM TRADEOFF STUDY	7-1
	General Approaches to Control System	7-1
	Comparison of Approaches	7-13
	Candidate Control Concepts	7-13
	Tradeoff Study	7-15
	Summary	7-21
8	SELECTED HEAT SINK SYSTEM	8-1
	Candidate Systems	8-1
	Selected System	8-3

CONTENTS (Continued)

Section		Page
9	HEAT EXCHANGER DESIGN	9-1
	Use of Freon -21	9-1
	Design Point Conditions	9-1
	Heat Exchanger Design Details	9-2
10	TEST SYSTEM AND TEST PROCEDURE	10-1
	Freon -21 Loop	10-1
	Hydrogen Loops	10-8
	Test Procedure	10-11
11	TEST RESULTS AND DISCUSSION	11-1
	Isothermal Pressure-Drop Measurement	11-1
	Testing With Warm Gaseous Hydrogen (Inlet Temperature Around $0^{\circ}F$)	11-7
	Testing With Cryogenic Hydrogen	11-11
	Discussion	11-19
12	OXYGEN HEAT SINK SYSTEM	12-1
	Weight of Consumables	12-1
	Heat Sink System Design	12-1
13	CONCLUSIONS AND RECOMMENDATIONS FOR FUTURE WORK	13-1
	Conclusions	13-1
	Recommended Future Work	13-2
	REFERENCES	R-1
Appendix		
	FLOW STABILITY CRITERION	A-1
	OPTIMUM THERMAL CONDUCTANCE RATIO ϕ FOR MINIMUM HEAT EXCHANGER VOLUME	B-1
	CONTROL SYSTEM MATHEMATICAL MODELS	C-1

ILLUSTRATIONS

Figure		Page
3-1	Modes of Operation on the Cryogenic Side of the Heat Exchanger	3-2
3-2	Heat Transfer and Flow Regimes in Forced Convection Boiling of Cryogenic Fluids	3-5
3-3	Two-Phase Flow Regimes	3-7
3-4	Martinelli-Nelson Correlating Term X_{tt} as a Function of Quality and Pressure for H_2	3-9
3-5	Martinelli-Nelson Correlating Term X_{tt} as a Function of Quality and Pressure for O_2	3-10
3-6	Types of Flow Transients	3-11
3-7	Schematic Diagram of System	3-14
5-1	Deviation from Optimum Heat Exchanger Design for Various Hot Fluids	5-5
6-1	Multipass Crossflow Plate Fin Heat Exchanger	6-3
6-2	Multipass Crossflow Tubular Heat Exchanger	6-4
6-3	Influence of Hydrogen Effectiveness on Heat Exchanger Core Weight - Design Conditions Are Listed in Table 2-3	6-7
6-4	Weight of Hydrogen Consumed During 2 Hr of Operation vs Hydrogen Inlet Temperature and Hydrogen Effectiveness	6-8
6-5	Weight of Hydrogen Consumed During 4 Hr of Operation vs Hydrogen Inlet Temperature and Hydrogen Effectiveness	6-9
6-6	Weight of Hydrogen Consumed During 6 Hr of Operation vs Hydrogen Inlet Temperature and Hydrogen Effectiveness	6-10
6-7	Influence of Hydrogen Effectiveness on Total Weight	6-12
6-8	Influence of Hydrogen Effectiveness on Heat Exchanger Core Weight	6-14

ILLUSTRATIONS (Continued)

Figure		Page
6-9	Effect of Cryogen Core Pressure Drop on Heat Exchanger Weight	6-15
6-10	Effect of Heat Exchanger Material on Core Weight	6-17
6-11	Influence of Hydrogen Effectiveness on Total Weight	6-18
6-12	Effect of Flow Configuration on Heat Exchanger Weight	6-20
7-1	Control Requirements	7-2
7-2	Control Approaches	7-3
7-3	Vernatherm Control Valve	7-8
7-4	Candidate Temperature Control Systems	7-10
7-5	Bode Plot for Position Control System	7-18
7-6	Bode Plot for Vernatherm Control System	7-19
7-7	Bode Plot for Position + Rate + Integral Control System	7-20
7-8	Compensated System Response to Hot Side Disturbance for $T_{C_{IN}} = 0^{\circ}F$	7-22
7-9	Compensated System Response to Hot Side Disturbance for $T_{C_{IN}} = -400^{\circ}F$	7-23
7-10	Compensated System Response to Hot Side Ramp Disturbance for $T_{C_{IN}} = 0^{\circ}F$	7-25
7-11	Compensated System Response to Hot Side Ramp Disturbance for $T_{C_{IN}} = -400^{\circ}F$	7-26
7-12	Compensated System Response to Cold Side Disturbance for $T_{H_{IN}} = 50^{\circ}F$	7-27
7-13	Compensated System Response to Cold Side Disturbance for $T_{H_{IN}} = 105.2^{\circ}F$	7-28
7-14	Electronic Circuit Schematic for Phase Compensation	7-29

ILLUSTRATIONS (Continued)

Figure		Page
8-1	Recommended Heat Sink Systems	8-2
8-2	Flow Control Valve and Actuator Schematic	8-4
8-3	Controller Block Diagram	8-7
9-1	Tubular Heat Exchanger Design	9-3
9-2	Cryogenic Heat Exchanger	9-7
10-1	Test System Schematic	10-2
10-2	Test System Showing Liquid/Gas Separation Tank (Far Right) and Uninsulated Cryogenic Heat Exchanger	10-3
10-3	Cryogenic Heat Exchanger Mounted in Test System	10-4
10-4	Test System Showing Cryogenic Hydrogen Tank, Insulated HX, and Part of Instrumentation	10-5
10-5	Hydrogen Liquid/Vapor Separation Tank	10-9
11-1	Isothermal Pressure Drop of Freon-21	11-4
11-2	Isothermal Hydrogen Pressure Drop	11-5
11-3	Schematic of ΔP_m Versus ΔP for Hydrogen Warm Gas	11-6
11-4	Heat Rejection Rate vs Hydrogen Flow Rate Hydrogen Inlet Temperature Is 0^0F	11-12
11-5	Hydrogen Pressure Drop Versus Hydrogen Flow Rate (Hydrogen Inlet Temperature Is 0^0F)	11-13
11-6	Hydrogen Side Effectiveness Versus Hydrogen Flow Rate (Hydrogen Inlet Temperature Is 0^0F)	11-14
11-7	Available UA Versus Hydrogen Flow Rate (Hydrogen Inlet Temperature Is 0^0F)	11-15
11-8	Temperature Profiles Along HX	11-19
11-9	Heat Rejection Rate Versus Hydrogen Flow Rate at Cryogenic Inlet Conditions	11-20
11-10	Hydrogen Core Pressure Drop at Cryogenic Inlet Conditions	11-21

ILLUSTRATIONS (Continued)

Figure		Page
11-11	Overall Heat Transfer, UA, Versus Hydrogen Flow Rate at Cryogenic Inlet Conditions	11-22
11-12	Estimated Temperature Distribution Along the Heat Exchanger for Run 7, Table 11-5	11-24
12-1	Total Weight of Consumables with Oxygen as Expendable Heat Sink	12-2
12-2	Comparison Between Oxygen and Hydrogen as Expendable Heat Sink Fluids	12-3
12-3	Oxygen Heat Sink System	12-4
12-4	Oxygen Heat Exchanger Design	12-6
A-1	Comparison of Stability Criterion and Experimental Data	A-2
B-1	Heat Exchanger Geometry	B-3
B-2	f, j, and F_l vs Reynolds Number for an Offset Fin Surface	B-5
C-1	Linear Heat Exchanger System Model	C-2
C-2	Analog Computer Simulation Schematic for System with Position + Rate + Integral Control	C-3
C-3	Cryogen Valve CA_c Function	C-4
Drawing		
168942	Heat Exchanger Assy. Cryogenic	9-6

TABLES

Table		Page
1-1	CONVERSION FACTORS TO SI UNITS	1-3
4-1	ENVIRONMENTAL CONTROL SUBSYSTEM HEAT LOADS BTU/HR	4-2
5-1	PHYSICAL PROPERTIES OF VARIOUS HOT SIDE FLUIDS	5-2
5-2	DESIGN CONDITIONS FOR FIGURE 5-1	5-6
6-1	RANGE OF DESIGN VARIABLES FOR THE HEAT EXCHANGER DESIGN TRADEOFF STUDY	6-1
7-1	CRYOGENIC HEAT EXCHANGER CONTROL CONCEPT COMPARISONS	7-14
9-1	DESIGN POINT VARIABLES FOR THE DESIGN OF THE CRYOGENIC HEAT EXCHANGER	9-2
10-1	INSTRUMENTATION LIST	
11-1	ISOTHERMAL PRESSURE DROP OF FREON-21	11-2
11-2	ISOTHERMAL PRESSURE DROP OF HYDROGEN	11-3
11-3	TEST DATA FOR HYDROGEN INLET TEMPERATURE AROUND $0^{o}F$	11-8
ii-4	REDUCED DATA FOR HYDROGEN INLET TEMPERATURE AROUND $0^{o}F$	11-10
11-5	TEST DATA FOR HYDROGEN AT CRYOGENIC INLET TEMPERATURES	11-16
11-6	REDUCED DATA FOR HYDROGEN AT CRYOGENIC INLET TEMPERATURES	11-17

SECTION 1

SUMMARY

The object of this study is to develop a prototype cryogenic heat exchanger (HX) for removal of waste heat from a spacecraft environmental control life support system (ECLS). The heat exchanger uses the heat sink capabilities of the cryogenic propellants and, hence, can operate over all mission phases from prelaunch to orbit, to post landing, with quiescent periods during orbit.

A survey of candidate warm fluids resulted in the selection of E-2, a fluorocarbon compound, because of its low freezing point and high boiling point. The final design and testing of the heat exchanger was carried out, however, using Freon-21, which is similar to E-2 except for its low boiling point. This change was motivated by the desire for cost effectiveness of the experimental program.

Based on a tradeoff study of the heat sink system, a heat exchanger effectiveness of 0.9 was selected, which resulted in the minimum total weight consisting of the weight of the heat exchanger, the weight of consumables, and the penalties weight.

The heat exchanger design study resulted in the selection of a tube-and-shell type with a ten-pass, cross-counter flow arrangement. The cryogen flows inside ring-dimpled, small-diameter (0.1 in. OD), tightly spaced tubes and the warm fluid flows outside the tubes. The entire heat exchanger is made of stainless steel. Certain unique features were included in the design to prevent any warm fluid freezing during all operating conditions.

Based on a control system tradeoff study, a position + rate + integral control scheme was selected. The control system consists of a flow control valve, an actuator, an electronic amplifier circuit for processing sensor signal, and a temperature sensor. Both upstream and downstream locations of the flow control valve, relative to the heat exchanger, were tested.

The cryogenic heat exchanger was optimally designed and tested using hydrogen as the heat sink fluid since it presents the most optimum solution from a system standpoint.

The heat exchanger was tested in one orientation with 0°F gaseous hydrogen and cryogenic gaseous and liquid hydrogen, and met the desired performance over the entire range of hydrogen inlet conditions.

Good agreement between the test data and the predicted performance was obtained which confirms the analytical techniques used in the design and performance prediction of cryogenic heat exchangers.

Minimum tube wall temperatures measured were about 130°F above the Freon -21 freezing point, and 110°F above the E-2 freezing point. The effectiveness of the design features included in the present design indicates that

the present design can be used for warm fluids with higher freezing points such as Coolanol 15 or even a glycol-water solution. Such fluids possess higher specific heats than Freon -21 and E-2, and their use should result in significant power and weight savings on spacecraft environmental control systems.

During liquid hydrogen testing, pressure fluctuations were observed at the inlet and outlet of the heat exchanger. These fluctuations, however, were repetitive in nature and never resulted in any apparent performance degradation, or any freezing of the warm fluid. These fluctuations were dampened by placing the cryogen flow modulating valve downstream of the heat exchanger.

The transient performance of the heat exchanger was demonstrated by an analog simulation of the heat sink system. Under the realistic transient heat load conditions (20 sec ramp from minimum to maximum Freon -21 inlet temperature), the control system was able to maintain the warm fluid outlet temperature within $\pm 3^{o}F$. For a 20-sec ramp from $0^{o}F$ to $-400^{o}F$ in the hydrogen inlet temperature, at maximum heat load, the warm fluid outlet temperature was maintained within $\pm 7^{o}F$.

A separate oxygen heat exchanger system, incorporating all the hydrogen system design features, is presented. The main difference between the two systems is the sizes of the heat exchanger and valves which are dictated by the higher oxygen flow rates. The tested hydrogen heat exchanger could have accommodated the oxygen flow rate at the $182^{o}R$ inlet condition while meeting the desired performance but the heat exchanger pressure drop would have been far in excess of the allowable 10 psi at the $0^{o}F$ inlet condition.

Finally, recommendations are made for future work to further evaluate the heat sink system developed herein and/or determine its suitability to other applications.

Recommendations for future work include testing with other heat transport fluids, testing in other orientations, transient performance testing, testing with supercritical cryogen and additional flow stability testing.

A list of conversion factors to SI units is given in Table I-I.

TABLE I-I

CONVERSION FACTORS TO SI UNITS

The following tables express the definitions of miscellaneous units of measure as exact numerical multiples of coherent SI Units, and provide multiplying factors for converting number and miscellaneous units to corresponding new numbers and SI Units.

The first two digits of each numerical entry represent a power of 10. For example, the entry "-02 2.54" expresses the fact that 1 inch = 2.54×10^{-2} meter by definition. Most of the definitions are extracted from National Bureau of Standards documents.

The conversion factors are listed by physical quantity.

The Listing by Physical Quantity includes only relationships which are encountered in the text.

Listing by Physical Quantity

To Convert from	To	Multiply by
	Acceleration	
ft/sec^2	$meter/sec^2$	-01 3.048
	Area	
ft^2	$meter^2$	-02 9.290
in^2	$meter^2$	-04 6.45
	Density	
lbm/ft^3	$kilogram/meter^3$	+01 1.602
	Energy	
British Thermal Unit (BTU)	joule	+03 1.055
lbf. ft	joule	+00 1.356
kilowatt-hr	joule	+06 3.60
	Energy per Area Time	
BTU/ft^2 sec	$watt/meter^2$	+04 1.135
BTU/ft^2 hr	$watt/meter^2$	+00 3.152
	Force	
lbm	Kilogram	-01 4.536
	Heat Transfer Coefficient	
BTU/ft^2-hr-°F	joule/$meter^2$. sec °K	+00 5.678

TABLE I-1 (Continued)

To Convert from	To	Multiply by
	Power	
BTU/sec	watt	+03 1.054
lbf. ft/hr	watt	-04 3.766
horsepower (550 lbf. ft/sec)	watt	+02 7.457
	Pressure	
in. of water (at 60°F)	newton/meter^2	+02 2.4884
in. of mercury (at 60°F)	newton/meter^2	+03 3.377
lbf/meter^2	newton/meter^2	+01 4.788
lbf/in^2 (psi)	newton/meter^2	+03 6.895
	Specific Heat	
BTU/lbm °F	joule/kilogram °K	+03 4.187
	Thermal Conductivity	
BTU/ft hr °F	joule/meter sec °K	+00 1.731
	Viscosity	
lbm/ft sec	newton sec/meter^2	+00 1.488

SECTION 2

INTRODUCTION

The removal of waste heat from environmental control and life support systems for space vehicles has commonly been accomplished by radiators, with water boilers or sublimators taking care of ascent or reentry transients.

Applications such as the space shuttle will require thermal control systems that can handle pre-launch, ascent, on orbit, reentry, cruise and ferry phases of the flight. Hence, water boilers and sublimators have to be augmented with other heat sink systems which can operate during the pre-launch, cruise and ferry periods. Another concept being considered for space shuttle application is the flash evaporator which uses water as an evaporant during orbit, ascent and reentry operation and Freon 22 or liquid ammonia during the rest of the phases of the flight.

Each of these systems can be considered to be in the development stage and in the case of sublimators and flash evaporators there are still technical problems to be solved before these systems can qualify for space shuttle application.

A potential means of removing waste heat from the environmental control and life support systems for space vehicles is provided by a heat exchanger using the heat sink capabilities of the cryogenic propellants. Such a system can operate over all mission phases although a space radiator for on-orbit operations may be a more efficient system for that period of operations.

The overall objective of the present study is to develop a prototype cryogenic heat exchanger for removal of waste heat from a spacecraft ECLS. The cryogenic heat exchanger will be able to operate from prelaunch to orbit with quiescent periods during orbit and until post landing.

SECTION 3

HEAT TRANSFER AND FLUID FLOW CONSIDERATIONS

PERFORMANCE PREDICTIONS OF THE CRYOGEN SIDE

The cryogen side of the heat exchanger represents a critical area in the heat exchanger design. This is primarily due to the wide variation in the inlet conditions of the cryogen. The cryogen conditions in the heat exchanger may range from all liquid operation to all gas to two-phase (vapor-liquid) operation.

Among these, the two-phase flow operation is the most critical one, at least in two areas: (1) potential freezing problems due to the high heat transfer coefficients obtained in boiling cryogens which result in very low wall temperatures, and (2) cryogen flow oscillations which can result in freezing of the hot fluid at conditions which would not cause freezing under stable operation.

The following discussion deals with the heat transfer, pressure drop and flow stability of the cryogen under various inlet conditions. The boundaries of each mode of operation are established and the methods of predicting the heat transfer, pressure drop and flow stability are discussed.

All-Gas Mode

This mode of operation, shown as Region 1 in Figure 3-1, has the following inlet conditions:

$$P < P_{crit}$$
$$T_{in} > T_{sat}$$

1. Heat Transfer

For flow inside tubes, References 1 and 2 recommend the following correlation to predict the heat transfer coefficient for the thermal entry length in turbulent flow and over a wide range of wall-to-bulk temperature ratio.

$$Nu_b = 0.045\ Re_b^{0.8}\ Pr_b^{0.4} \left(\frac{T_w}{T_b}\right)^{-0.55} \left(\frac{L}{D}\right)^{-0.15} \qquad (3\text{-}1)$$

where subscript b denotes that properties are evaluated at bulk temperature.

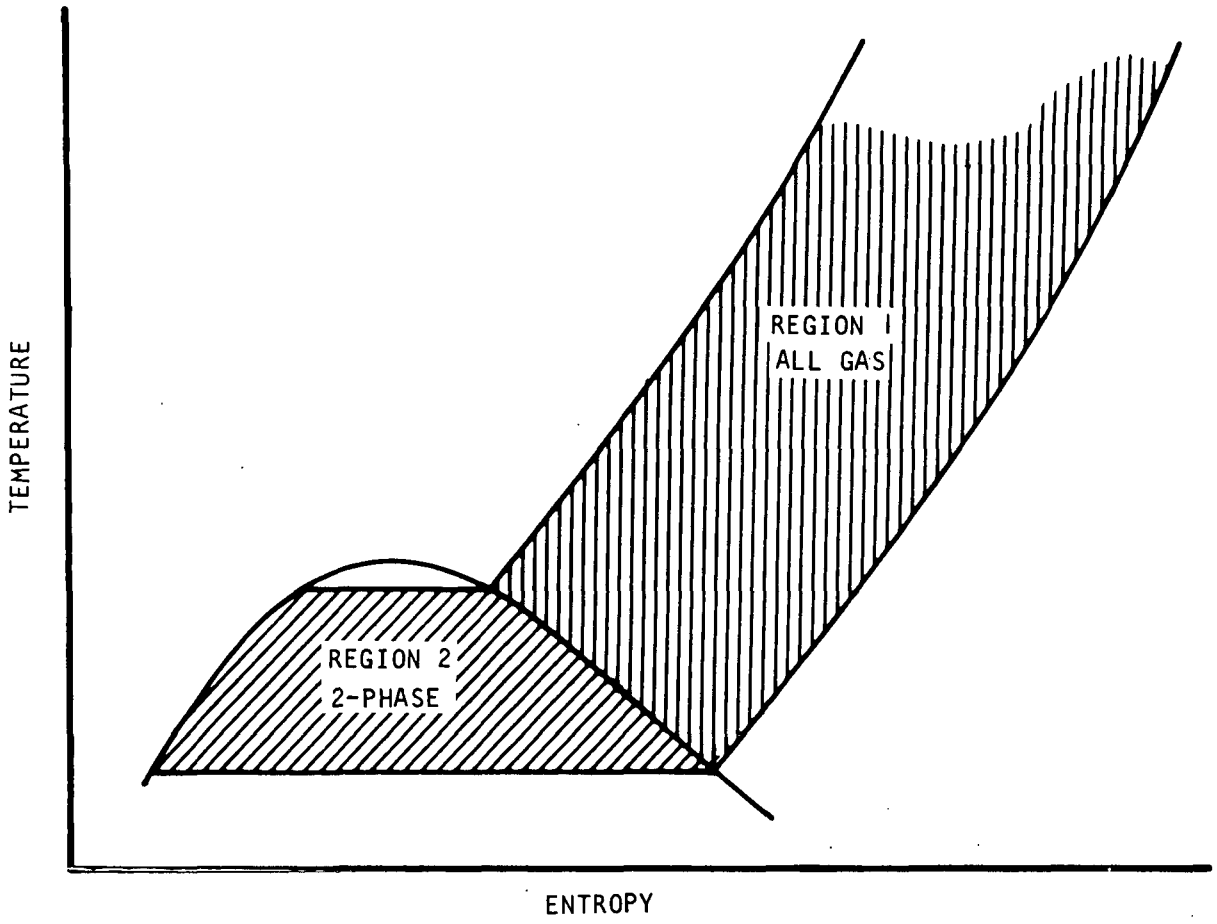

S-68253

Figure 3-1. Modes of Operation on the Cryogenic Side of the Heat Exchanger

For flow inside dimpled tubes and finned passages, the AiResearch heat transfer data on the surfaces were used with the correction $\left(\frac{T_W}{T_b}\right)^{-0.55}$ to account for the wall-to-bulk temperature ratio.

2. Pressure Drop

The AiResearch data were used for the friction factor inside the tubes and various finned passages. The pressure drop within a core section is predicted by

$$\Delta P = \frac{G^2}{2\rho_1 g_c}\left[\left(K_c + 1 - \sigma^2\right) + 2\left(\frac{\rho_1}{\rho_2} - 1\right) + \frac{4fL}{D_h}\cdot\frac{\rho_1}{\rho_m} - \left(1 - \sigma^2 - K_e\,\frac{\rho_1}{\rho_2}\right)\right]$$

where ρ_1, ρ, and ρ_m = inlet, outlet and mean densities, respectively

$2\left(\frac{\rho_1}{\rho_2} - 1\right)$ = flow acceleration

$\frac{4fL}{D_n}\frac{\rho_1}{\rho_m}$ = frictional pressure loss

f = friction factor

D_h = hydraulic diameter

L = flow length

G = mass velocity in HX

K_c, K_e = contraction and expansion loss coefficients at entrance and exit of HX, respectively

σ = ratio of free flow area to frontal area

3. Flow Instability

Flow instability is unlikely during this mode of operation. Flow instability caused by variation of viscosity with temperature, as explained later under performance predictions of the hot fluid side, is unlikely to occur. The increase in viscosity with temperature as the cryogen heats up is a stabilizing factor and results in a positive slope of pressure drop vs flow rate.

All-Liquid Operation

This mode of operation is characterized by highly subcooled liquid flowing in the heat exchanger where it heats to a temperature close to its saturation temperature without vaporization taking place. Hence, the cryogen conditions are

$$P < P_{crit}$$

$$T_{in} < T_{sat}$$

$$T_{out} < T_{sat}$$

1. Heat Transfer and Pressure Drop

The same methods, as in the case of all-gas operation, are used for predicting the heat transfer and the pressure drop.

2. Flow Instability

Flow instability is unlikely during this mode of operation.

Two-Phase (Liquid-Vapor) Mode

This mode of operation, shown as Region 2 in Figure 3-1, has the following operating conditions:

$$P < P_{crit}$$

$$T_{in} \leq T_{sat}$$

$$T_{out} \geq T_{sat}$$

1. Flow Regimes

Forced convection vaporization takes place on the cryogenic side of the heat exchanger until vaporization is completed. In general, this process involves a continuous change in the flow patterns as the vapor quality changes. The most common and distinctive flow patterns observed in forced convection boiling of fluids, other than cryogens, are the bubbly flow, plug or slug flow, annular flow, and mist flow. In case of forced convection vaporization of cryogenic fluids, the temperature difference ΔT between the wall and the fluid is usually large and, hence, the flow patterns may be somewhat different. Based on the observations and conclusions of References 3 and 4, the forced convection vaporization process of cryogenic fluids may be divided into three regions (see Figure 3-2).

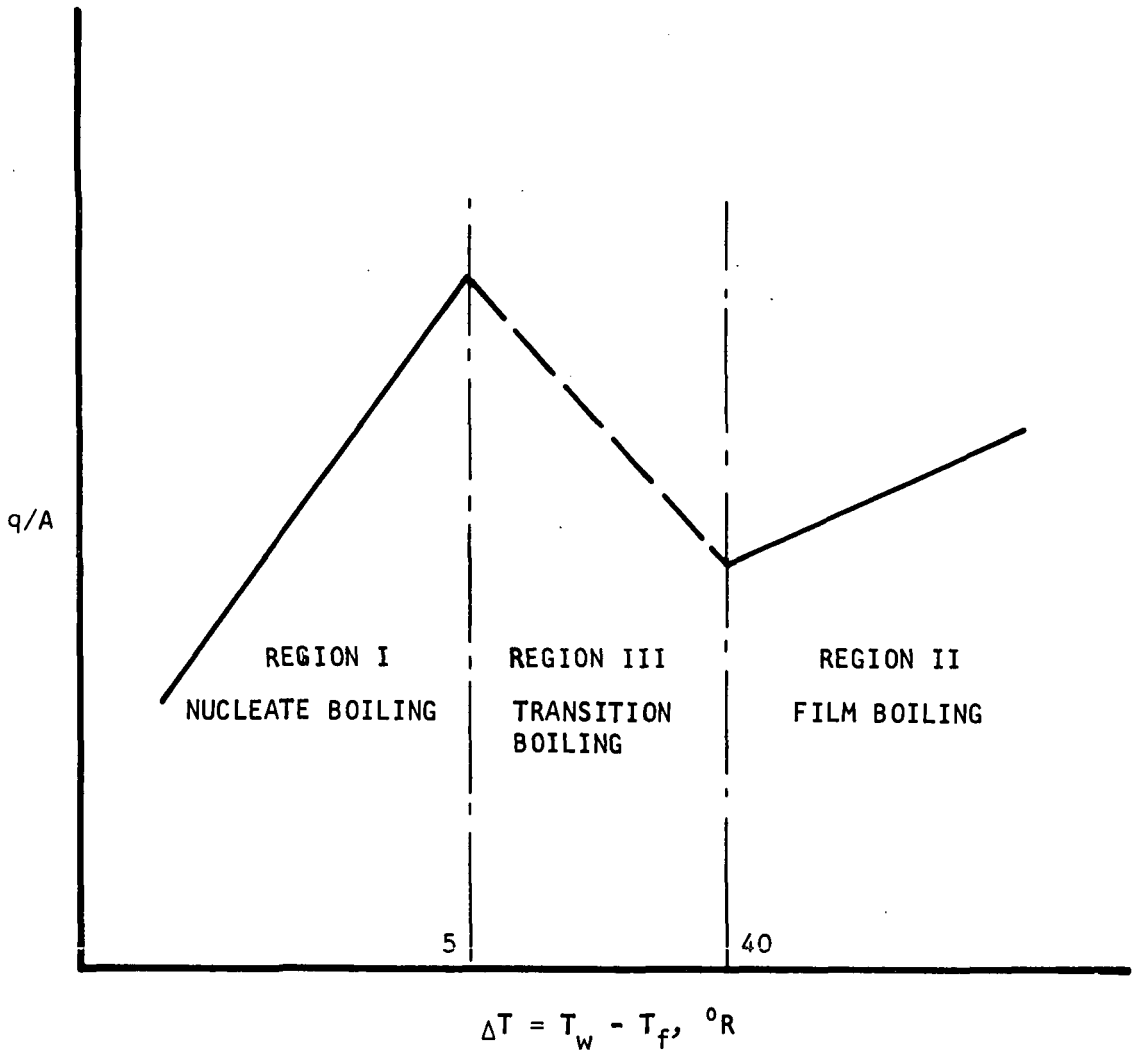

Figure 3-2. Heat Transfer and Flow Regimes in Forced Convection Boiling of Cryogenic Fluids

a. Region I.

For $\Delta T = T_w - T_f \leq 5^{\circ}R$ and may be called nucleate boiling regime and includes the bubbly-plug-annular flow patterns shown in Figure 3-3. This regime results in very high heat transfer coefficients. Based on the ranges of the parameters in the present problem statement, it can be easily shown that the presence of nucleate boiling would result in the completion of vaporization in a very small fraction of the cryogen flow length. Such a short length is not sufficient for a flow pattern to be established and the occurrence of this flow regime is highly unlikely in the present application.

b. Region II.

For $\Delta T \geq 40^{\circ}R$ and may be called film boiling regime. Due to the high temperature difference between the wall and the cryogen, a thin vapor film is established adjacent to the wall as soon as the cryogen enters the heat exchanger. A turbulent exchange occurs at the interface between the vapor film and the liquid core and evaporation takes place at this interface until complete vaporization is reached (i.e., 100-percent quality). The heat transfer coefficients in this case are considerably lower than in Region I.

Based on the inlet conditions of both oxygen and hydrogen and the inlet and outlet conditions of the hot fluid in the present application, this flow regime is the most likely one to occur over most of the two-phase operating conditions.

c. Region III.

For $5 < \Delta T < 40^{\circ}R$ and may be called transition boiling. In this case a nonstable vapor film is established adjacent to the wall. The exchange mechanism between the vapor and the liquid at the interface represents a nonequilibrium condition with the vapor film breaking off at times and the liquid touching the wall. The higher the ΔT the more stable the vapor film becomes until Region III is reached.

The heat transfer coefficients range from the high value of Region I to those values characteristic of Region III.

The likelihood of this flow regime occurring in the present application is limited to the areas adjacent to Region II in Figure 3-2. The heat transfer and flow processes are quite similar to Region II.

2. Heat Transfer

Based on the above discussion, film boiling will dominate the two-phase portion of the heat exchanger tubes. For flow inside tubes, the heat transfer coefficient in this portion of the tubes is predicted by the correlation of Reference 3.

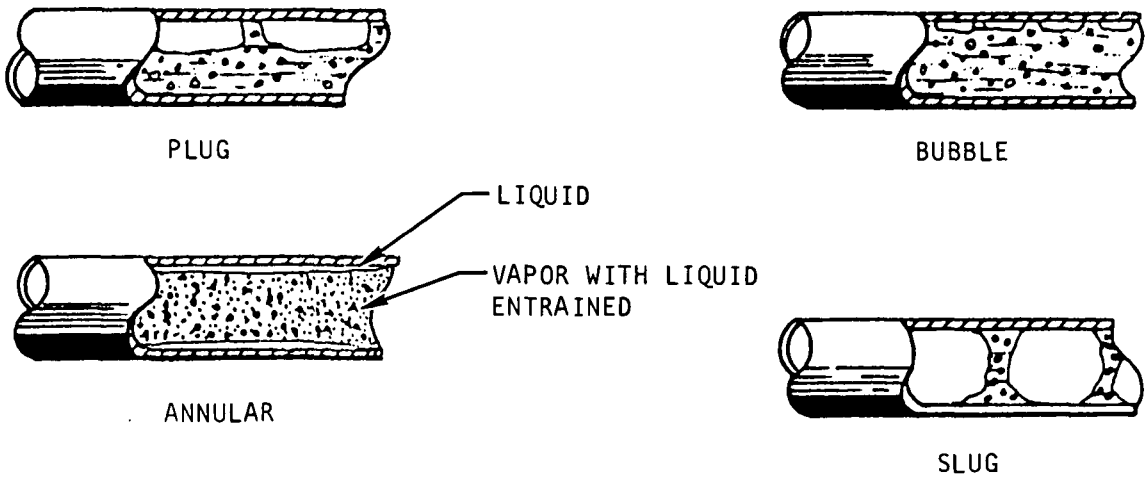

REGION I - NUCLEATE BOILING

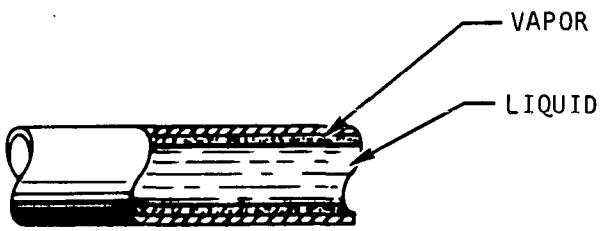

REGION II - FILM BOILING

S-68963

Figure 3-3. Two-phase Flow Regimes

$$\left(\frac{Nu_{calc}}{Nu_{exp}}\right)_f = 0.611 + 1.93\ \chi_{tt,f} \qquad (3\text{-}3)$$

where $$Nu_{calc} = 0.023 \rho_{fm}^{0.8} \left(\frac{U_{av} D_H}{\mu_f}\right)^{0.8} (P_{r_f})^{0.4} \qquad (3\text{-}4)$$

f denotes the temperature conditions halfway between wall and bulk, and the density ρ_{fm} is defined as

$$\frac{1}{\rho_{fm}} = \frac{x}{\rho_{g,f}} + \frac{1 - x}{\rho_\ell}$$

where $\rho_{g,f}$ = gas density evaluated at film temperature

ρ_ℓ = density of saturated liquid

x = quality, mass fraction of gas in the mixture

The velocity, U_{av}, is based on bulk conditions.

The variable χ_{tt} is the Martinelli parameter, Reference 7, which is a coefficient accounting for the shear at the wall and at the boundaries between the two phases. Figure 3-4 and 3-5 show χ_{tt} as a function of quality and pressure for hydrogen and oxygen, respectively.

For the case of flow inside finned rectangular channels, the heat transfer coefficients predicted by Equation 3-3 should give conservative results.

3. Pressure Drop

The frictional pressure drop in the two-phase portion of the HX tubes is predicted by a modified Martinelli-Nelson correlation, Reference 8.

$$\Delta P = \int_o^L \left(\frac{dP}{dz}\right)_\ell \phi_{\ell tt}^2\ dz \qquad (3\text{-}5)$$

where $\left(\frac{dP}{dz}\right)_\ell$ is the liquid phase pressure gradient, $\phi_{\ell tt}$ is a parameter defined in Reference 7 and is a function of χ_{tt} only, and L is the two-phase flow length.

The pressure gradient $\left(\frac{dP}{dz}\right)_\ell$ is defined as

$$\left(\frac{dP}{dz}\right)_\ell = \frac{4f}{D_H} \cdot \frac{G_\ell}{2\rho_\ell g_c} \qquad (3\text{-}6)$$

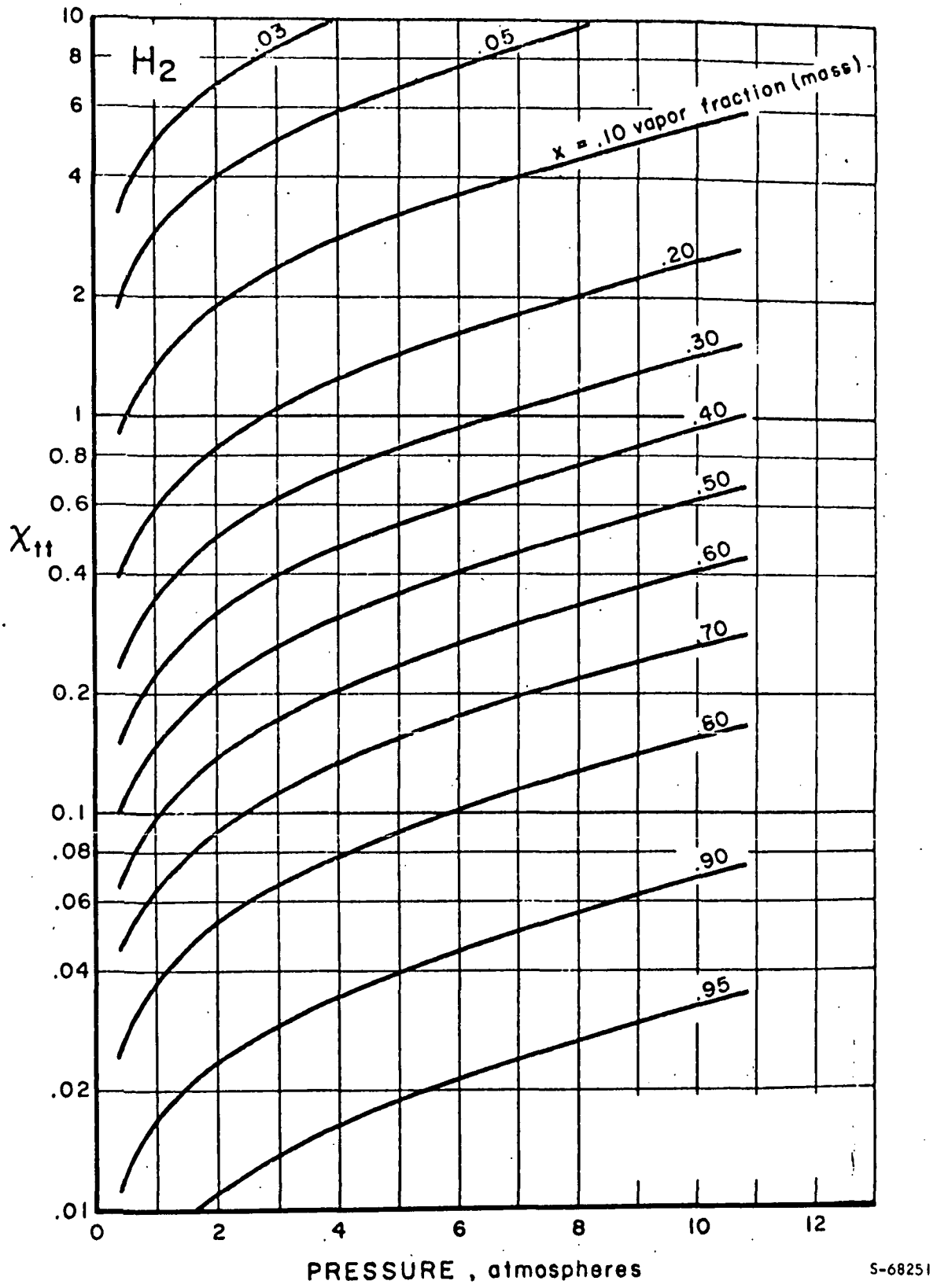

Figure 3-4. Martinelli-Nelson Correlating Term X_{tt} as a Function of Quality and Pressure for H_2

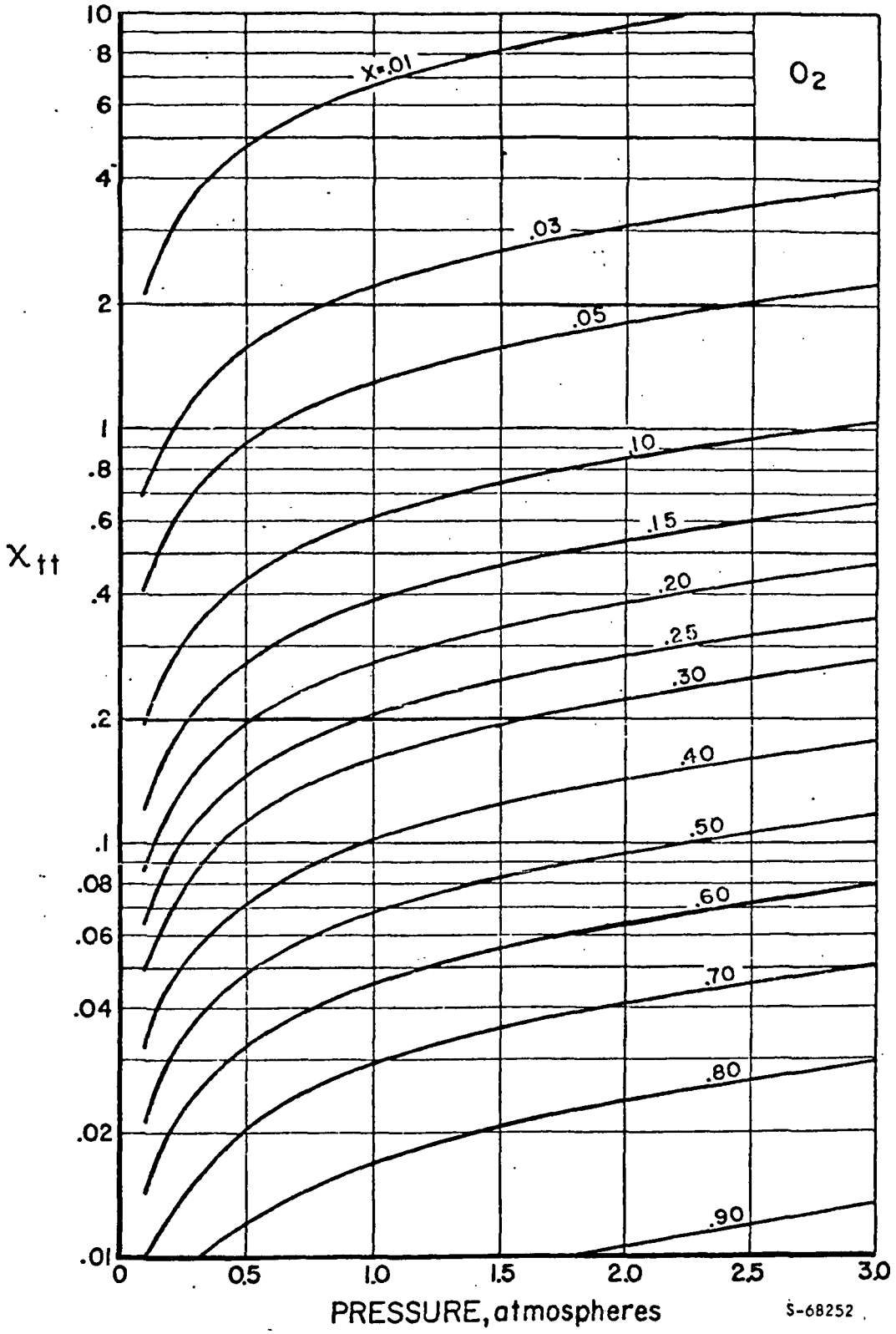

Figure 3-5. Martinelli-Nelson Correlating Term X_{tt} as a Function of Quality and Pressure for O_2

where x is the vapor quality, G_ℓ is the liquid mass flow rate per unit area of the flow channel and f is the one-phase friction factor. In case of flow inside tubes, f is given by

$$f = 0.046\ Re_o^{-0.2} \tag{3-7}$$

and for flow in dimpled tubes and finned passages, f is obtained from AiResearch data for the particular surface used.

4. Flow Instability

The different types of flow behavior that can occur in boiler tubes are depicted in Figure 3-6. No harmful effects result from types (A), (B) and (C) as long as the oscillations are within tolerable limits. The flow instability exhibited by (D), if encountered, would lead to the deterioration of the exchanger performance and may cause freezing of the warm fluid at conditions where stable flow calculations would indicate wall temperatures above the freezing point. Since two-phase flow instabilities are common in boiling systems they require special attention. The main objectives in this section are to identify the potential sources of flow instability in the present application and to establish a flow stability criterion that can be used during heat exchanger design.

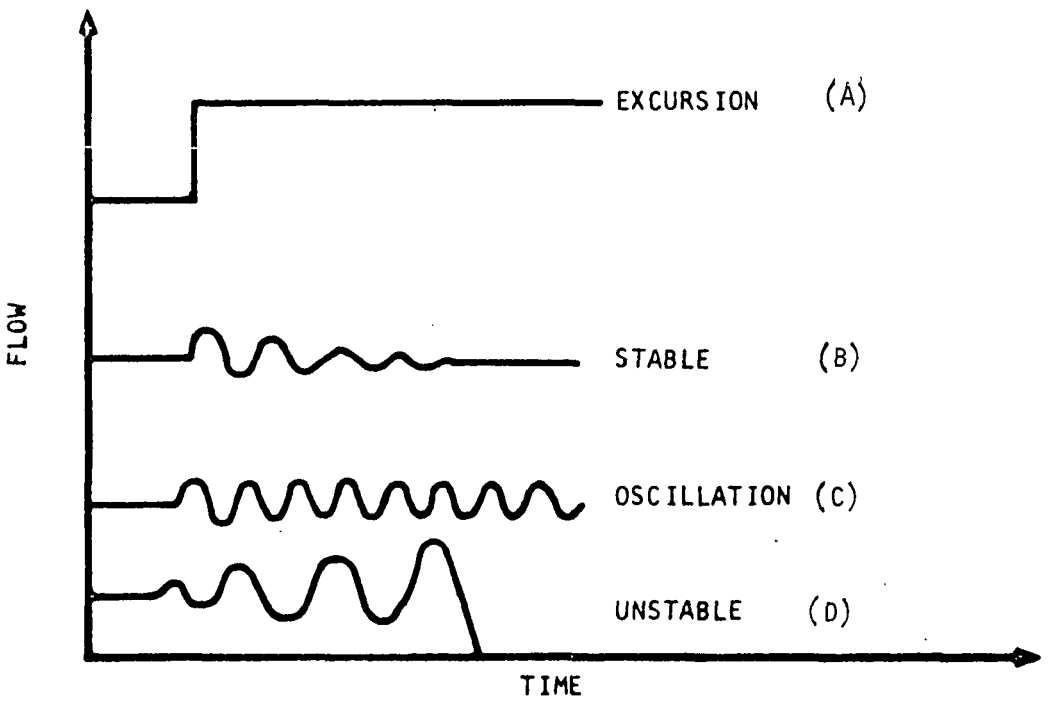

Figure 3-6. Types of Flow Transients

Flow stability in boilers has been extensively studied, both experimentally and analytically. These boiling studies dealt with fluids in subcritical conditions as well as with fluids in the near to supercritical states. Several sources provide sufficient information for the problems of interest in the present application. These are the experimental work carried out at AiResearch, References 9 and 10, and the investigations of Friedly and Zuber, References 12, 14 and 15, respectively.

The physical variables affecting flow stability of fluids boiling under subcritical conditions were grouped in References 9 and 10 into six pertinent dimensionless parameters, which can be expressed as follows:

$$\frac{\Delta P_{\ell}}{\Delta P_{TP}} = f\left(\frac{Cp\Delta T}{h_{fg}}\ ,\ \rho_{\ell}/\rho_{v},\ \frac{\Delta P_{TP}}{P}\ ,\ X,\ L/D_{H}\right) \qquad (3\text{-}8)$$

The term on the left-hand side is the ratio of the subcooled liquid pressure drop to the two-phase pressure drop. This parameter was selected as a dependent parameter because the results of References 11 and 12; and others, had shown that two-phase flow could always be stabilized with a large enough pressure drop in the subcooled-liquid region.

The parameters on the right hand side of Equation 3-8 are the ratio of subcooling to latent heat of vaporization, liquid to vapor density ratio, ratio of tow-phase pressure drop to pressure level, exit quality and ratio of length to hydraulic diameter.

An extensive experimental program was carried out at AiResearch to investigate, quantitatively, the effect of the various parameters in Equation 3-8. The main conclusions of this investigation were:

(a) A stable flow can be achieved by inserting, at the entrance of the boiler, an orifice valve which has a pressure drop ΔP_{ℓ} of from 5 to 90 percent of the two-phase pressure drop ΔP_{TP}.

(b) An increase in the two-phase pressure drop ratio $\Delta P_{TP}/P$ and a decrease in the density ratio ρ_{ℓ}/ρ_{v} are stabilizing factors.

(c) An increase in heat transfer acts to stabilize the flow.

(d) The pressure and flow fluctuations result from the nonhomogeneous nature of the flow in the bubbly-plug flow region or in the transition from bubbly-plug flow to annular flow. It can also be inferred that this transition is from a region where the fluid is incompressible to a region where the flow becomes compressible.

As explained previously, the flow regime in the present application is different from the flow regimes observed and studied in References 9 and 10 due to the high wall to bulk temperature difference. Hence, it is important to establish whether the conclusions listed above are still valid.

The flow regime on the cryogenic side of the heat exchanger will be characterized by a vapor film adjacent to the warm wall and a liquid core up to a point where vaporization is completed. This is quite similar to the flow regime observed with cryogenic fluids flowing in the near to supercritical states. In this case a light density fluid flows adjacent to the hot walls and a heavy density fluid in the core. This flow model is sometimes referred to as a homogeneous model and was extensively analyzed by Zuber (13) then by Friedly (14). The conclusions made on the basis of such a model, regarding flow stability, should be applicable for the present application, if the unique behavior of the physical properties in the near and supercritical states is discounted.

Friedly et al, in References 14 and 15 presented a simplified analysis based on the work of Zuber. They arrived at a simplified criterion which they correlated with experimental data from various sources. Their criterion was further simplified and adapted to the present application (Appendix A). The final result of this criterion is that for the flow to be stable, the following inequality must be satisfied:

$$\frac{\Delta P_\ell + \Delta P_{TP} + 2(\rho_v/\rho_\ell)\,\Delta P_{fv} + 0.5\,(\rho_v/\rho_\ell)\,\ln\,(\rho_\ell/\rho_v)\,\Delta P_a}{(\rho_v/\rho_\ell)\,\Delta P_{fv} + (\rho_v/\rho_\ell)\,\Delta P_a} > (\rho_\ell/\rho_v)^{1-H} \qquad (3\text{-}9)$$

where, ΔP_ℓ = pressure drop across orifice valve upstream of heat exchanger

ΔP_{TP} = pressure drop in the two phase region

ΔP_{fv} = frictional pressure drop in the vapor region

ΔP_a = acceleration pressure drop

and

$H = \dfrac{hA_H}{A_c \rho_\ell C_p}$ is a heat transfer parameter.

To demonstrate the similarity between the criterion in Equation 3-9 and the observations made in References 9 and 10, Equation 3-8 is regrouped. The liquid subcooling term, exit quality and length to diameter ratio can be combined and replaced by another dimensionless parameter which is the ratio of heat transfer to the amount of subcooling (Reference 9). In this case, Equation 3-8 takes the form

$$\frac{\Delta P_\ell}{\Delta P_{TP}} = f\left(\rho_\ell/\rho_v,\ \frac{\Delta P_{TP}}{P},\ \frac{Q}{WCp\Delta T}\right) \qquad (3\text{-}10)$$

Knowing that both ΔP_a and ΔP_{fv} were essentially zero in the experiments of References 9 and 10 and that H is essentially the heat transfer term in Equation 3-10, it is interesting to note that both results contain the same parameters. Equation 3-9 supports the experimental findings of References 9 and 10. For example, (a) an increase in the orifice pressure drop can always stabilize the flow, (b) an increase in ΔP_{TP} and a decrease in ρ_ℓ/ρ_v are stabilizing factors, and (c) an increase in heat transfer is also stabilizing.

An orifice pressure drop is not very practical in the present application since it requires providing orifices on the individual HX tubes. The density ratio is determined by the operating pressure and temperature of the cryogen in the HX, and little can be done in this area. The flow-stabilizing effect by increasing the heat transfer along the HX tubes can be achieved by using highly efficient heat transfer surfaces. Another stabilizing effect is to increase the ratio of the two-phase pressure drop ΔP_{TP} to the overall pressure drop in the HX tube. While this is possible to achieve in case of oxygen, it is difficult in the case of hydrogen because of the following reason: A high oxygen side effectiveness is one of the design objectives in the present HX to minimize the amount of oxygen expended. In case of liquid oxygen (inlet temperature = $180^{\circ}R$), the portion of the HX tubes occupied by vapor is comparable to that occupied by two-phase flow (see Figure 3-7). Hence, ΔP_{TP} becomes comparable to ΔP_{fv}. On the other hand, in case of liquid hydrogen (inlet temperature = $40^{\circ}R$) the two-phase flow portion is a small fraction of the overall length of the HX tubes and ΔP_{TP} is small compared with the overall ΔP.

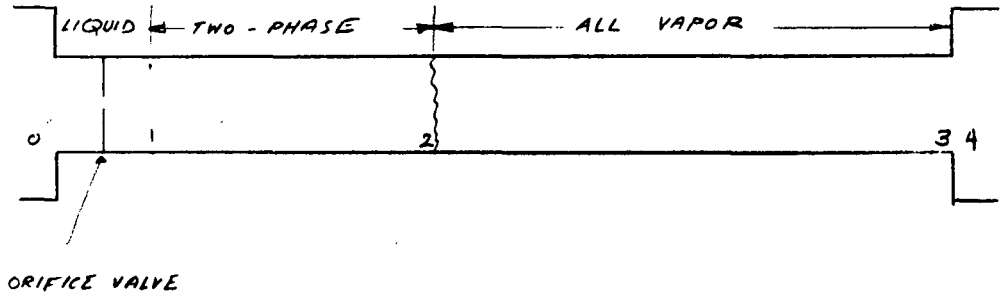

Figure 3-7. Schematic Diagram of System

PERFORMANCE PREDICTIONS OF THE WARM FLUID SIDE

Heat Transfer and Pressure Drop

The pressure drop and heat transfer in the hot fluid passages were predicted by the f and j data stored in AiResearch computer library for flow inside tubes and finned passages of various geometries and for flow over tube and finned tube banks.

Flow Instability

Flow instability on the hot fluid side could cause freezing or congealing, even though calculations may show the wall temperature to be above the freezing point, Reference 16. While flow instability is known to be common in two-phase (boiling or condensing) flow, it is generally not considered in single-phase flow. The following paragraphs discuss the feasibility of such an instability in a heat exchanger where liquid is being cooled, and describe the necessary means to avoid it.

This one-phase instability is analogous to one occurring in forced-convection vaporization. In both cases, there is a negative slope of pressure drop vs flow rate. In boiling, it is due to the phase change and the increased pressure drop with vapor over that with liquid at higher flow rate. In liquid cooling, it is due to the increased viscosity of liquid with decreasing temperature. The negative slope of the pressure drop flow rate curve is a classical cause of flow instability and is referred to as the Ledinegg criterion (Reference 17).

The adverse effect of viscosity on one-phase pressure drop is more pronounced in laminar flow than in turbulent flow as shown below.

In laminar flow, pressure drop is given by

$$\Delta P = \frac{32\ L}{g_c D^2 \rho A}\ \mu W \qquad (3\text{-}11)$$

where ΔP is the pressure drop, μ is the viscosity and W is the cooled fluid flow rate.

For a fixed heat sink capacity, decreasing the flow rate decreases the outlet temperature and, if the increase in viscosity is faster than the decrease in flow rate, a higher ΔP is obtained. The increased pressure drop then leads to lower flow, more cooling, and more increase in pressure drop with still lower flow, until the fluid freezes.

In turbulent flow, pressure drop is given by

$$\Delta P = \frac{4fL}{D} \cdot \frac{W^2}{2g_c \rho A^2}$$

or

$$\Delta P = 0.143 \frac{\mu^{0.2} W^{1.8}}{g_c \rho D^{4.8}} \qquad (3\text{-}12)$$

Thus, the pressure drop in turbulent flow is proportional to $\mu^{0.2} W^{1.8}$. It seems unlikely that there will be many practical cases in which the change in viscosity to the 0.2 power will overcome the increased pressure drop due to the $W^{1.8}$ term.

The factors affecting the flow instability of the hot fluid are summarized below.

Factors Favoring Freezing and Instability	Factors Favoring Stable Operation
Laminar flow	Turbulent flow
High change in liquid viscosity	Low change in liquid viscosity
Pump flow strongly dependent on ΔP	Constant displacement pump

The above discussion reveals that the variation of viscosity with temperature along the warm fluid path must be considered in calculating the pressure drop and that a positive slope for the pressure drop vs flow is mandatory to ensure flow stability.

SECTION 4

INTERFACE DEFINITION

The various interfaces necessary for the design and tradeoff study of the heat exchanger and control system were defined. These definitions were guided by previous AiResearch experience on the Gemini and Apollo programs and current experience with the Skylab and the Space Shuttle. The interfaces of interest are:

(a) Inlet condition profile of hydrogen

(b) Inlet condition profile of oxygen

(c) Heat load profile

(d) Penalties attached to the weight of expendables

(e) Weight penalty of hot fluid pumping power

(f) Typical rates of change of the heat load

(g) Typical rates of change of the cryogen inlet condition.

The inlet condition profile of the cryogen depends on the exact location of the heat exchanger in the system and the nature of the cryogen source. This source may be either vent gases or subcritical cryogenic tanks.

Typical subcritical pressures in the oxygen and hydrogen tanks are in the range of 40 to 50 psia. This corresponds to a hydrogen saturation temperature of about -417°F and to an oxygen saturation temperature of about -275°F. Location of the gaseous and liquid phases may change due to acceleration fields to an extent that cryogen gases may be fed into the heat exchanger for periods of time. These gases should be at temperatures close to the liquid cryogen temperature for all conditions except when large storage tanks are almost depleted of liquid cryogen. Under the latter, although the gas temperature may be considerably higher than the liquid temperature (possibly up to 0°F), the condition would most probably occur during reentry or subsequent phases where known acceleration fields and, therefore, known liquid location exists, thus allowing proper location of outlet ports on the tank to maintain liquid cryogen flow. The final weight of consumables should be based on either 0°F in case of vent gases or -417°F and -275°F in case of hydrogen and oxygen, respectively.

The heat load profile was determined on the basis of typical environmental control system heat loads being used on the Space Shuttle and given in Table 4-1. Except for the time spent in orbit, the heat exchanger has to operate very close to maximum heat load (60,000 Btu/hr in the present application) for a period of about 2.6 hr. In orbit, the heat exchanger acts as a topping device for the space radiator. The exact amount and duration of the peak heat loads are very difficult to determine since it depends on

TABLE 4-1

ENVIRONMENTAL CONTROL SUBSYSTEM HEAT LOADS BTU/HR

Phase	Time	Heat Rejection Total (Btu/hr)
Prelaunch	5 min	TBD
Liftoff-Separate	3 min	64,000
Assent/Insertion	8 min	64,000
Coast-radiator Deploy	30 min	57,000
Coast	60 min	57,000
Coast Circular	50 min	58,000
Orbit-Max Active*	116 hr	54,000
Orbit-Min Sleep*	48 hr	39,000
Radiator Stowage	30 min	55,000
De-Orbit	5 min	65,000
Re-Orbit	20 min	63,000
Entry	35 min	64,000
Approach Go-around	15 min	28,000
Post Landing	10 min	TBD

*Cryogenic Heat Exchanger is acting as a topping device

the details of the spacecraft subsystems as well as on the details of the mission. For the purpose of this study it will be assumed that the cryogenic heat exchanger will be required to reject a heat load of 60,000 Btu/hr over a period of 2 to 6 hr.

The penalties attached to the weight of expendables include weight of the tanks, controls, etc. Approximate values are assumed on the basis of large tanks:

For hydrogen = 1.7 lb/lb of H_2

For oxygen = 1.2 lb/lb of O_2

The weight penalty of hot fluid pumping power will be determined on the basis of 1 lb/kwh. This penalty will be confined to the heat exchanger tradeoff study where a higher hot fluid pressure drop means more pumping power and, hence, a weight penalty. Since the heat exchanger operation is limited to a few hours, this penalty will be small.

Approximate rates of change of the heat load are determined by considering a typical overall environmental control system as a lumped capacity located at the inlet of the cryogenic heat exchanger. The rate of change of the temperature at the inlet of the heat exchanger (which is the outlet of the lumped system) is determined subject to a step function in the heat dissipation in the lumped system. Typical rate of change may be 2.5°F per sec. The present HX is investigated, however, using the conservative time assumption of 20-sec ramp from minimum to maximum heat load.

Changes in the cryogen inlet condition of any significant consequences are the ones occurring at the lowest cryogen temperatures, i.e., when the cryogen source is the subcritical propellant tanks. As discussed previously, a sudden change in the outlet temperature of these tanks is highly unlikely, and any change must take place gradually. The present control system is investigated using the conservative assumption of 20 sec ramp from 0°F to -400°F.

SECTION 5

WARM FLUID SELECTION

WARM FLUID SURVEY

The candidate hot side fluids and pertinent physical properties are listed in Table 5-1. The liquids are placed in three groupings, which consist of water and water mixtures, dielectric coolants, and fluorocarbon compounds. The primary properties of interest are fluid specific heat, freezing or pour point, boiling point, density and viscosity. The number of hot side fluids can be narrowed down on the basis of the physical properties listed.

The fluid specific heat is a direct measure of the required flow rate, and, thus the pumping power required. With the inlet and outlet temperatures and maximum heat load fixed, the required flow rate for each fluid is defined by the value of specific heat. Water and the water glycol mixture require the lowest flow rates, whereas the fluorocarbons require the maximum mass flows. If pumping power were the only requirement, water would be the obvious fluid choice.

The physical property of prime importance is the freezing or pour point of the fluid. The fluids with the lowest values of this temperature allow the greatest flexibility in heat exchanger design from the freezing standpoint.

The third fluid property variable listed in Table 5-1 is the normal boiling point at 14.7 psia. This temperature determines the required system operating pressure. A low boiling temperature thus dictates a high operating pressure to ensure all liquid operation. In fact, the most attractive fluid from a freezing standpoint, Freon-14, would have to be operated at supercritical pressure (at $T_c = -50^{\circ}F$) to ensure single phase operation.

The density and viscosity values listed in the table are indications of the pressure drop in the system and, thus, pumping power. The pressure drop is inversely proportional to the fluid density and a weak function of the fluid viscosity.

From a heat transport standpoint, water is quite attractive as a hot side fluid. Freezing characteristics, however, would make the system extremely complex and, therefore, water should be rejected as a candidate fluid. Water-glycol has the advantage of a high specific heat and, at the same time, a reasonably low freezing point; hence, it is a good candidate fluid.

Among the fluids in group B, which are characterized by specific heat values in between the water-mixtures and the Fluorocarbons, Coolanol 15 seems to be the most attractive one. While it has the lowest freezing point in this group, its specific heat is not much different from Coolanol 45. The boiling point at 1 atm is quite high, which is desirable.

TABLE 5-1

PHYSICAL PROPERTIES OF VARIOUS HOT SIDE FLUIDS

Coolant	Specific Heat, Btu/lb °F	Freezing or Pour Point, °F	Boiling Point at 1 atm, °F	Density, lb/ft^3	Viscosity lb/ft-hr
A. Water and water mixtures					
Water	1.0	32	212	62.3	2.37
Eutectic mixture of ethylene glycol-water	0.77	-40	235	65.3	8.7
B. Dielectric coolant fluids					
Coolanol 15	0.431	-140	432	55.8	4.56
Coolanol 25	0.441	-120	590	56	12.6
Coolanol 45	0.45	-80	> 600	58	22.0
C. Fluorocarbon compounds					
FC-75	0.247	-135	216	105	6.6
Freon-14	0.294	-299	-198	82	0.5
Freon-21	0.256	-211	48	85.3	0.82
E-1	0.247	-246	105	94	1.55
E-2	0.242	-190	220	103	3.87
E-3	0.240	-160	306	107	7.8
E-4	0.239	-138	381	110	19.5
E-5	0.238	-119	436	111	31

Among the fluorocarbon compounds, FC-75 is comparable to E-2, except that E-2 has a lower freezing point and is more attractive. Freon-14 can be rejected on the basis of its low boiling point and consequently high system pressure. Although Freon-21 also has a low boiling point, it is maintained in the selection since it is commonly used on current spacecraft systems. Among E-1, E-2 and E-3, E-2 has a reasonably high boiling point and a reasonably low freezing point; therefore, it is the most attractive one.

The hot side fluids can be narrowed down to the following fluids:

Eutectic mixture of ethylene glycol-water

Coolanol 15

E-2

Freon-21

The final selection of one candidate hot side fluid is made on the basis of heat exchanger size and weight and freezing considerations, as shown in the following paragraphs.

WARM FLUID FINAL SELECTION

The method usually employed to prevent freezing involves designing the heat exchanger with unbalanced heat transfer conductances on each side. The wall temperature is defined by the relative magnitude of the two heat transfer conductances. The defining equation is as follows:

$$T_W = \frac{T_c + \phi T_H}{1 + \phi} \tag{5-1}$$

where $$\phi = \frac{(\eta hA)_H}{(\eta hA)_c} , \tag{5-2}$$

η is the fin effectiveness, h is the heat transfer coefficient and A is the heat transfer area. The subscripts H and c refer to the hot and cold side, respectively.

For every hot fluid there is a minimum value of ϕ required to maintain the wall temperature above the freezing point of that fluid. For example, if hydrogen at $-417^{\circ}F$ is used as the cold fluid and the minimum hot fluid temperature is taken as $40^{\circ}F$, Equation 5-1 can be written as:

$$\phi = \frac{T_W + 417}{40 - T_W} \tag{5-3}$$

To maintain the wall temperature 10°F above the freezing point, the following minimum values ϕ result for the various candidate hot fluids:

Hot fluid	Value of ϕ required to eliminate freezing
Ethylene glycol-water	5.55
Coolanol 15	1.7
E-2	1.08
Freon-21	0.91

In addition to the required minimum values shown above, the parameter ϕ has an optimum value for which the volume of the heat exchanger is minimized. The derivation of this ϕ value is given in Appendix B. The final result is

$$\phi \simeq \left(\frac{\alpha_c}{\alpha_H}\right)^{0.6} \left[\frac{W_H\ (\rho\Delta P)_H}{W_c\ (\rho\Delta P)_C}\right]^{0.2} \left(\frac{J_H}{J_c}\right)^{0.4} \qquad (5\text{-}4)$$

where $\alpha = Pr^{2/3}/Cp$, W is flow rate, ρ is density, ΔP is pressure drop and J is ratio of colburn factor to hydraulic radius of the flow passage.

The optimum values of the conductance ratio, as calculated by Equation 5-4, are shown in Figure 5-1 for the four candidate hot fluids. The conditions used to evaluate ϕ are listed in Table 5-2. These conditions were selected since they result in the lowest values of ϕ over the desired operating conditions, and they may be considered conservative. These values of ϕ correspond to minimum heat exchanger volumes. A conductance ratio which deviates considerably from the values shown in Figure 5-1 would indicate a heat exchanger design deviating from the minimum volume design and, consequently, a volume and a weight penalty.

The minimum values of the conductance ratios, required to maintain the heat exchanger wall 10°F above the freezing point of the hot fluid considered, are also shown in Figure 5-1. These values were obtained from Equation 5-3 with the assumption that the cryogen inlet temperature is -417°F.

Figure 5-1 demonstrates the disadvantages in using water-glycol as a hot fluid versus E-2 or F-21. Each candidate fluid is represented in the figure by a curve (equation 5-4) and a horizontal line (equation 5-3). The curve indicates the optimum ϕ values required to achieve minimum heat exchanger volumes and the horizontal line indicates the minimum ϕ values required to avoid freezing. For F-21 and E-2 the optimum ϕ values are higher than those indicated by the horizontal lines over most of the range of J_H/J_C. Hence, it is feasible, in this case, to achieve an optimum design which satisfies the freezing criterion. On the other hand, to satisfy the freezing criterion for water-glycol one must deviate considerably from the optimum ϕ values, thus resulting in substantial volume and weight penalties.

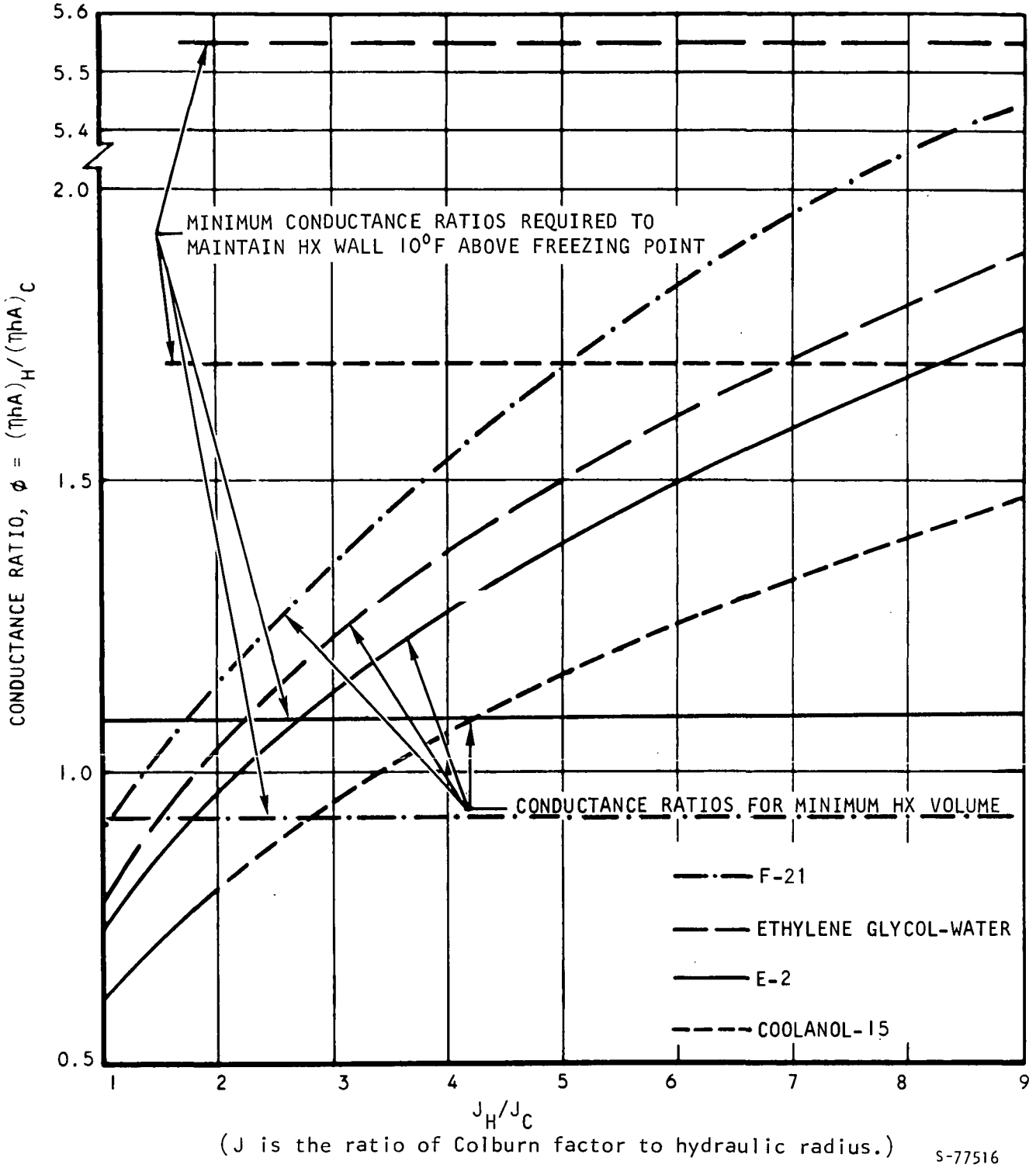

Figure 5-1. Deviation from Optium Heat Exchanger Design for Various Hot Fluids

TABLE 5-2

DESIGN CONDITIONS FOR FIGURE 5-1

Side	Cold Side	Hot Side			
	Hydrogen	Water-Glycol	Coolanol 15	E-2	F-21
Flow, lb/hr	237	1305	2340	4150	4300
Inlet temperature, ^{o}F	0	100	100	100	100
Outlet temperature, ^{o}F	-	40	40	40	40
Effectiveness	0.7	0.6	0.6	0.6	0.6
Heat load, Btu/hr	60,000	60,000	60,000	60,000	60,000
Inlet pressure, psia	40	100	100	100	100
Core pressure drop, ΔP, psi	1.0	2.5	2.5	2.5	2.5

Based on the above discussion and on AiResearch experience, both the water-glycol and Coolanol 15 are eliminated as candidate hot fluids and the heat exchanger and control study are confined to either E-2 or Freon-21.

Experience, such as on the Dyna Soar program, which utilized a glycol-water to liquid hydrogen heat exchanger, indicates that considerably complex heat exchanger and control system designs are required to eliminate freezing problems.

In the present application, E-2 is favored over Freon-21 because of its high boiling point relative to Freon-21. A low boiling point requires a high system operating pressure and, therefore, increases the overall system complexity. Hence E-2 was selected as the candidate warm fluid for the heat sink system design tradeoff study.

The final selection of the hot fluid was confined to the cryogenic heat exchanger and the entire environmental control system was not considered. A consideration of the impact of this selection on the various components in the system is beyond the scope of this study.

SECTION 6

HEAT EXCHANGER TRADEOFF STUDY

GENERAL APPROACH

In addition to having an optimum design from the standpoint of weight and volume, the heat exchanger must maintain a wall temperature sufficiently higher than -190°F to eliminate any freezing problems.

The worst design condition for the heat exchanger, relative to heat transfer and pressure drop, is at maximum heat load with the inlet temperature of the cryogen at its maximum value.

On the other hand, the worst design point from freezing and flow instability standpoints is at the cryogen lowest inlet temperature. The design tradeoff study, therefore, is carried out at the maximum cryogen inlet temperature, with the thermal conductance ratio selected such that the wall is always maintained above -190°F regardless of the cryogen inlet temperature. The other design conditions for the tradeoff study are listed in Table 6-1. Hydrogen was selected for the tradeoff study since it presents the most severe freezing problem in the HX design.

TABLE 6-1

RANGE OF DESIGN VARIABLES
FOR THE HEAT EXCHANGER DESIGN TRADEOFF STUDY

Side	Hydrogen	E-2
Flow, lb/hr	184 to 554	4150
Inlet Temperature, °F	0*	100
Outlet Temperature, °F	30 to 90	40
Effectiveness	0.3 to 0.9	0.6
Heat load, Btu/hr	60,000	60,000
Inlet pressure, psia	40	100
System pressure drop, psi	1 to 10	1 to 5

*The conductance ratio must be selected such that when the hydrogen inlet temperature drops to -417°F, the wall temperature is maintained above -190°F

The cold side effectiveness is considered as a design variable, and thus cold side flow rate and outlet temperature are variables. A range of cold side effectiveness of 0.3 to 0.9 has been selected for this study. As effectiveness increases, cryogen flow required decreases. On the other hand, both core size and weight increase with increasing effectiveness.

The range of pressure drops on the hot side ΔP_H is from 1 to 5 psi and on the cold side ΔP_c is from 1 to 10 psi. The hot side pressure drop affects the heat exchanger design and it has a weight penalty associated with the required pumping power. The cryogen side pressure drop merely affects the heat exchanger design and performance.

For every set of design variables listed in Table 6-1, such as cold side effectiveness E_c, ΔP_H, and ΔP_c, the heat exchanger is optimized and a specific design is selected. This design must have a conductance ratio ϕ sufficiently high to maintain the wall temperature above freezing when cryogen inlet temperature drops to its lowest value.

The various designs will be compared in terms of the total weight which is the sum of the heat exchanger weight, weight of consumables, and pumping power penalty. The weight of the control system is assumed fixed in this tradeoff study. The procedure is repeated for each heat exchanger concept considered.

CANDIDATE HEAT EXCHANGER DESIGNS

For both plate-fin and tubular heat exchangers, a wide range of flow arrangements can be used. The choice in the present application is dependent on freezing and effectiveness, which determine the heat exchanger size and weight. The typical flow arrangements are (a) counterflow, (b) parallel flow, (c) crossflow, (d) multi-pass cross-counterflow, and (e) multi-pass cross-parallel flow.

Counterflow configuration can produce the smallest size heat exchanger; however, the possibility of freezing is greater in this configuration. Pure parallel flow produces the largest size heat exchanger while the possibility of freezing is the least. This flow configuration, however, does not offer any advantages over multi-pass cross-parallel flow configuration. Furthermore, the manifolding of both fluids in the parallel and counterflow arrangements is complicated. Hence, both of these flow configurations have been eliminated from the heat exchanger tradeoff study.

A multipass crossflow arrangement with the hot fluid making several crossflow passes is preferred in this application to avoid excessively cold corners within the matrix caused by the transverse temperature gradient inherent in crossflow heat exchangers. The multipass arrangement also provides a reasonable packaging shape. The various candidate crossflow configurations are shown in Figures 6-1 and 6-2.

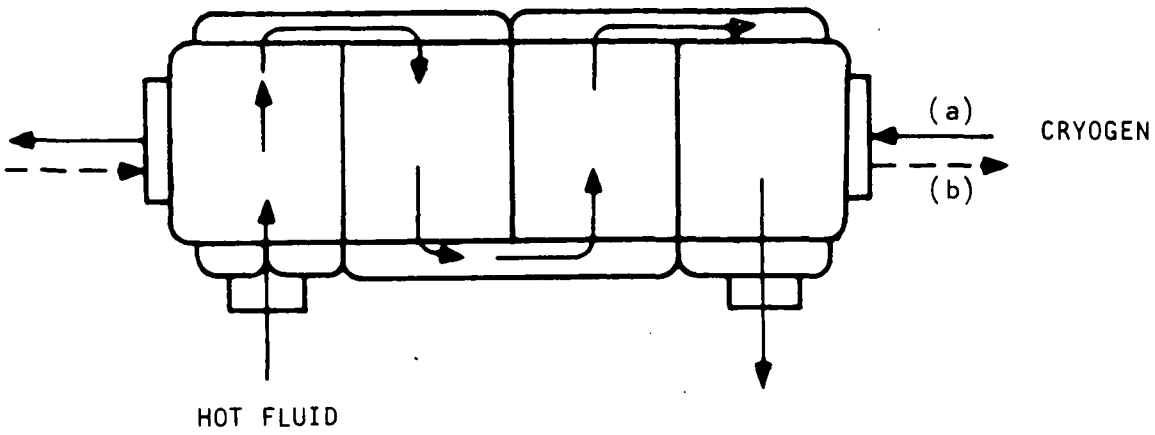

(a.) Cross-Counter Flow

(b.) Cross-Parallel Flow

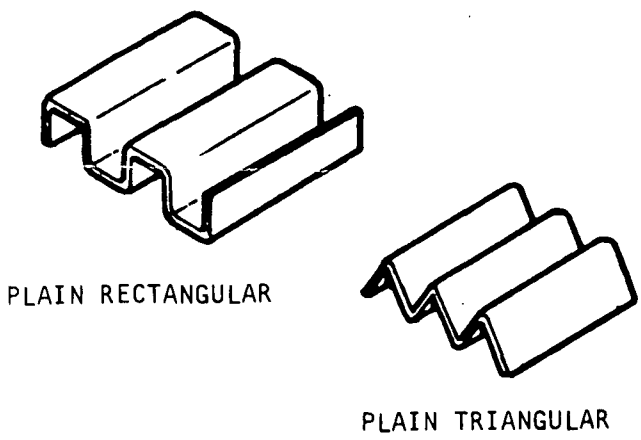

COLD SIDE FIN GEOMETRIES

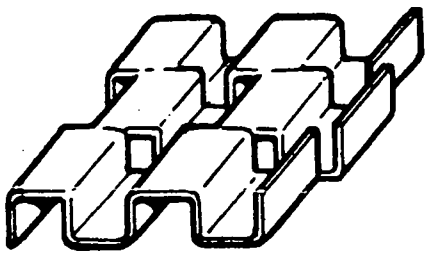

HOT SIDE FIN GEOMETRIES

S-68602

Figure 6-1. Multipass Crossflow Plate Fin Heat Exchanger

(a.) Cross-Counter Flow

(b.) Cross-Parallel Flow

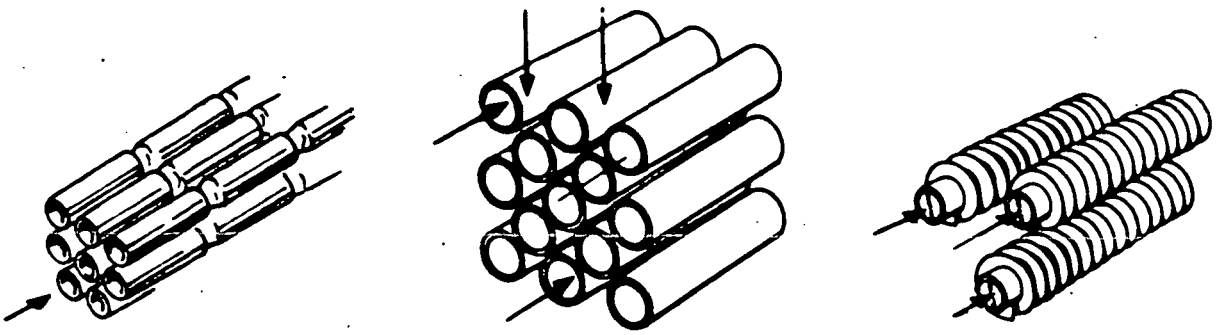

DIMPLED TUBE

PLAIN TUBULAR

DISC FINNED TUBE

S-68604

Figure 6-2. Mulitpass Crossflow Tubular Heat Exchanger

Figure 6-1 shows a multipass crossflow plate fin arrangement. The hot fluid makes four crossflow passes. The cryogen makes one pass to avoid any turning which could induce freezing, particularly in the two-phase mode of operation. The cryogen can flow either counter or parallel to the hot fluid. The latter flow arrangement results in a heavier heat exchanger but is attractive from the freezing standpoint.

The candidate heat transfer surfaces in the plate-fin design also are shown in Figure 6-1. Rectangular offset fins are used on the hot fluid side to augment the heat transfer. Typical f and j values for these kinds of fins are given in Appendix B, Figure B-2. Less effective heat transfer surfaces are required on the cryogen side to increase the thermal conductance ratio ϕ; therefore, plain rectangular or plain triangular fins are used.

Figure 6-2 shows a multipass crossflow tubular heat exchanger, which is another candidate design. The cryogen flows inside the tubes and the hot fluis makes several cross-flow passes outside the tubes for the reason given previously. An additional advantage of not flowing the warm fluid inside the tubes is the elimination of thermal stress loads resulting from freezing inside the tubes. Should freezing begin to build up, the flow in the tube would decrease and the temperature of the fluid in the tube would drop. The wall temperature would then drop, allowing more freezing until partial or complete flow blockage occurs. The mean tube wall temperature would then approach the mean cryogen temperature. The resulting temperature gradient between the cold tubes and its adjacent tubes at the containing header could then cause severe thermal stresses. This danger is prevented by flowing the hot fluid across the tubes since partial blockage would not affect individual tubes.

The candidate heat transfer surfaces for the tubular design also are shown in Figure 6-2. For internal heat transfer surfaces (the heat transfer existing on the inside of the tubes), both smooth and artificially roughened tubes are used, depending on which type yields the best heat exchanger. Turbulence-promoting devices, such as ring dimples (uniform small contractions in tube diameter occuring at regular intervals along the tube), may be used to ensure good flow distribution and to improve heat exchanger shape.

For external heat transfer surfaces, the tubes are arranged so that they give staggered rows for two reasons: (1) The staggered-tube rows create high turbulence in the fluid flowing over them, which results in a large heat transfer coefficient for a given requirement; and (2), The turbulent mixing of the fluid flowing over the offset tubes eliminates cold stagnant areas associated with the in-line configuration. Thus, the possibility of freezing is reduced when the staggered-tube configuration is used.

Extended surfaces may be added to the outside of the tubes by using fins; however, these fins can introduce large temperature gradients which could result in freezing temperatures at the hot fin root. Furthermore, tightly spaced fins provide quasi-stagnation zones and would act as points of initial freezing on the warm fluid side. When freezing occurs in finned tubes, an unstable situation exists whereby the loss of hot-side extended

surface area from frozen fluid build-up sufficiently reduces the wall temperature and promotes an additional loss of the effective heat transfer area. This can cause substantial reductions in overall heat transfer performance, as well as sharp increases in the hot-fluid pressure drop.

TRADEOFF STUDY FOR PLATE-FIN, CROSS-COUNTERFLOW HEAT EXCHANGER

The first candidate design, shown in Figure 6-1, was investigated over the range of variables listed in Table 6-1. The heat load was assumed at its maximum value of 60,000 Btu/hr. Hot fluid flow rate, inlet and outlet temperatures were held constant during this tradeoff while the allowable pressure drop ΔP_H was varied between 1 and 5 psi. The hydrogen inlet temperature and pressure were held constant. The cryogen side effectiveness and the cryogen pressure drop were varied from 0.3 to 0.9 and 1 to 10 psi, respectively.

For every set of design variables, such as cold side effectiveness E_c, ΔP_H, and ΔP_c the heat exchanger was optimized and a specific design was selected using AiResearch Computer Program H0480A (gas to liquid multi-pass cross-counterflow plate-fin design). For every heat transfer surface combination specified, the program optimizes the heat exchanger within the specified design variables and prints out several possible solutions. The optimum heat exchanger was considered to be the lightest which would maintain practicability and reasonable dimensions. All heat exchangers selected had approximately the same thermal conductance ratio ϕ. The value of ϕ was selected high enough so that when hydrogen inlet temperature falls to -417°F, the warm fluid will not freeze.

Typical results of this design procedure are shown in Figure 6-3. The heat exchanger core weight is shown vs the hydrogen effectiveness for various hot fluid pressure drops (ΔP_H). The hydrogen side pressure drop (ΔP_c) was fixed in this case at 1 psi. All pressure drops are for the core only and do not include pressure drops in manifolds, ducts, and control valves.

Raising the cold side allowable core pressure drop ΔP_c, introduced restrictions on the design due to the increase in heat transfer effectiveness on the cold side. This required an increase in hot side heat transfer to maintain the conductance ratio at the desired value and, consequently, resulted in unreasonable core shape and weight penalty. The only advantage in raising ΔP_c is to eliminate flow instability during the two-phase mode of operation. This flow instability can be eliminated, however, by imposing a pressure drop in the hydrogen path by such means as orificing the hydrogen flow passages.

The most important tradeoff parameter in the heat sink system is the weight of hydrogen required to meet the heat load profile. This depends on the heat exchanger cryogen side effectiveness, hydrogen inlet temperature, and period of operation. Figures 6-4, 6-5, and 6-6 show the total hydrogen consumed vs hydrogen inlet temperature after 2, 4, and 6 hrs of operation, respectively. The hydrogen side effectiveness is varied in these figures between 0.3 and 0.9. The heat load was fixed at its maximum value during

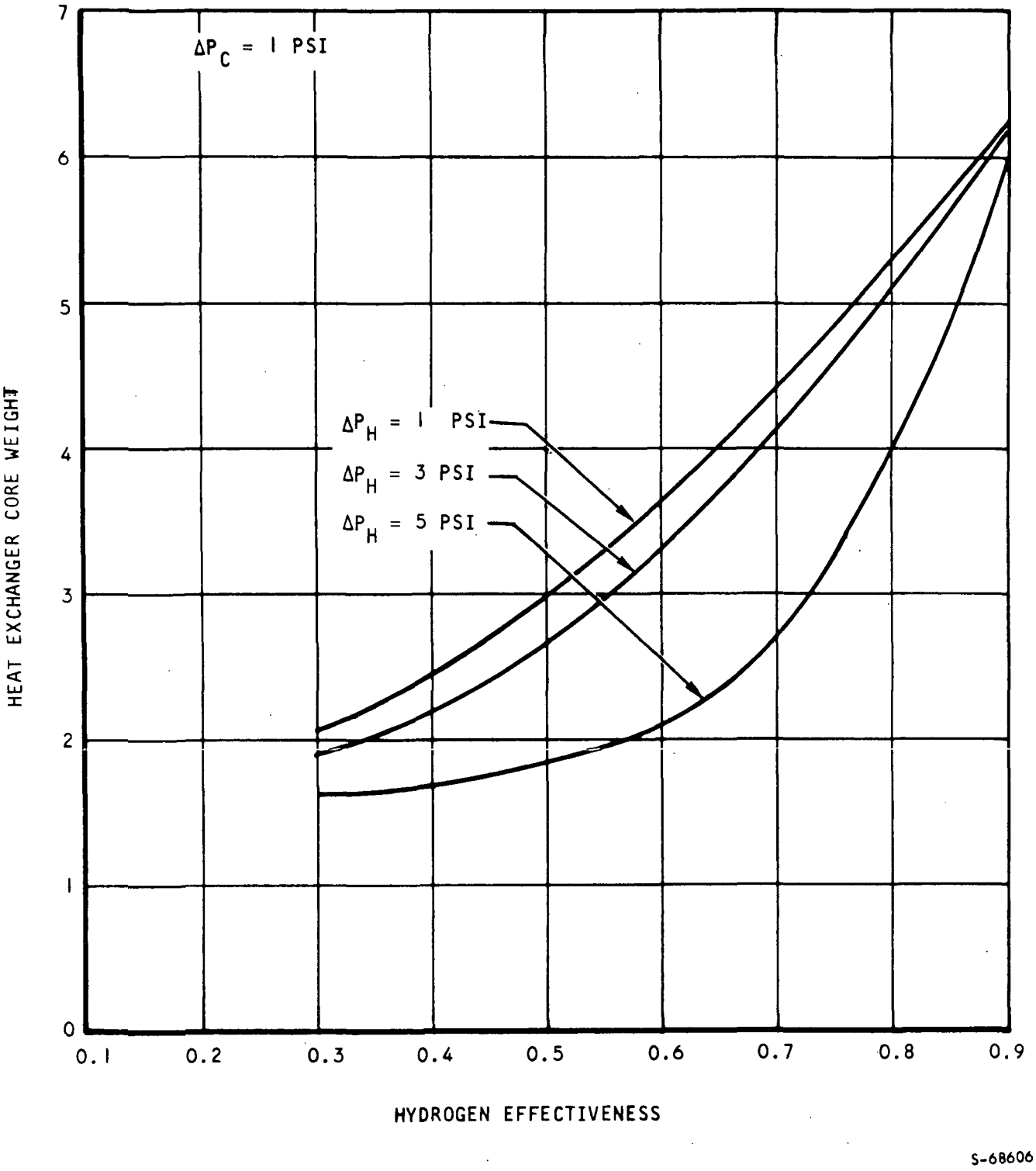

Figure 6-3. Influence of Hydrogen Effectiveness on Heat Exchanger Core Weight - Design Conditions Are Listed in Table 6-1

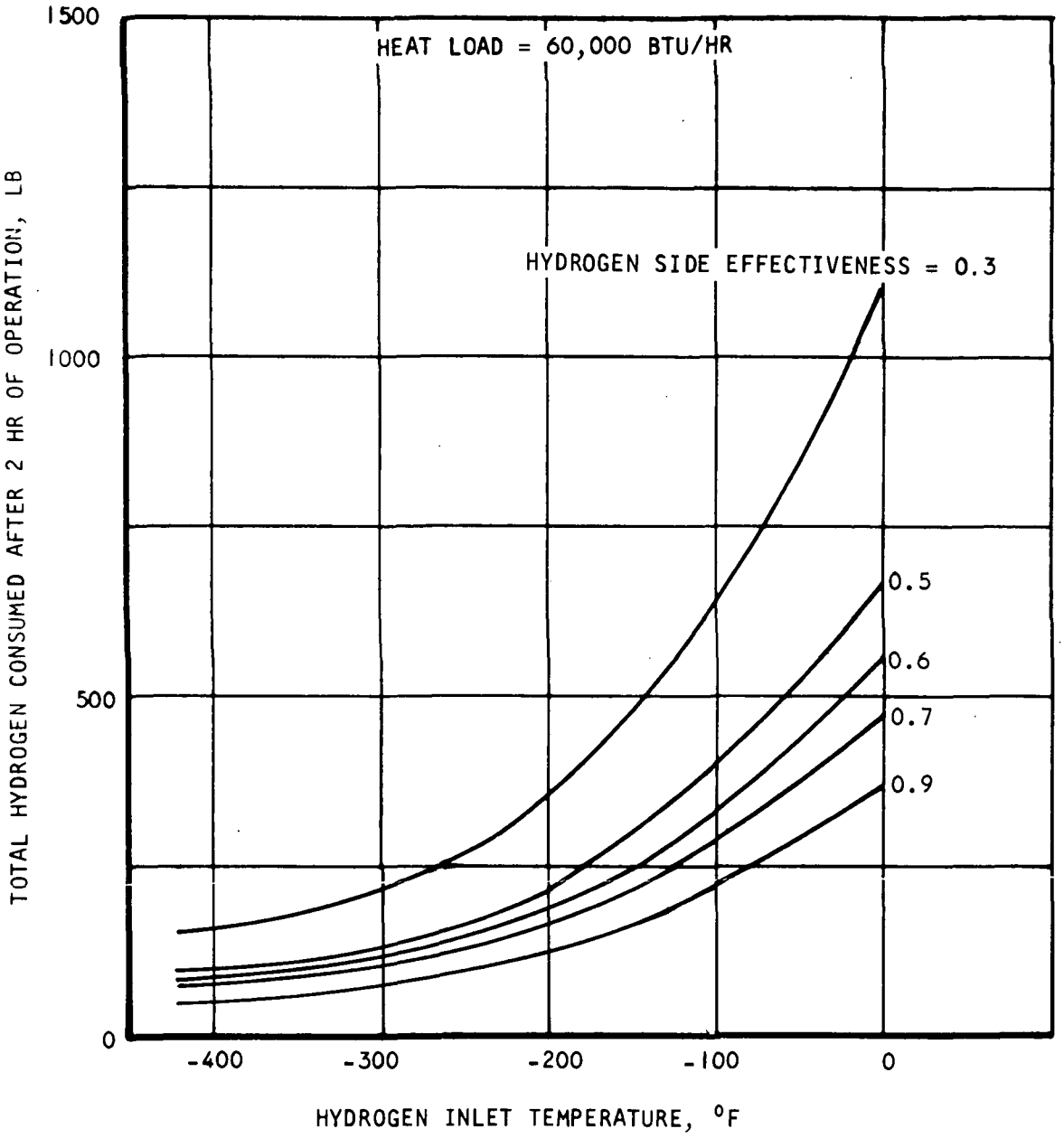

S-68608-A

Figure 6-4. Weight of Hydrogen Consumed During 2 Hr of Operation vs Hydrogen Inlet Temperature and Hydrogen Effectiveness

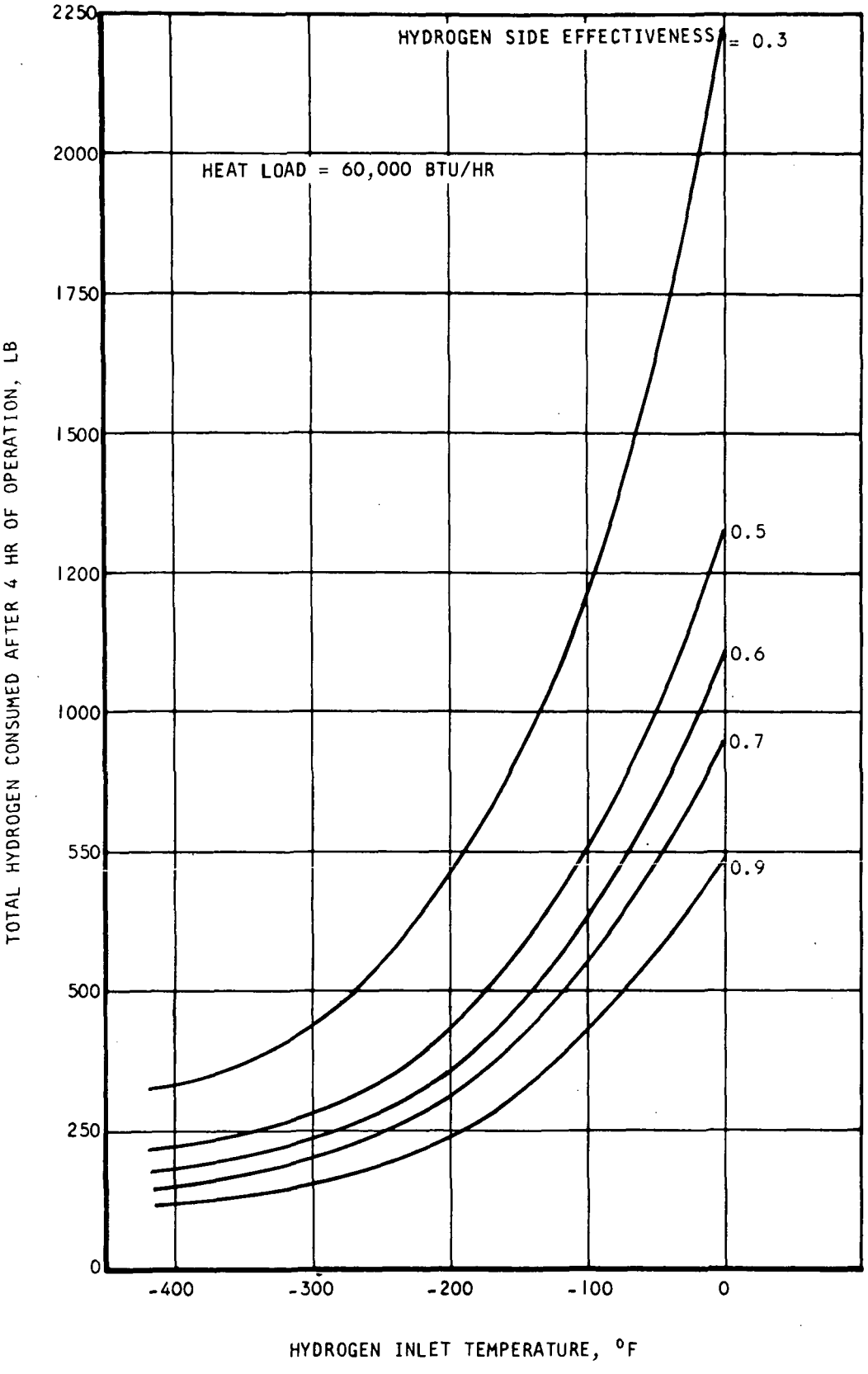

S-68609 -A

Figure 6-5. **Weight of Hydrogen Consumed During 4 Hr of Operation vs Hydrogen Inlet Temperature and Hydrogen Effectiveness**

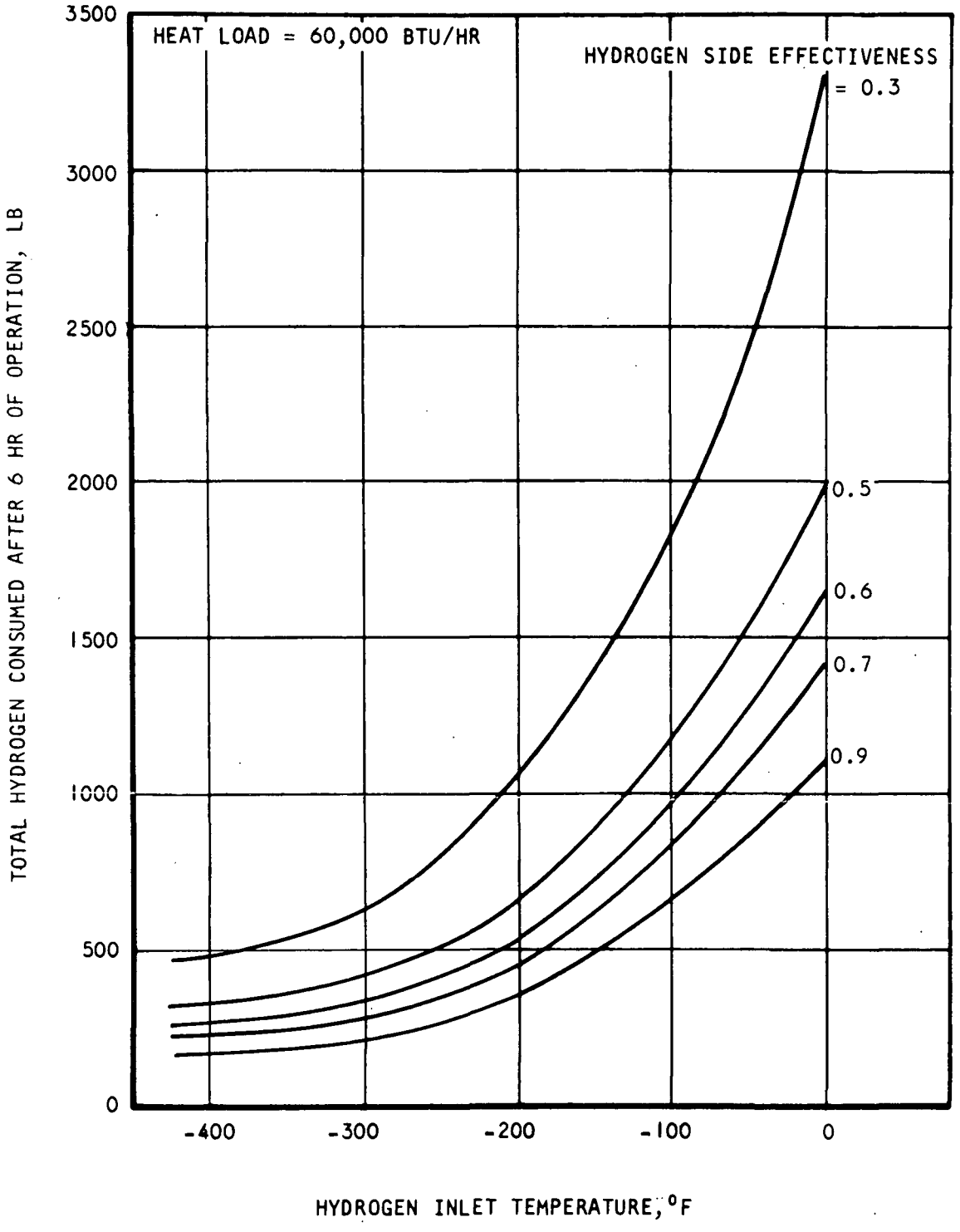

Figure 6-6. Weight of Hydrogen Consumed During 6 Hr of Operation vs Hydrogen Inlet Temperature and Hydrogen Effectiveness

the entire period of operation which was shown under the interfaces definition to be a reasonable assumption.

Figures 6-3 through 6-6 demonstrate that as hydrogen side effectiveness E_c increases, the heat exchanger weight increases, and the weight of the hydrogen consumed decreases. This behavior is further demonstrated in Figure 6-7 which shows the total weight vs E_c. The total weight consists of the hydrogen weight, penalties attached to hydrogen weight, heat exchanger core weight, and penalties attached to hot fluid pressure drop. The weight of the last item is very small. A period of operation of 4 hr was considered which represents an average value on the basis of Table 4-1.

Figure 6-7 shows the importance of a high E_c in reducing the total weight. The results also demonstrate that the heat exchanger core weight is small compared to the total weight and, hence, weight optimization of the core weight, at least in this particular heat exchanger design, is of secondary importance. Obviously, for longer period of operation or for other cryogens such as oxygen the contribution of the heat exchanger weight to the total weight would become even less important.

TRADEOFF STUDY FOR TUBULAR, CROSS-COUNTERFLOW HEAT EXCHANGER

The second candidate design, shown in Figure 6-2a, was investigated over a range of variables listed in Table 6-1. The same procedure, described for the plate-fin cross-counterflow design, was used in this case to select optimum heat exchanger designs. The heat load was assumed at the maximum value of 60,000 Btu/hr. Hot fluid flow rate, inlet and outlet temperatures were held constant during this tradeoff while the allowable pressure drop ΔP_H was varied between 1 and 5 psi. The hydrogen inlet pressure and temperature were held constant while the hydrogen side effectiveness and pressure drop varied from 0.3 to 0.95 and 1 to 10 psi, respectively.

Other design variables investigated during this tradeoff study were

- Tube diameter
- Tube wall thickness
- Heat exchanger material
- Tube arrangement and spacing
- Finned tubes
- Plain tubes versus tubes with ring dimples
- Number of passes

Various tube sizes were investigated. It was found that a lighter and

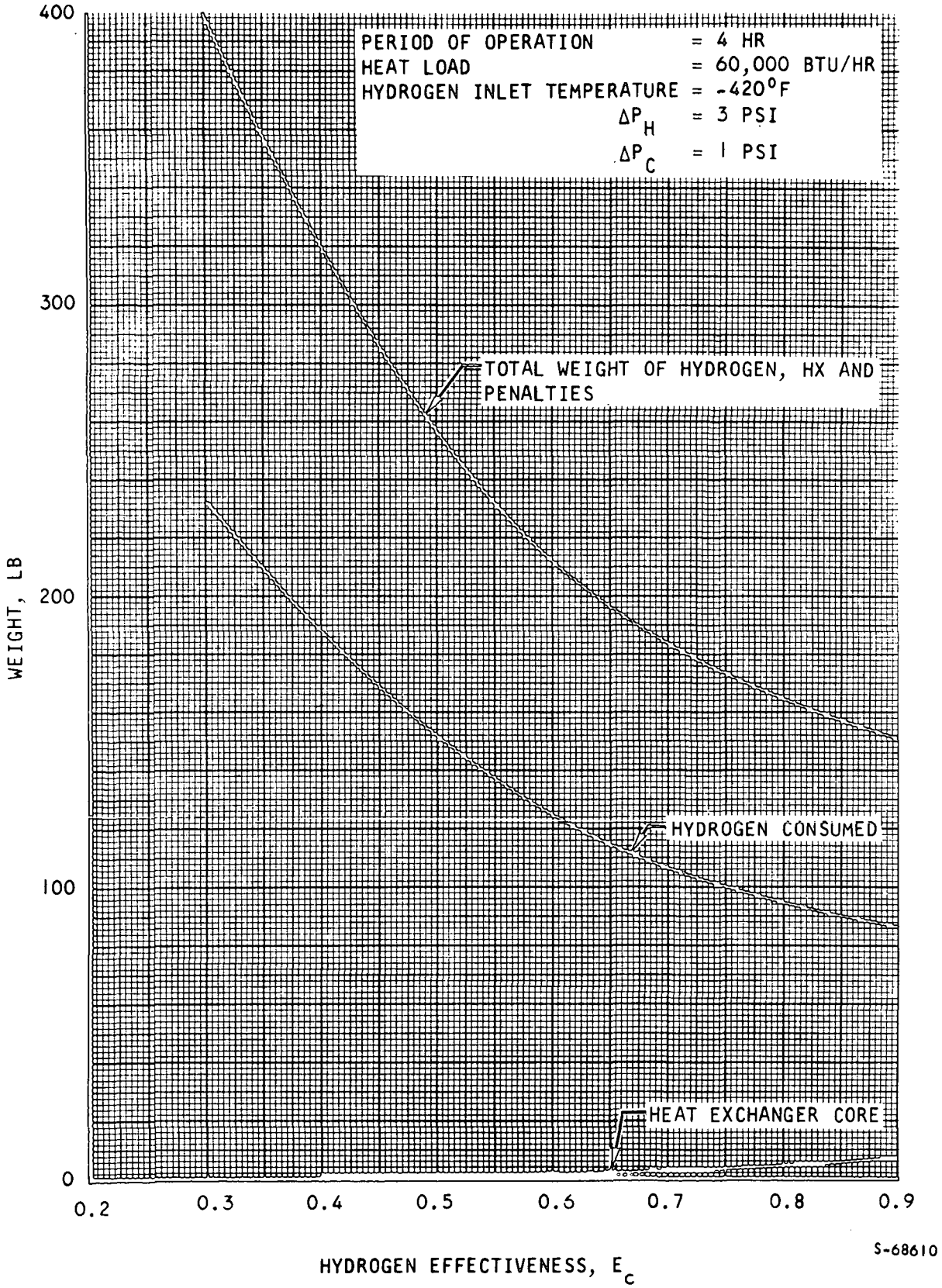

Figure 6-7. Influence of Hydrogen Effectiveness on Total Weight

more packagable heat exchanger is obtained with smaller inner tube diameters. Hence, the tube ID was fixed by manufacturing considerations to be about 0.084-in. The tube wall thickness depends on the material of construction as well as on the operating pressure. The pressure inside the tubes correspond to that in the subcritical cryogenic tanks which is below 100 psia for both oxygen and hydrogen. For stainless steel the wall thickness is limited by minimum guages to 0.006 to 0.008-in. and for aluminum the wall thickness was taken as 0.02-in. The tube OD is 0.125-in. for aluminum and 0.1-in. for stainless steel.

Both aluminum and stainless steel were considered as heat exchanger materials in the tradeoff study.

A staggered-equilateral tube arrangement was selected for two reasons: (1) The staggered-tube rows create high turbulence in the fluid flowing over them, which results in a large heat transfer coefficient for a given pressure drop and thus a small heat transfer matrix for a given requirement. (2) The turbulent mixing of the fluid flowing over the offset tubes eliminates cold stagnant areas associated with the in-line configuration. Thus, the possibility of freezing is reduced when the staggered-tube configuration is used.

A very tight tube transverse pitch was found to be favorable from the heat exchanger weight and freezing standpoints. Hence, the tube spacing was limited by fabrication capabilities to about 0.020-in.

Extended surfaces were added to the outside of the tubes by using fins of different configurations. These fins, however, can be added only to tube diameters of not less than 0.25-in. The increase in heat transfer on the warm fluid side is overshadowed by the weight increase resulting from a large tube ID with the net result of a weight penalty. Consequently, this tube configuration was dropped from further consideration during the tradeoff study.

For every set of design variables, such as cold side effectiveness E_c, ΔP_H and ΔP_c the heat exchanger was optimized using various configurations of ring dimples, plain tubes and various numbers of passes. A specific design was then selected which was the minimum weight and the same thermal conductance ratio ϕ. The value of ϕ was selected high enough so that when hydrogen inlet temperature drops to -417°F the tube wall temperature remains above -190°F. This procedure was carried out using AiResearch Computer Program H0414 (gas to liquid multipass cross-flow tubular design).

The results of this design procedure are shown in Figure 6-8 for the case of aluminum. The heat exchanger core weight excluding manifolds and ducts is shown versus the hydrogen side effectiveness for various hot fluid pressure drops. The hydrogen side pressure drop ΔP_c was fixed a 1 psi. All pressure drops are for the core only and do not include pressure drops in manifolds, ducts, and control valves.

The effect of the allowable cryogen pressure drop is shown in Figure 6-9 for the aluminum case and for a hot side pressure drop of 3 psi. An increase

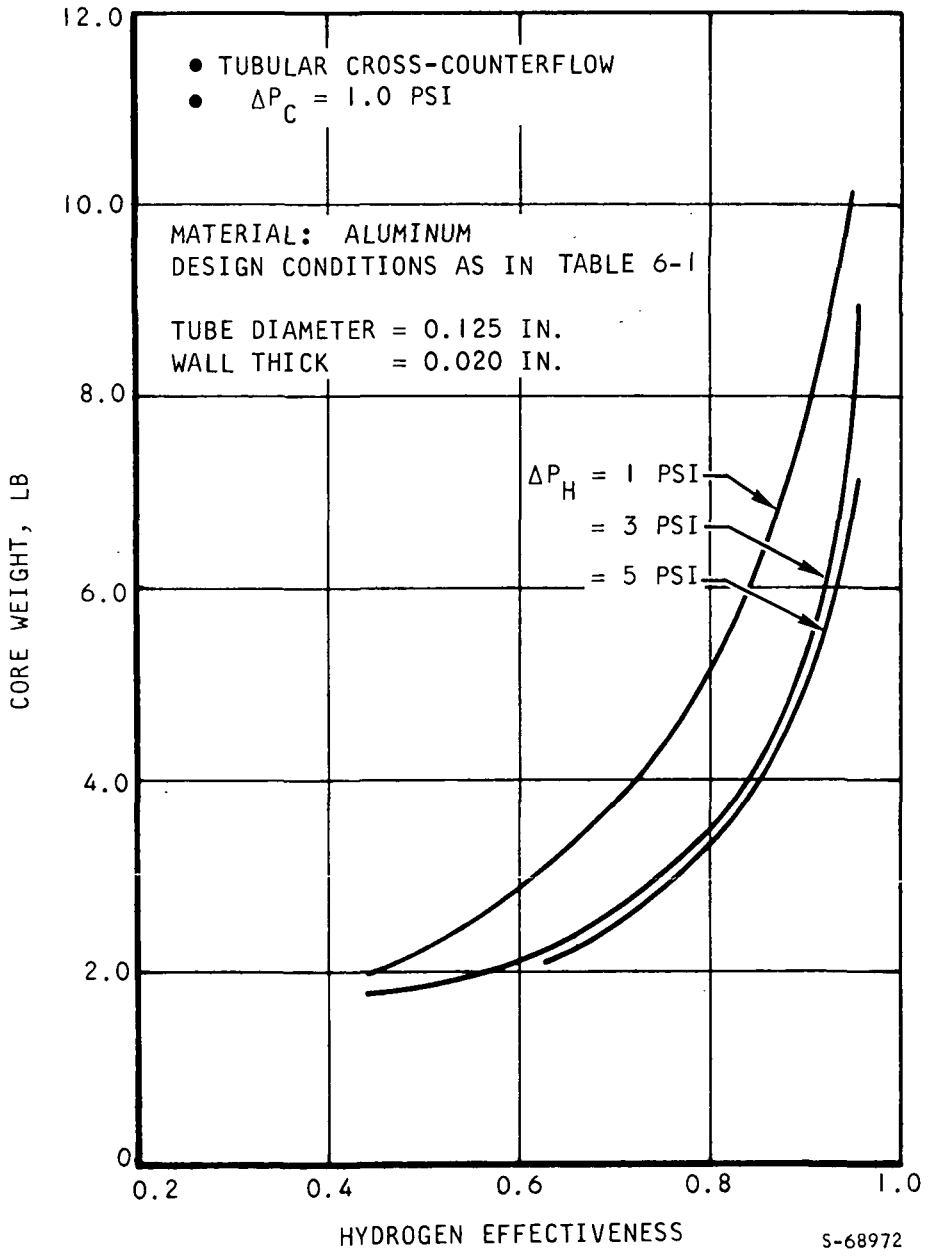

Figure 6-8. Influence of Hydrogen Effectiveness on Heat Exchanger Core Weight

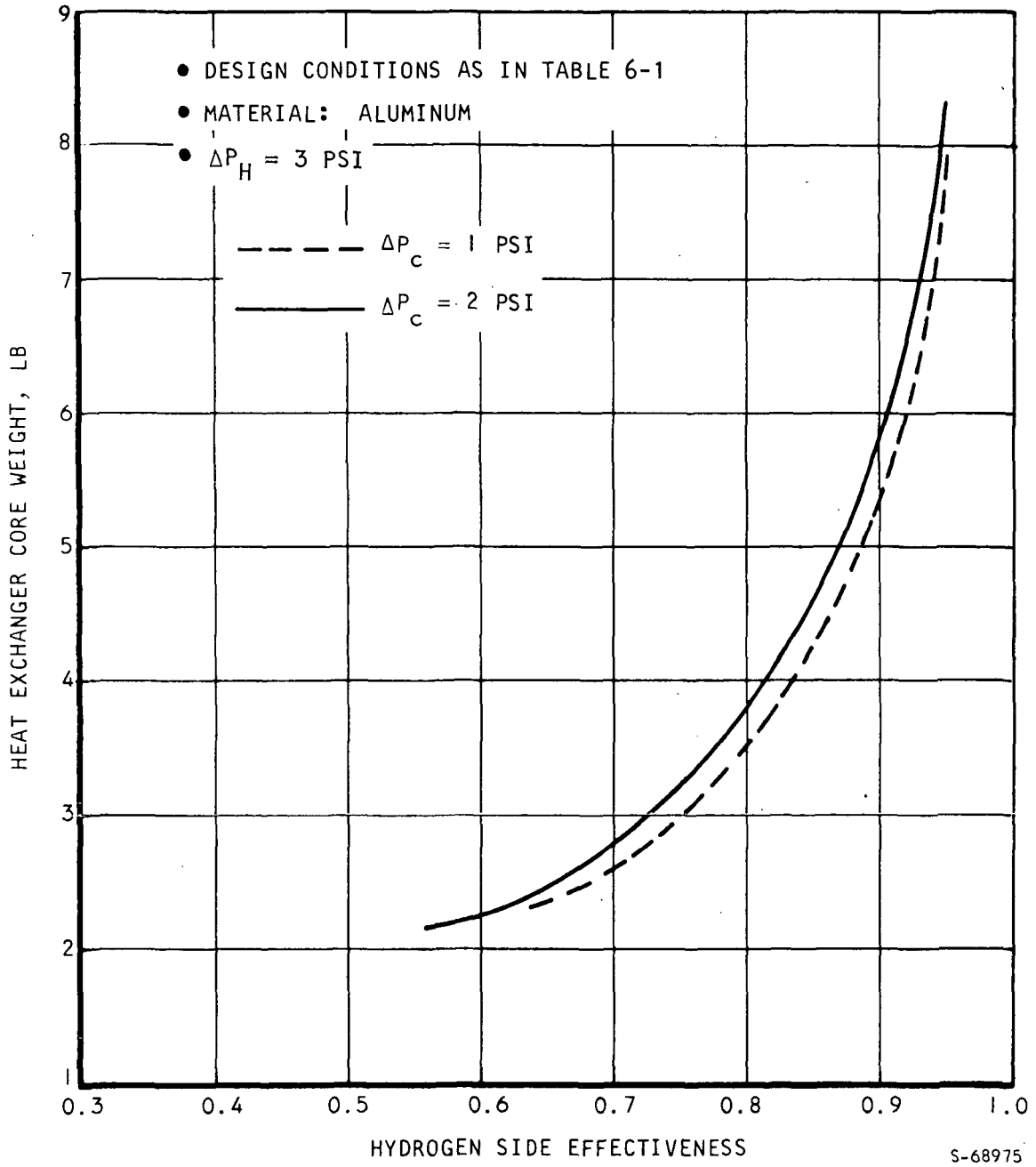

Figure 6-9. Effect of Cryogen Core Pressure Drop on Heat Exchanger Weight

in the allowable ΔP_c results in a slight weight penalty. This is due to the increase in heat transfer on the cryogen side and the necessary increase in hot side heat transfer to maintain the thermal conductance ratio at the desired level. On the other hand, a high core pressure drop on the cryogen side relative to manifold pressure drop is necessary to ensure uniform flow distribution in the core. A slight weight penalty may be necessary to achieve this purpose. The limiting factor in this case is the core shape which starts becoming unreasonable as ΔP_c gets larger.

The effect of the heat exchanger material is depicted in Figure 6-10 for ΔP_c = 1 psi and ΔP_H = 3 psi. As shown, changing the material from aluminum to stainless steel results in little change in heat exchanger core weight. This is due to the small wall thickness used in case of stainless steel. The selection of the heat exchanger material should be based on fabrication considerations.

The total weight of consumables, penalties and heat exchanger core versus hydrogen side effectiveness is shown in Figure 6-11. The case shown in this figure is for a period of operation of 4 hr, maximum heat load, and an inlet cryogen temperature of -417°F. The penalties attached to the cryogen weight include the weight of tanks, controls, etc., and was estimated before to be 1.7 lb/lb of hydrogen. The other weight penalty included in the total weight is the hot fluid pumping power which is quite small for short periods of operation. The heat exchanger weight did not include the weight of manifolds, ducts and controls which were assumed to be constant in this design tradeoff study.

Figure 6-11 demonstrates the importance of a high hydrogen side effectiveness in reducing the total weight up to E_c = 0.9. Increasing E_c beyond that does not result in any further decrease of the total weight; therefore, a value of E_c = 0.9 appears to be most desirable.

TRADEOFF STUDY FOR CROSS-PARALLEL FLOW HEAT EXCHANGER

This concept was shown in Figures 6-1 and 6-2. A serious limitation is imposed on this design due to the flow configuration. This limitation is described by a parameter known as the sum of effectivenesses,

$$\Sigma E < 1$$

where $$\Sigma E = E_H + E_c = \frac{(T_{H,in} - T_{H,out}) + (T_{c,out} - T_{c,in})}{T_{H,in} - T_{c,in}}$$

The value $\Sigma E = 1$ is the theoretical maximum limit of a parallel flow configuration.

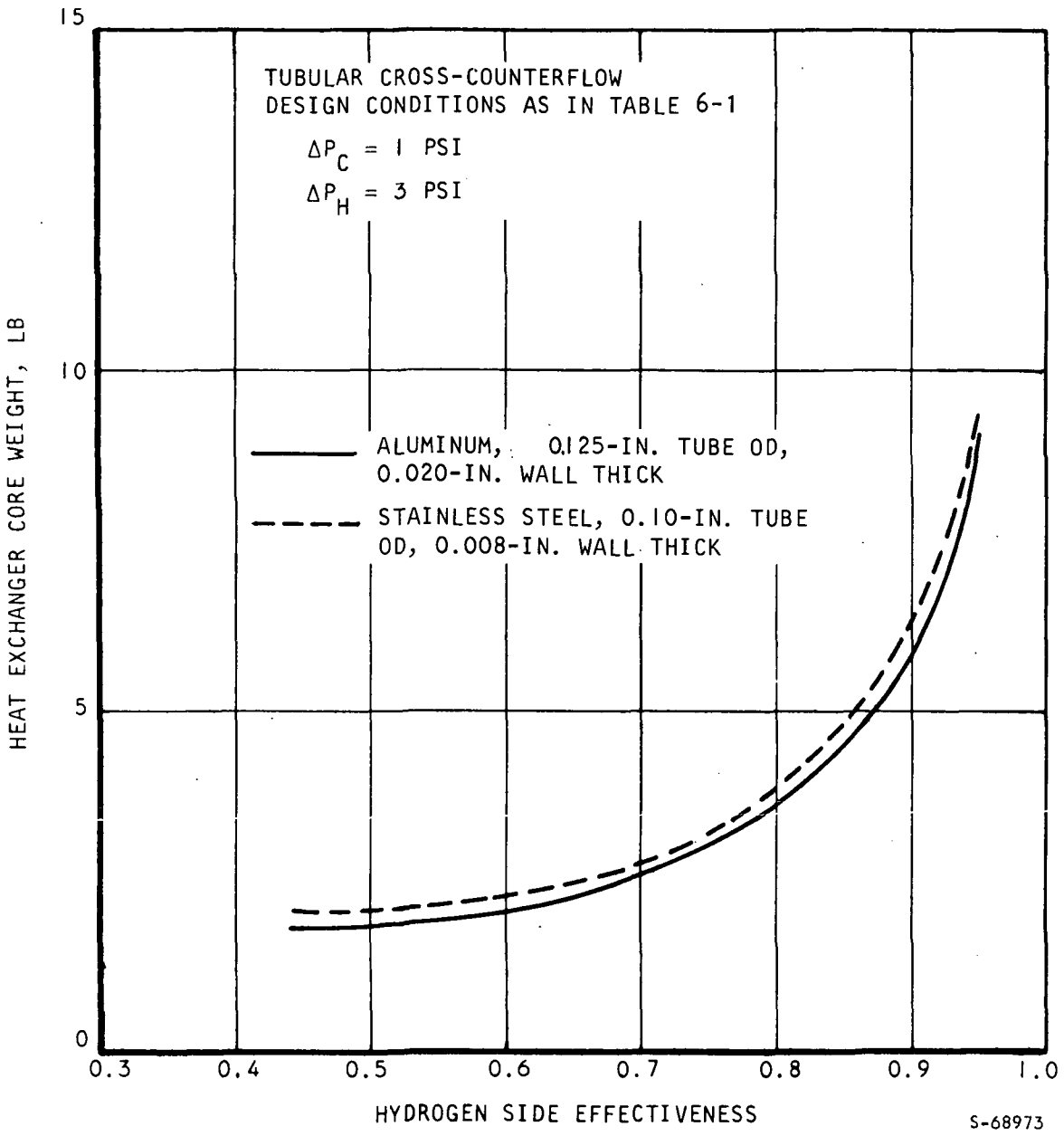

Figure 6-10. Effect of Heat Exchanger Material on Core Weight

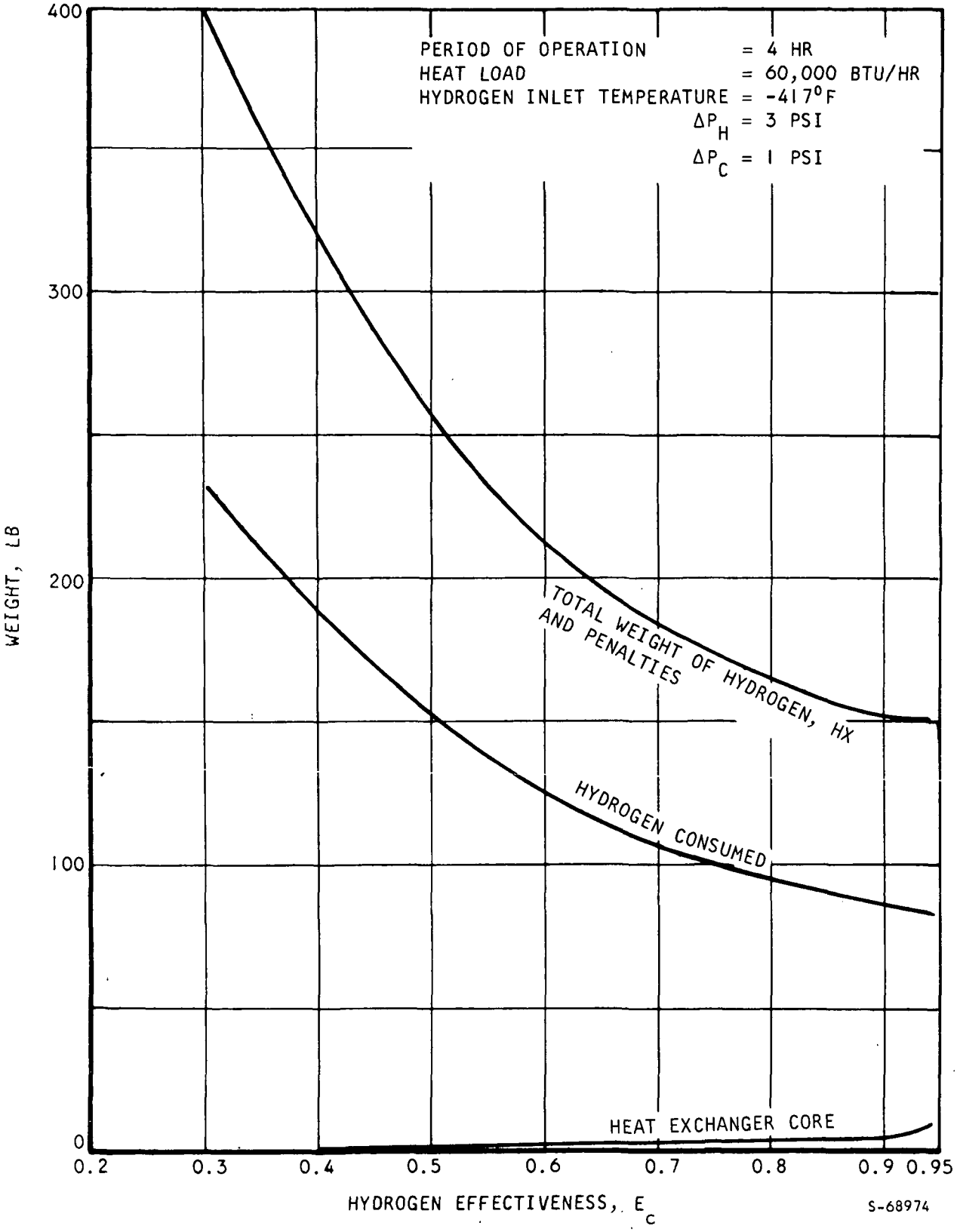

Figure 6-11. Influence of Hydrogen Effectiveness on Total Weight

Since the hot side effectiveness is fixed by the design inlet and outlet temperatures of the hot fluid as $E_H = 0.6$, the hydrogen side effectiveness has the following upper bound

$$E_c = 0.4$$

Such a low effectiveness results into the a substantial weight penalty in terms of the weight of consumables as shown in Figures 6-4, 6-5 and 6-6.

In addition to the weight penalty introduced by the limited low effectiveness there is a weight penalty associated with a cross-parallel flow design over a counterflow design. Figure 6-12 demonstrates this effect for the case of aluminum and $\Delta P_c = 1$ psi and $\Delta P_H = 3$ psi. At $E_c = 0.35$ the weight of the cross-parallel flow heat exchanger is almost twice that of the cross-counter flow. This difference becomes much more pronounced at higher effectivenesses if they were thermodynamically possible.

The only advantage of a cross-parallel flow design over a cross-counter flow design is in less susceptibility to freezing in the heat exchanger portions close to the cryogen inlet, since the hot fluid is at a relatively higher temperature in this case. This, however, did not present any severe problems in the cross-counter flow designs presented in the previous sections, and a cross-parallel flow design cannot be justified in the present case.

SUMMARY OF THE TRADEOFF STUDY

On the basis of the tradeoff study, several conclusions can be made. These conclusions are summarized below.

1. The weight of consumables, consisting of the cryogen weight and the weight of penalties attached to the cryogen weight, is quite substantial.

2. The heat exchanger weight is a very small fraction of the total weight.

3. It is essential to design a heat exchanger with a high cryogen side effectiveness to minimize the weight of cryogen used.

4. Increasing the cryogen side effectiveness beyond 0.9 does not result in any weight saving, and hence an effectiveness of 0.9 is selected.

5. A multipass cross-counterflow arrangement with the hot fluid making several cross flow passes is the best arrangement.

6. Both plate-fin and shell and tube designs are capable of meeting the desired performance.

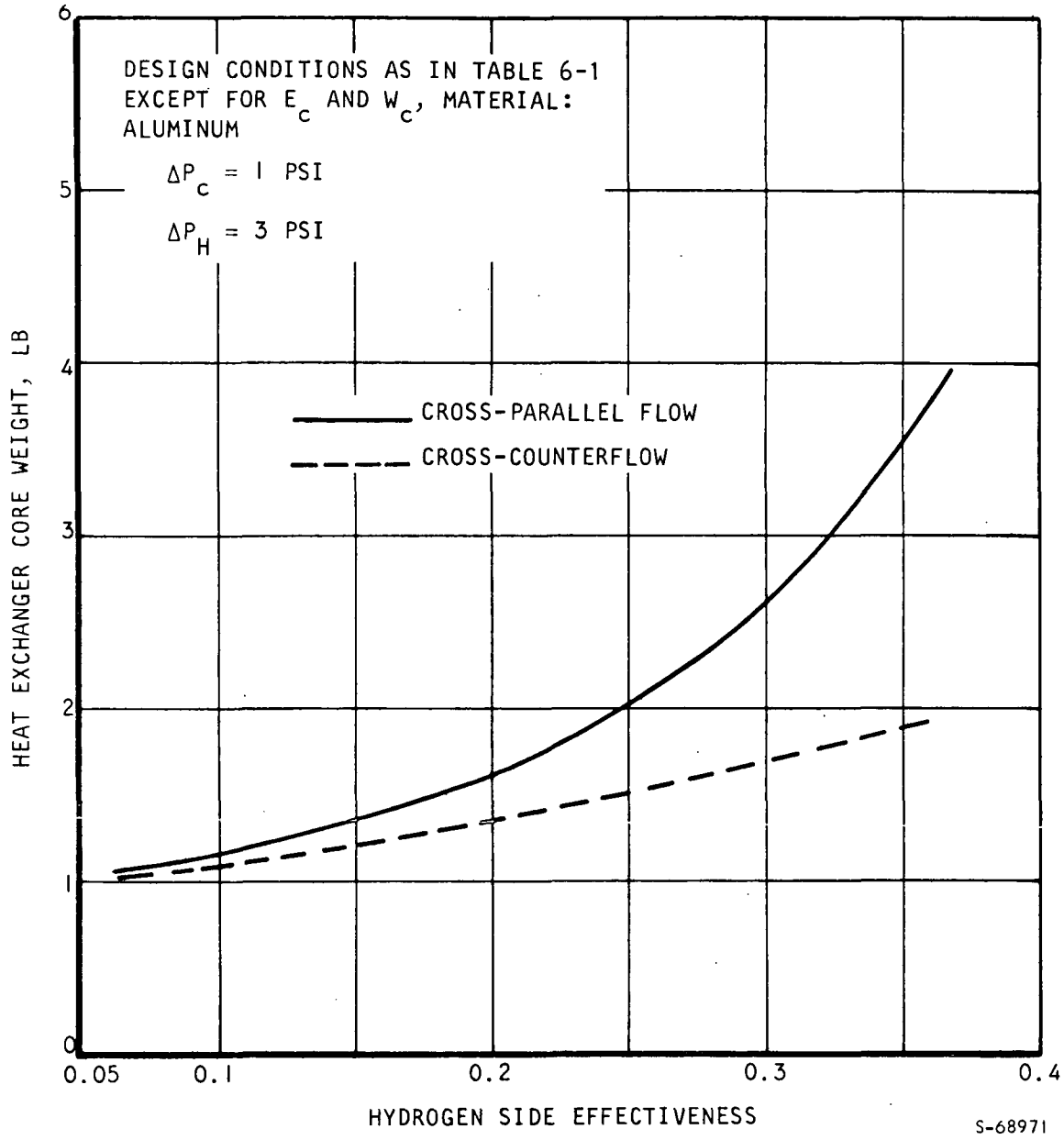

Figure 6-12. Effect of Flow Configuration on Heat Exchanger Weight

7. The plate-fin design consists of compact offset fins on the hot fluid side for effective heat transfer and of loose plain rectangular or triangular fins on the cryogen side.

8. The tubular design consists of straight dimpled tubes with the smallest possible inner diameter. No fins are added on the hot fluid side.

9. Both aluminum and stainless steel can be used in the tubular design with little difference in the heat exchanger weight.

10. An increase in the warm fluid allowable pressure drop in the core results in a slight saving of the heat exchanger weight; a value of ΔP_H = 3 psi appears to be reasonable to allow 2 psi for the pressure drop in ducts, manifolds, etc.

11. Increasing the allowable pressure drop on the cryogen side results in small penalty due to the minimum desired value of ϕ. On the other hand, a high ΔP_c is desirable to ensure flow distribution and flow stability.

12. Although the tradeoff study was carried out using hydrogen as the heat sink fluid, the same conclusions hold for the case of oxygen. On the other hand, an optimum heat exchanger design for hydrogen is not optimum for oxygen. The amount of oxygen required for the present heat load removal is substantially larger than that shown in Figures 6-4 to 6-6 for hydrogen. For example, for 4 hr of operation the minimum amount of hydrogen needed is shown in Figure 6-5 to be 125 lb. If liquid oxygen is used about 1800 lb would be required.

SECTION 7

CONTROL SYSTEM TRADEOFF STUDY

A control system is required to provide the flow control of cryogen to the cryogenic heat exchanger to satisfy the heat rejection requirements of the ECS coolant loop. The control system must also maintain a fixed temperature of the ECS coolant returning to the ECS heat sources.

GENERAL APPROACHES TO CONTROL SYSTEM

Requirements for control of the cryogenic heat exchanger are shown in Figure 7-1. The figure shows that the coolant flow rate in the ECS subsystem is constant, and the inlet temperature to the heat exchanger changes according to the total heat rejection required. The initial conditions of the cryogen vary over wide ranges including liquid, subcooled liquid and vapor states, and vapor at temperatures ranging from saturated liquid to $0^{\circ}F$. The control system must therefore provide for the variables of cryogen heat capacity and the ECS heat rejection required.

An important operational requirement, not shown in Figure 7-1, is the operating back pressure on the cryogen side of the heat exchanger. It is assumed that the heat exchanger will be operated at any altitude from sea level to orbit; therefore, the back pressure on the cold side of the heat exchanger may vary from approximately 14.7 psia to nearly zero psia. This variation in back pressure must be considered in the selection of the control components to achieve the desired cryogen flow rates.

The principal elements of prospective control systems include a sensing element to determine temperature of the ECS coolant, a controller which provides logic for cryogen flow control, and the cryogen flow control valve. Figure 7-2 presents 12 control systems arrangements which have been synthesized to show application and allow comparison of advantages and disadvantages of each. The approaches presented are not all-inclusive, but rather show representative equipment arrangements which are candidates for this application. The arrangement of these functional elements, and the integration with the heat exchanger, is the subject of the discussions in the paragraphs that follow.

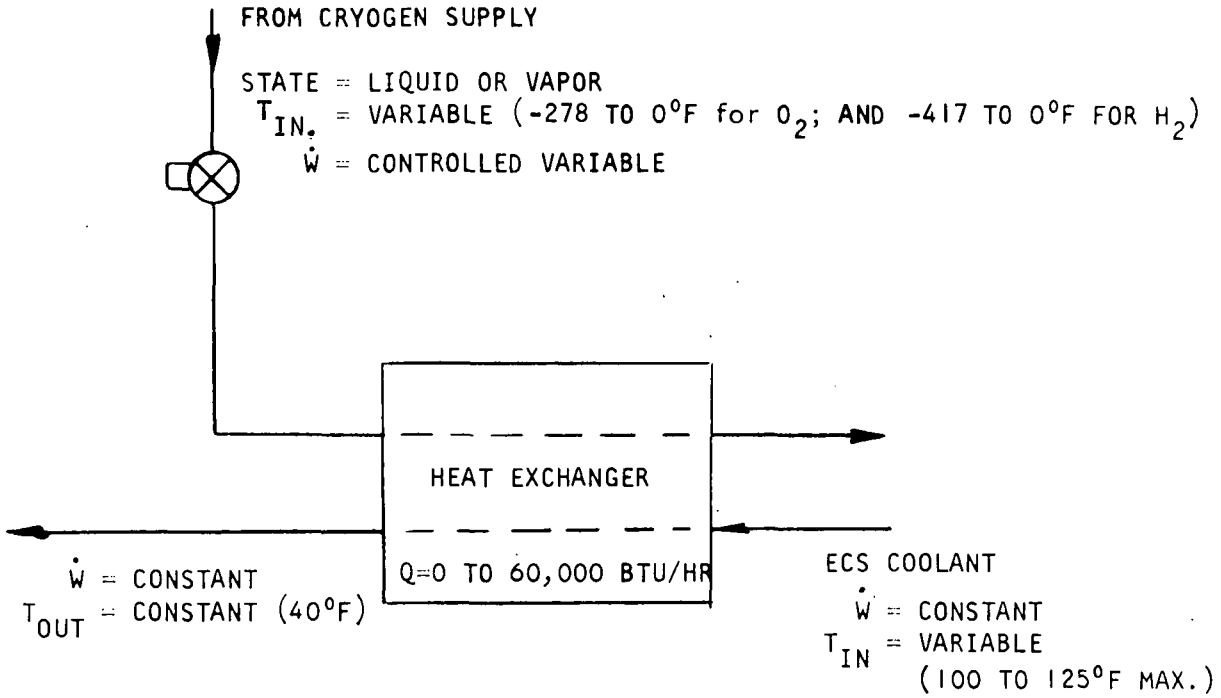

HEAT EXCHANGER PRESSURE DROP

- COLD SIDE: 1 TO 5 PSID GOAL
- HOT SIDE: 1 TO 10 PSID

TRANSIENT VARIATIONS

- 20 SEC RAMP IN ECS COOLANT HEAT LOAD
- 20 SEC RAMP IN CRYOGEN INLET TEMPERATURE TO BE CONSIDERED

CRYOGEN SOURCES

- SUBCRITICAL PROPELLANT TANKS
- VENT GASES.
- RECIRCULATION OF CRYOGEN TO TANK WILL BE CONSIDERED

S-77515

Figure 7-1. Control Requirements

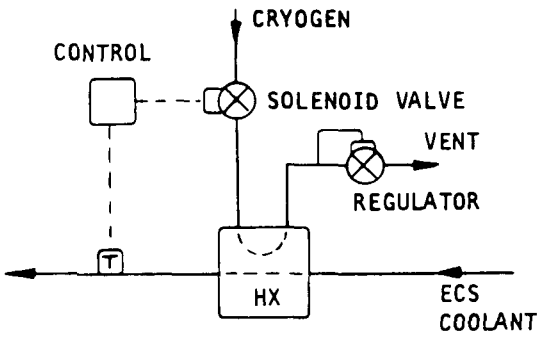

PULSED CRYOGEN FEED

A

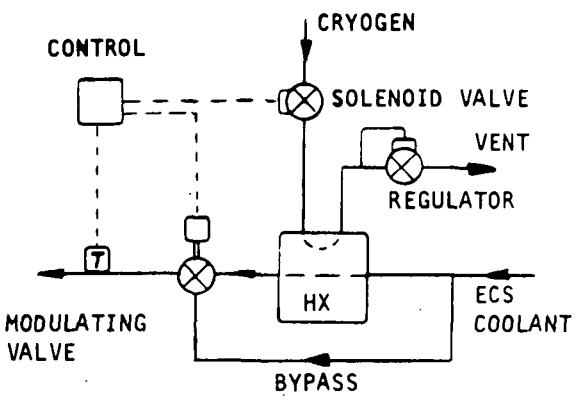

PULSED CRYOGEN FEED WITH
PROPORTIONAL HOTSIDE BYPASS

B

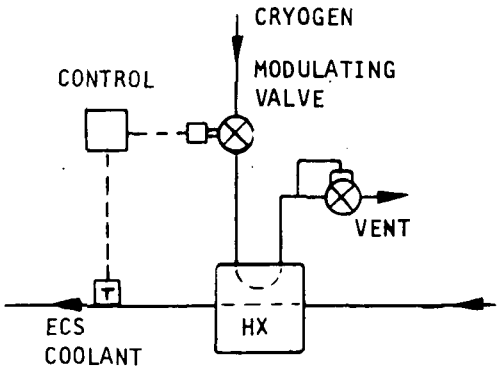

MODULATED CRYOGEN FEED CONTROL
WITH REGULATOR VENT

C

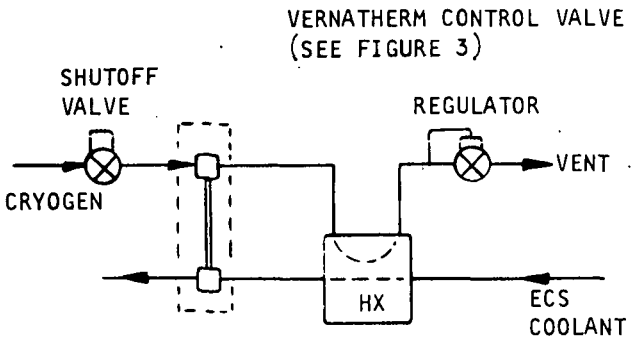

VERNATHERM MODULATION OF
CRYOGEN SUPPLY

D

S-68618

Figure 7-2. Control Approaches

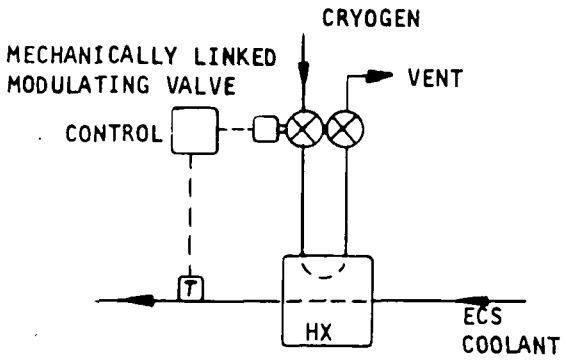

ACTIVE CONTROL WITH MECHANICALLY LINKED CRYOGEN AND VENT FLOWS

E

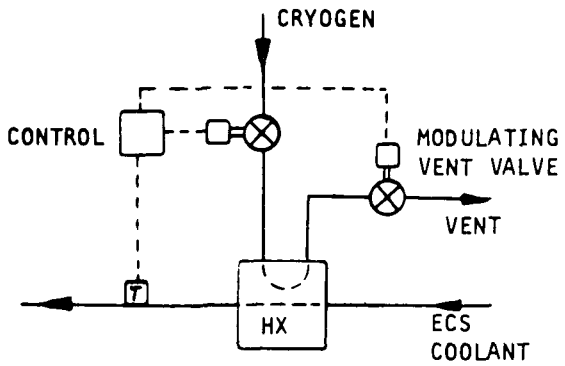

ACTIVE CONTROL WITH ELECTRICAL FLOW CONTROL OF CRYOGEN AND VENT

F

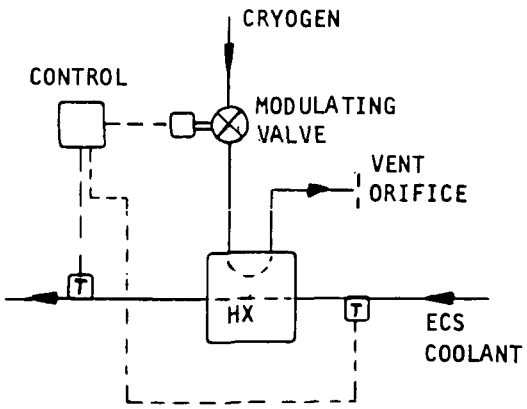

ANTICIPATING TEMPERATURE CONTROL IN ECS COOLANT

G

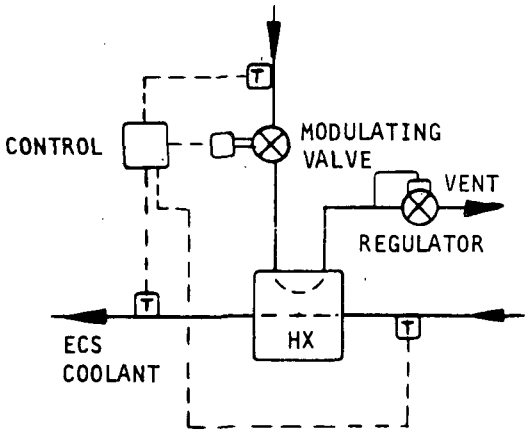

ANTICIPATING TEMPERATURE CONTROL IN CRYOGEN AND ECS FLUIDS

H

S-68619

Figure 7-2. (Continued)

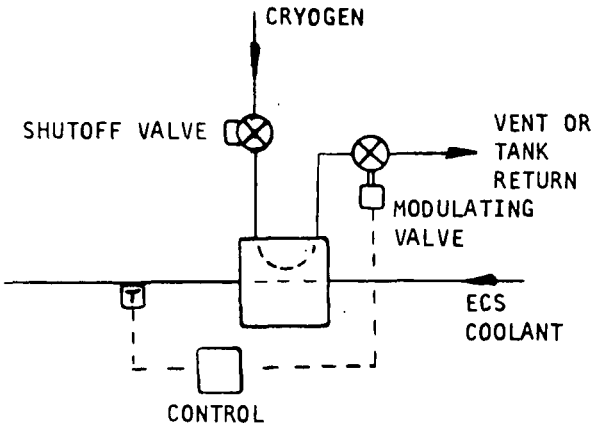

ACTIVE CRYOGEN CONTROL BY DOWN-STREAM FLOW MODULATION

I

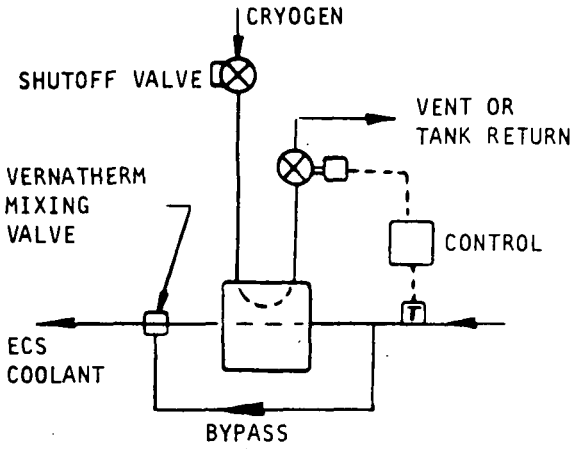

VERNATHERM CONTROLLED BYPASS AND ACTIVE CRYOGEN FLOW CONTROL

J

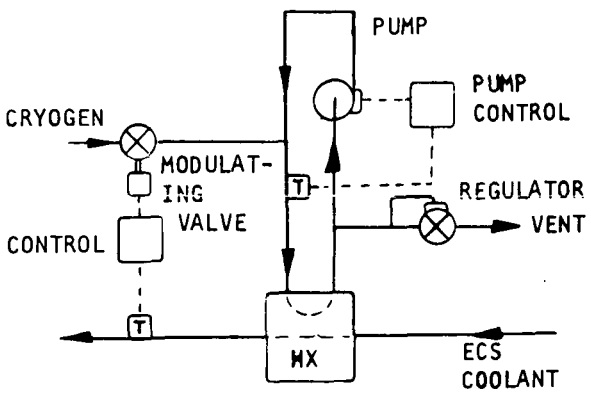

RECIRCULATING BUFFER LOOP

K

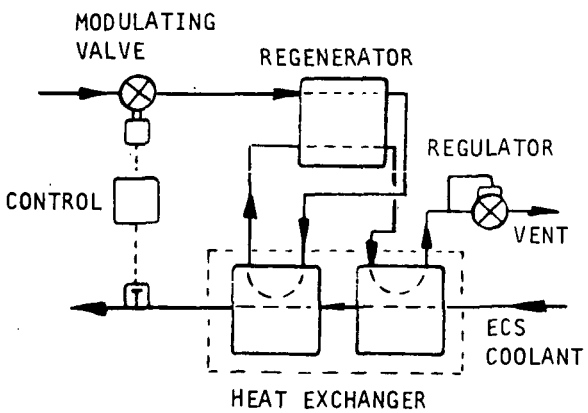

INCLUSION OF REGENERATOR INTO ACTIVE CONTROL APPROACH

L

S-68620

Figure 7-2. (Continued)

Cryogen Feed Control

Two methods are considered as principal candidates for feeding cryogen to the heat exchanger: pulsed and proportional.

Figure 7-2A shows a solenoid valve for cryogen feed control which also serves as a shutoff valve. Control of the valve could be accomplished by actuating the valve open for short pulses; the duration of the on-time and the frequency of repetition would result in a specific average value of cryogen flow. The on-time of the solenoid valve is limited by the hold-up capacity in the cold side of the heat exchanger, and the rate of required heat rejection from the ECS coolant loop. Design consideration also must be given to the resulting pressure excursion and the pulsing heat rejection capability. Thermal inertia, however, can be added to the heat exchanger at the expense of weight to minimize this consideration.

Although this approach may provide a relatively simple design, the valve life may be limited due to the number of operational cycles experienced in a shuttle application where service life of 10 years is desired.

Figure 7-2B presents an approach that offers improved temperature control of the ECS coolant when pulsed cryogen feed control is used. Here the ECS coolant is bypassed around the heat exchanger when the outlet temperature is lower than the desired value, and mixed with the heat exchanger outlet fluid. The improved temperature control is achieved by reducing the ECS coolant flow through the heat exchanger at the exact time when the ECS coolant is the coldest, and, therefore, tends to increase the freezing problem of cryogenically cooled heat exchangers.

Figure 7-2C shows a method of providing cryogen feed control using a modulating valve. This approach provides a continuously variable feed rate of cryogen to the heat exchanger in response to the cooling requirements. The schematic illustrates, by comparison with Figure 7-2B, that a single feed control valve provides the necessary control in a smooth and continuous manner, and that the freezing problem of the ECS coolant is reduced by eliminating the bypass. This control is identical to that of Figure 7-2A except for valve type.

Proportional control of the cryogen feed is shown as the dominant method of cryogen feed in the approaches considered for the following reasons:

(a) Provides smooth transition from one flow to another to compensate for cryogen and ECS coolant variations

(b) Minimizes thermal and pressure transients

(c) Potential for improved valve life

Due to these advantages, all of the control approaches except for those depicted in Figures 7-2A and 7-2B utilize modulating valves for cryogen flow control.

Control Components

Two categories of control components were considered for the control of the cryogen supply:

(a) Mechanical vernatherm

(b) Electronic

Figure 7-2D shows the use of a vernatherm controlled cryogen flow control valve, and Figure 7-2J shows the vernatherm approach applied to bypass flow control. The bypass valve of Figure 7-2B could also be of the vernatherm type. Figure 7-3 presents a schematic of the operating principle of the flow control valve shown in Figure 7-2D. The temperature of the ECS coolant is sensed by the vernatherm element located in the ECS coolant stream. As the ECS coolant temperature rises, the element expands. Expansion occurs by converting the volumetric change of a phase-changing wax compound into a linear output. The wax-based material is selected to provide a phase change within the desired temperature range. The resultant volumetric change displaces a diaphragm which acts upon a force transfer rubber plug amplifying the diaphragm which acts upon a force transfer rubber plug amplifying the diaphragm motion. The increased linear motion is directly transmitted through the bellows seals to the cryogen flow control element. The flow control surfaces are arranged so that the cryogen flow is increased with increasing ECS coolant temperature.

Vernatherm valve control elements used either for cryogen flow control or heat exchanger bypass flow mixing control, modify flow area (CA) by sensing a change in the ECS coolant temperature. Control of ECS coolant temperature to a moment value, therefore, with zero steady state error is not possible since a change in the control temperature is required before a change in flow control is achieved. The mechanical gain of the currently available vernatherm elements is sufficient, however, to maintain the operating band within 2 to 3°F of the nominal temperature for applications where high sensed flows exist, low power for valve positioning is required and small temperature differences exist between the sensed and controlled fluids.

Disadvantages of the vernatherm valve are its relatively high time constant, seal problems in applications where one fluid is sensed and another is being controlled, and axial thermal conduction affecting the sensed temperature when high temperature differentials exist between the sensed and controlled fluids. These characteristics tend to make this type of valve applicable to the ECS coolant bypass control and not applicable to the cryogen flow control.

The electronic controls are designed to provide a specific ECS coolant temperature at the heat exchanger outlet. The ability of the electronic control to achieve a close tolerance in controlled temperature depends upon the temperature data available, the type of control logic designed into the controller, and the type of valve drive used to vary the cryogen flow.

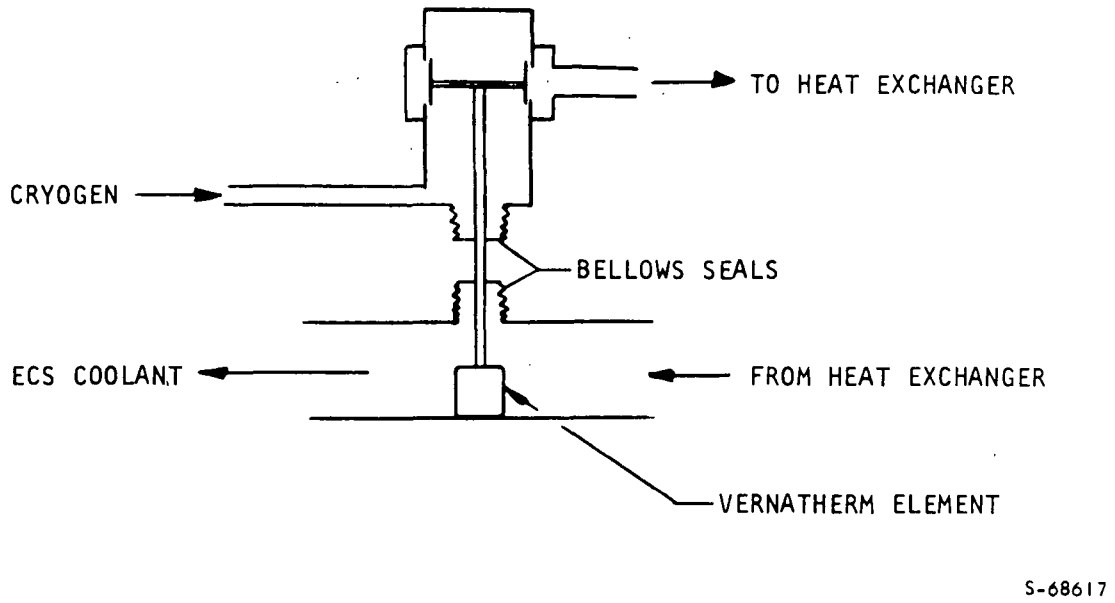

Figure 7-3. Vernatherm Control Valve

In Figure 7-4, two simplified representations of candidate control schemes and implementations are shown. In the case of Figure 7-4A, an electronic motor-actuated valve is used. This type of valve lends itself to use in an integrating control scheme. As long as the controlled temperature resides in a predetermined deadband about the setpoint, no control action occurs. If the controlled temperature departs from this deadband, the controller delivers pulse-width modulated power to the valve, driving it in the appropriate direction at a slow rate approximately proportional to the sensed error.

Figure 7-4B represents a proportional temperature control system. In this case, the valve--possibly pneumatically actuated and electronically controlled-assumes a modulated position proportional to a low-level analog electrical control signal applied to it. At sensed ECS coolant temperatures below a predetermined control band, the controller delivers zero control signal to the valve, which remains closed. At sensed temperatures above the control band, the maximum control signal is applied to the valve, and it remains fully open. At intermediate sensed temperatures within the control band, the valve control signal and the valve opening are modulated in proportion to the sensed temperature error.

The electronic control circuitry will feature those dynamic compensation networks that will result in the most desirable control system stability and dynamic response characteristics, regardless of what basic control concept and type of valve is selected.

The controls shown in Figure 7-2A and 7-2B show a method of active control of cryogen flow based on a single sensor sensing the ECS coolant heat exchanger outlet temperature. This approach can accept varying inputs of temperature in the ECS coolant and also the inlet conditions in the cryogenic stream to certain limits. This feed control concept is the simplest but its acceptability is dependent on the magnitude and dynamics of the inlet transients of ECS coolant and cryogen, and system characteristics. Variations to the single sensor control are shown in Figures 7-2E and 7-2F where the cryogen outlet vent restriction is varied in addition to control of cryogen flow.

The control systems shown in Figure 7-2G and 7-2H allow additional versatility with little added complication. The use of anticipating sensors to detect transients in either or both of the two fluid streams allows compensation of the flow control valve prior to a sensed temperature excursion in the ECS coolant outlet. The compensation network has provisions to account for the operating characteristics and thermal inertia of the heat exchanger along with the valve operating characteristics.

Electronic controls are shown on the majority of the control concepts of Figure 7-2 because of the adaptability of this approach. Versatility in meeting performance requirements, adjustability of control ranges and set points, are factors which favor the use of the electronic approach.

Maintainability of the competing approaches is also an important consideration. The basic reliability of the vernathern is higher than the

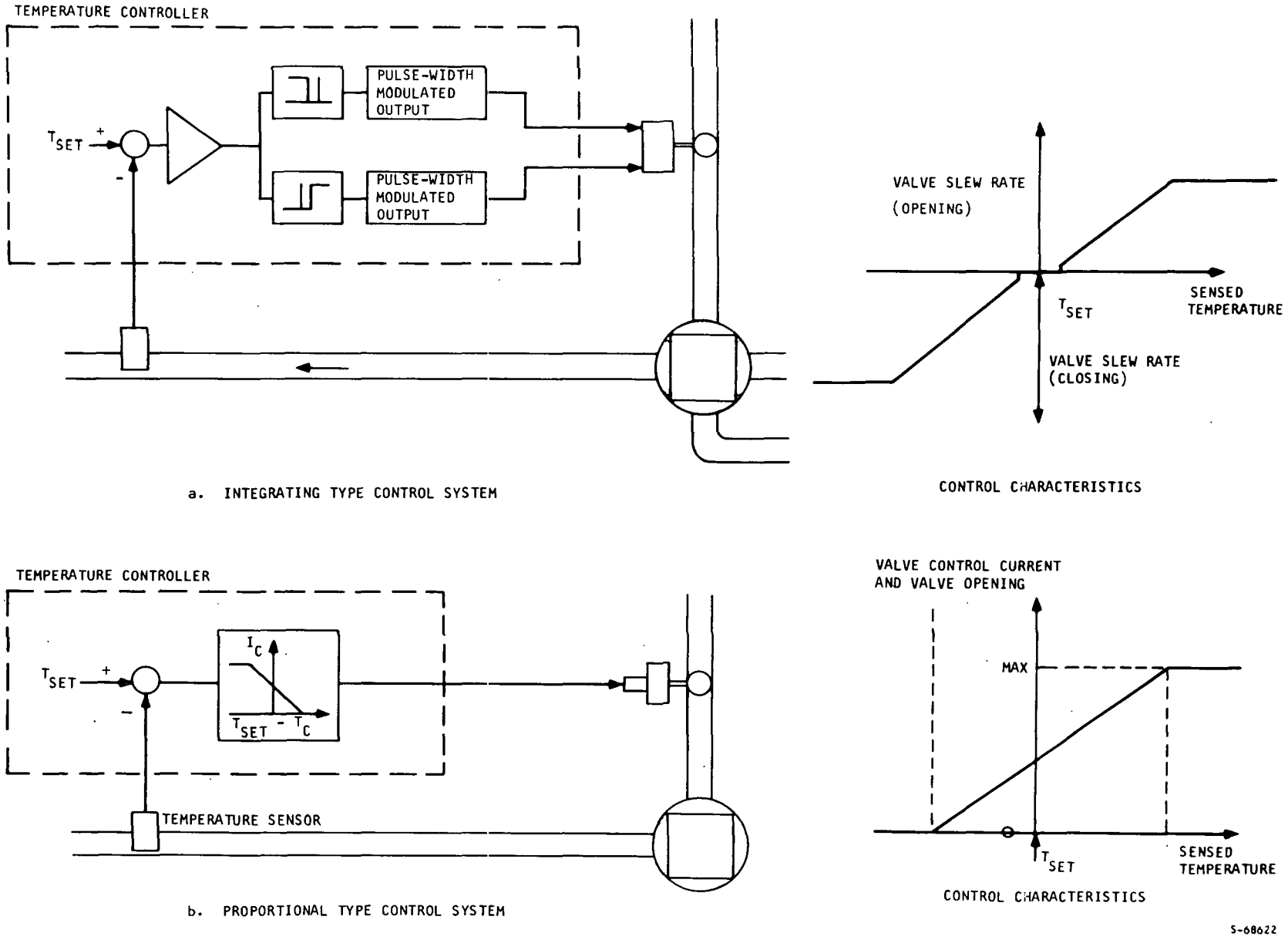

Figure 7-4. Candidate Temperature Control Systems

combination of control elements comprising an electronic control system. Failure of the vernatherm valve, however, requires the ECS coolant line to be broken and a new valve inserted in place of the failed one. This maintenance action requires time for ECS coolant system servicing as well as the normal time required for replacement of the failed valve.

Failure of a part in the electronic control system may not require violation of any part of the cryogenic or ECS fluid lines. The use of strap-on temperature sensors, or sensors inserted in wells, allows replacement of sensors without opening a fluid line. The electronic controller can be replaced by disconnecting appropriate electrical connectors, replacement of the controller and performing the necessary checkout of the unit. Valve drive motor or actuator failure may also be corrected without violating the fluid loop if the motor is connected to the valve element through an appropriate seal.

Cryogenic Vent Control

As mentioned earlier, it may be desirable to provide a fixed outlet pressure on the cold side of the heat exchanger to provide more uniform heat transfer at all conditions of altitude and cryogenic flow rate. Four types of vent control are considered in this preliminary screening study:

(a) Proportional control matched to the cryogen feed

(b) Active downstream flow control

(c) Free vent through a fixed orifice

(d) Active pressure regulator

Figures 7-2E and 7-2F show two approaches to the proportional control of the vent pressure by modulating the outlet flow to correspond to the inlet flow rate. The electrical approach shown in Figure 7-2F allows greater versatility in the matching of the valve orifice values (CA) since separate electrical compensation could be included to account for such factors as heat exchanger inlet condition changes in the cryogen, and altitude pressure.

Figure 7-2I and 7-2J show a method of providing a nearly constant cold side pressure by controlling flow to the heat exchanger by downstream valves. These valves, therefore, serve as the principal cryogen flow control, and also maintain the coldside heat exchanger cavity at a pressure approximately equal to the supply pressure of the cryogen. The shutoff in the cryogen supply provides isolation of the unit during periods of quiescence. The simplicity of the single control valve to perform basic flow control and vent back-pressure control is augmented by the limited environmental exposure of the valve. Since the valve is located in the relatively warm cryogenic outlet vapor, the environmental design requirements for the valve are significantly reduced.

Flow of subcooled cryogen through the heat exchanger and return to the tank could be accomplished using the approach shown in Figures 7-2I and 7-2J. The modulating flow control valve could be replaced with a cryogenic pump. The control of the pump could be accomplished by a speed control adjusted by temperature of the ECS coolant. As ECS cooling demand increases, the pump speed would increase to provide a greater cooling capability within the allowable operating temperature increase of the subcooled coolant.

Figure 7-2G shows a method of providing the simplest back pressure control: use of an orifice. The backpressure of the cryogenic side will vary according to the flow rate into the heat exchanger and the heat load in the ECS coolant. It is, however, the simplest approach of the four considered. The control orifice may be in the form of an overboard vent duct as dictated by final packaging and installation.

Figure 7-2A is one of several systems shown which utilizes a pressure regulator in the cryogenic vent to control the back pressure. This provides complete freedom in the selection of cryogenic feed control approach. The regulator responds directly to the cryogen feed rate without complicated interface constraints.

Of the four approaches to back pressure control it appears that the downstream modulating flow control valve (Figure 7-2I and 7-2J) is most applicable to systems using recirculation of subcooled cryogen to provide ECS coolant heat rejection. The regulator-controlled back pressure concept has greatest application to the widest variety of system arrangements and cryogen flow control approaches based on the assumption that a positive cold-side backpressure is required to meet heat exchanger performance goals. It is clear that the orifice is the simplest approach.

Thermal Buffers

The control approaches synthesized here are compatible with several types of thermal buffers.

The simplest type of thermal buffer is the design of low effectiveness thermal surfaces on the cold side of the heat exchanger, such that the ECS coolant freezing problem is reduced. This approach to buffering is also the least flexible to accommodate variations in operating conditions.

Figure 7-2K shows a method of providing a buffer using a recirculating loop of the cryogen. Cryogen feed is mixed with the warm cryogen from the heat exchanger outlet to provide a more uniform cryogen inlet temperature. This arrangement also allows the use of liquid cryogen as a feed to the unit, while designing the cold side heat transfer surfaces for vapor. The recirculation rate of the buffer flow could be either constant or variable as a function of temperature. The use of a constant flow rate simplifies the control and the pump design; however, the use of a variable flow control allows greater flexibility in meeting diverse operating conditions of the unit.

The second type of buffer considered is shown in Figure 7-2L. Here, the regenerator serves to provide the ECS heat exchangers with vapor even when the cryogen feed is in the liquid state. An advantage of this approach is that the ECS cryogenic heat exchanger is never subjected to the extremes of thermal shock imposed by liquid/vapor flow conditions. These design problems are imposed upon the regenerator. The concept shown requires that the ECS heat exchanger be fabricated in two sections.

COMPARISON OF APPROACHES

Table 7-1 shows the various control concepts described earlier, and presents comparative comments. The table includes a set of columns showing estimated weight, power and reliability for the control approaches. The values shown are limited to the control components only, and do not include weights for the heat exchanger(s), pumps or regenerators. The weight column indicates that the weight range for the various concepts is from 4.1 lb to 9.3 lb. Although the percentage difference is high, the other factors such as performance may dictate that the slight weight penalty be accepted. A similar comment can be made about the continuous power variation from one concept to the other.

In the reliability area, the failure rate data indicate the probability of performing unscheduled maintenance on the control system, and the requirements for spare parts.

The table includes a set of columns headed "compatibility with cryogen source". A check mark in all three columns indicates the control system can be used, without modification, in a cryogenic heat exchanger application supplied by all vapor at various temperatures, or all liquid, or a combination of liquid and vapor. A control system capable of operating in liquid, vapor, or liquid and vapor offers significant advantages to overall operational flexibility and versatility.

The two columns under the heading "Features", indicate two important system features for comparison. First, the location of the cryogen flow control valve in the cold ambient cryogen stream imposes severe design requirements on the valve. Arranging the components to locate the modulating valves in the downstream vapor which is near ambient temperature reduces the design environmental requirement, and may offer advantages in reliability, weight, and cost.

Second, the control approaches are judged to determine the potential for close tolerance control of the ECS coolant outlet temperature. The comment column indicates that in some control concepts, close temperature control is achieved at the expense of introducing potential freezing problems in the ECS coolant.

CANDIDATE CONTROL CONCEPTS

The purpose of this preliminary control approach survey was to synthesize several candidate control approaches, compare these approaches, and to select

TABLE 7-1

CRYOGENIC HEAT EXCHANGER CONTROL CONCEPT COMPARISONS

Control Approaches	Figure No. 2-10	Estimate of Control Components only*			Compatibility with Cryogen Source			Features		Comments
		Weight lb	Power Watts	Failure Rate $\lambda \times 10^{-6}$ hr	Vapor	Liquid	Vapor and/or Liquid	Control Valve in Ambient Temperature Location	Capable of Close Temperature Control	
Pulsed cryogen feed	A	6	6	19.75	x	x	x	No	No	1) Limited valve life. 2) Control stability considerations.
Pulsed cryogen feed with proportional hot side bypass	B	8	8	24.25	x	x	x	No	Yes	1) Approach limited by freezing of ECS coolant during high bypass flows.
Recirculating buffer loop	K	8.6	12	26.25	x	x	x	No	Yes	1) High power demand, high weight, and low reliability; 2) approach provides reasonable protection against freezing at high recirculation rates
Proportional feed control with regulator vent	C	6.5	6	22.25	x	x	x	No	Yes	1) Close temperature control possible with limitations on inlet transients; 2) approach offers limited versatility but good growth potential
Active control with electrical flow control of cyrogen and vent	F	7	8	23	**	x	No	No	Yes	1) Matching the flow control areas (CA) of the two valves is a design problem for all values of inlet conditions.
Active control with mechanically linked cryogen and vent flows	E	5	6	20	**	x	No	No	Yes	1) Matching the flow control areas (CA) is more difficult with mechanical linkage than for electrically driven networks
Anticipating temperature control in ECS coolant	G	4.1	6	19.5	x	x	x	No	Yes	1) Simplest cold-side backpressure control; 2) impact of uncontrolled backpressure on heat exchanger performance unknown.
Anticipating temperature control in cryogen and ECS fluids	H	6.6	7	22.25	x	x	x	No	Yes	1) Offers versatility and growth capability; 2) active backpressure control, if needed; 3) anticipating networks for all fluid temperature changes.
Vernatherm modulation of cryogen supply	D	6.7	0	6.75	x	x	No	No	Yes	1) No electrical power required; 2) high reliability; 3) large temperature difference across valve, seal design, slow response make application questionable.
Inclusion of regenerator into active control approach	L	6.5	6	22.25	x	x	x	No	Yes	1) Thermal stress problems in regenerator; 2) minimizes freezing problems in ECS coolant passages; 3) concept imposses weight penalty
Active control by downstream flow modulation	I	5.5	6	20.5	x	x	x	Yes	Yes	1) Shut off valve cycled only when heat exchanger is activated; 2) heat exchanger exposed to full pressure of cryogen supply; possible weight penalty
Vernatherm controlled bypass and active cryogen flow control	J	9.3	6	21.5	**	x	No	Yes	Yes	1) Little versatility or growth potential; 2) bypass on hotside enhances possibility of ECS coolant freezing.

*Estimates for weight, power and failure rate are for control components only. Power shown is continuous demand. Power for vaives is estimated to be 200 watts, intermittant. No power allocation is made for the pump shown in Figure 2-10K.
**Considered only is cryogen inlet temperature and condition is known and predictable.

one or more for further study when applied to the specific heat exchanger configuration. Within this frame work preliminary selection was made.

This control concept providing the greatest simplicity with reasonable versatility and allowing reasonably simple modifications for greater versatility is the modulated cryogen feed control shown in Figure 7-2C. This system in a slightly simpler form would utilize the fixed orifice vent of Figure 7-2G. Modifications to provide greater control could include the addition of an anticipating sensor in the inlet ECS coolant line and corresponding control logic which would then be per the Figure 7-2G configuration. An additional sensor in the cryogen feed line with corresponding control logic would confirm to the Figure 7-2H configuration.

The thermally buffered heat exchanger shown in Figure 7-2L offers excellent protection against freezing of the ECS coolant and is rated well above the recirculating buffer loop of Figure 7-2K because of considerations of power, weight, and reliability. Buffering appears to be a significant adjunct to any control system to assist in the prevention of freezing of the hot side fluid. This control concept was not considered further, however, since freezing problems were overcome in the heat exchanger design phase.

Control of cryogen flow by downstream modulation (Figure 7-2I) shows promise because of the simplified design problem of operating the flow control valve in a relatively warm vapor as opposed to the cold and varying cryogen feed line. Application of this principal was investigated for the final design of the control approach.

The vernatherm control system shown in Figure 7-2D is rated consistently high in all aspects of the comparisons. The control approach is simple, reliable, requires no electrical power, and provides sufficiently tight temperature control for the application within certain design limits as discussed previously. This control appears more applicable to a liquid-bypass system or possibly a cryogen feed control if the cryogen was always in the vapor phase at temperatures significantly above the subcritical storage temperature. The latter conditions would reduce the problem of axial conduction in the valve and the reduced heat sink capacity would tend to offset the relatively high response time of the vernatherm element. This control concept was considered further in the tradeoff study.

TRADEOFF STUDY

General Approach

To analyze the dynamic characteristics of the basic cryogenic heat exchanger system and to subsequently synthesize a control system for it, both a linear and a nonlinear mathematical model of the heat exchanger system were generated. Both system models were used to evaluate the candidate control systems at the critical operating conditions. These systems and the analysis used to generate the two system mathematical models are described in Appendix C.

The candidate control systems which evolved from the previous survey are grouped under three main concepts:

Modulated Cryogen Feed Control (Position Control)

Vernatherm Control

Modulated Cryogen Feed Control--Position + Rate (and/or integral) Control

In both the first and third concepts, the flow-modulating valve may be located either upstream or downstream of the heat exchanger.

The first candidate scheme for control uses a temperature sensor and an actuator (generally pneumatic with a torque motor driven valve). The dynamics of the actuator can be described in general by a single small first order lag time constant of the order of about 0.5 seconds. The dynamics of the sensor can also be described by a single first order lag time constant but with a somewhat higher value of about 2 seconds (minimum). The overall response of this type of system is reasonably fast but results in a steady state control error of up to the control band in magnitude.

The second candidate scheme for control packages the sensor and actuator into a single unit. This vernatherm controller's dynamic characteristics can be described by a single first order lag time constant. Because temperature sensing and cryogen valve actuation are achieved through the expansion of a wax substrate within the vernatherm unit, the time constant is quite large: 20 or 30 seconds, minimum. As a consequence, the system response is slow. Since this system is also a position controller, it has the same steady state error characteristic of the first candidate control scheme.

The third control scheme contains the same elements as the first control scheme but processes the sensor temperature position signal through electronic circuitry to achieve rate and integral error control signals. The rate signal is used to anticipate temperature excursions and thus increase system response. The integral error signal is used to eliminate any steady state error generated by the position + rate control.

The two main control system characteristics used in the tradeoff study were system stability margin and system response to disturbances. Although absolute stability was a requirement, gain margin for stable systems was a characteristic that could be compromised in favor of system response. Both these system characteristics were readily obtainable from the analog computer simulation transient responses resulting from hot and cold fluid temperature disturbances. Stability was indicated by the number and amplitude of temperature oscillations after the initial temperature excursion. Generally no more than one measureable oscillation is desirable. System response was measured by the magnitude of the initial temperature excursion. Less than $10^{\circ}F$ difference from the $40^{\circ}F$ set point is desirable for a response characteristic.

Position Control

To prevent large steady state errors the temperature control band must be $\pm 10^{\circ}F$ or less, the limit for desired transient excursions. With this maximum control band (and thus lowest gain) the heat exchanger system is very difficult to stabilize. A typical example is shown in the Bode plot of Figure 7-5 that exhibits instability by 9 db of gain. Such a control system can be stabilized, however, but the resultant system would be very lightly damped or have a very slow response. In either case the system would exhibit very large temperature excursions as a result of system disturbances. As a result, this type of control system is not considered appropriate for the heat exchanger system.

Vernatherm Control

Since the vernatherm controlled system is essentially second order (vernatherm first order lag and heat exchanger first order lag), the system has inherent stability. With a control band of $\pm 10^{\circ}F$, a vernatherm with a 30 second first order lag time constant will afford the system characterized by the Bode plot of Figure 7-6. The system is stable with good damping as shown by the phase margin of 30 degrees. The system has a very slow response, however, as dictated by the large vernatherm time constant. Although the controlled temperature will have unpronounced oscillatory behavior, temperature excursions due to system disturbances will be prohibitively large. Consequently, this type of controller is considered inadequate for the heat exchanger system.

Furthermore, the seal problems and the axial conduction in this kind of valve between the warm and cold portions of the valve could significantly affect the accuracy of the sensed temperature. For these reasons, this control scheme was dropped from further consideration.

Position + Rate + Integral Control

The control system which offers the best stability and response is one that incorporates position, rate and integral modes of control. The rate mode affords the system high response and recovery from disturbances by anticipating temperature excursions. The position mode provides response when no error rate signal exists. The integral mode eliminates any steady state error that would otherwise exist.

The rate and position control signals are generated by processing the sensor temperature signal through an electronic lead-lag phase compensation network. The transfer function of such a network could be $\frac{1.333\ S + 1}{0.0667\ S + 1}$. The integral control signal is achieved in a parallel signal path by integrating the error between the sensor signal and the reference set point of $40^{\circ}F$. The transfer function of such an integrator could be $\frac{0.5}{S}$. Since the parallel integration signal path eliminates any steady state error, the control band for cryogen flow valve actuation can be expanded to $\pm 20^{\circ}F$ as an example. The Bode plot of this system at the critical operating condition is shown in Figure 7-7. The plot shows a highly stable system (13.5 db of gain margin) with good damping (28 degrees of phase margin).

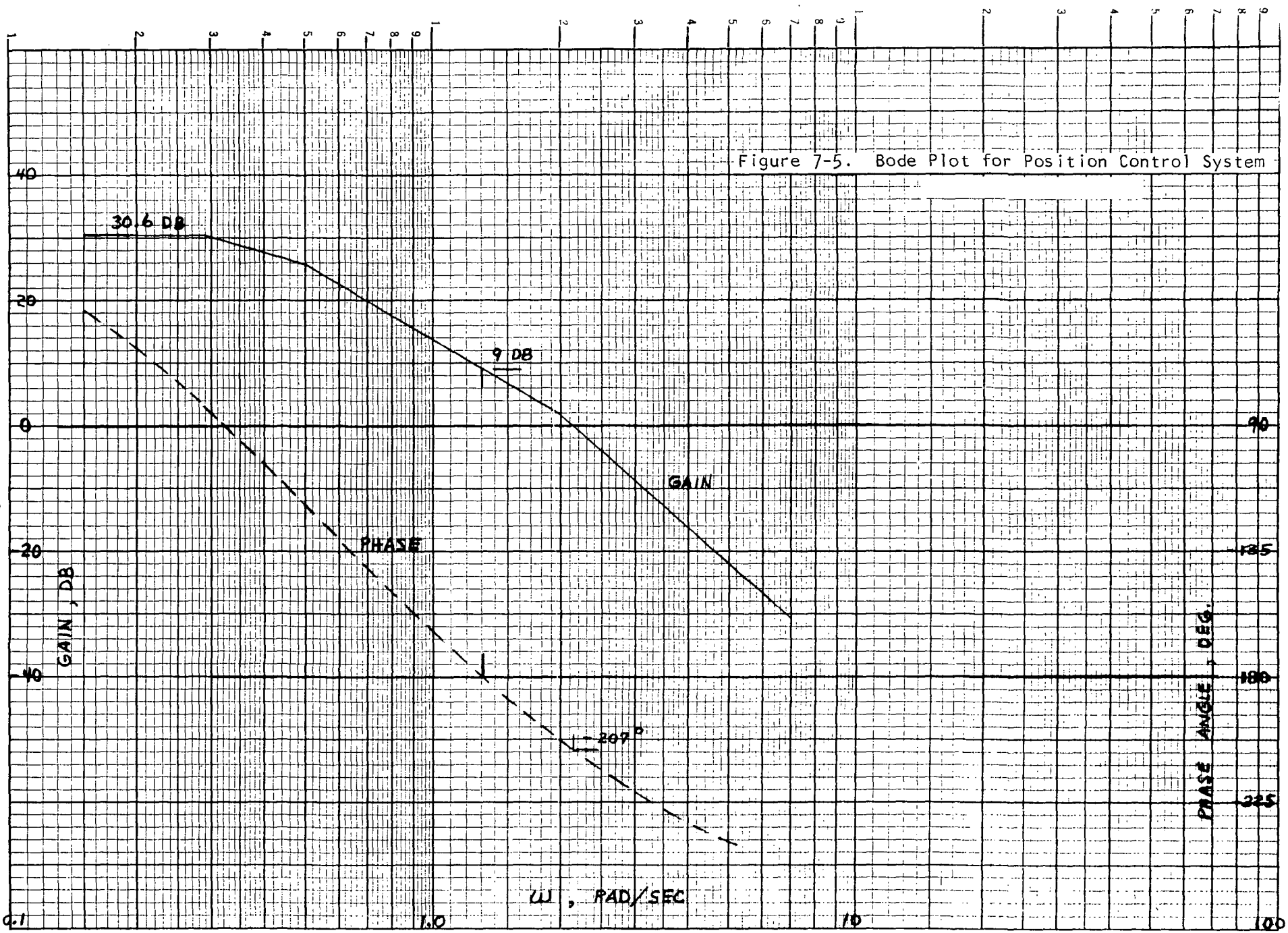

Figure 7-5. Bode Plot for Position Control System

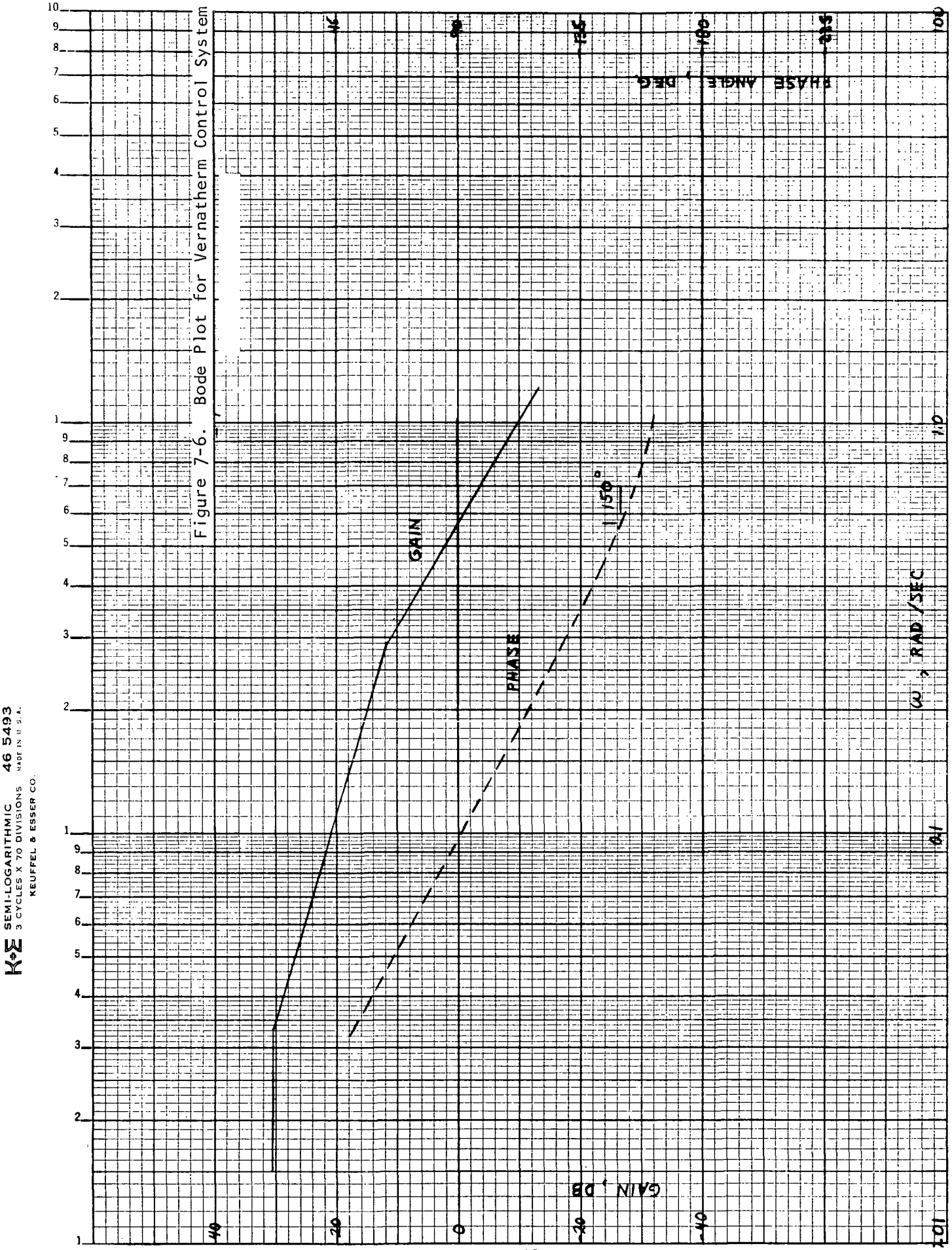
Figure 7-6. Bode Plot for Vernatherm Control System
GAIN
PHASE
150°
GAIN, DB
PHASE ANGLE, DEG
ω, RAD/SEC
SEMI-LOGARITHMIC 46 5493
3 CYCLES X 70 DIVISIONS MADE IN U.S.A.
KEUFFEL & ESSER CO.

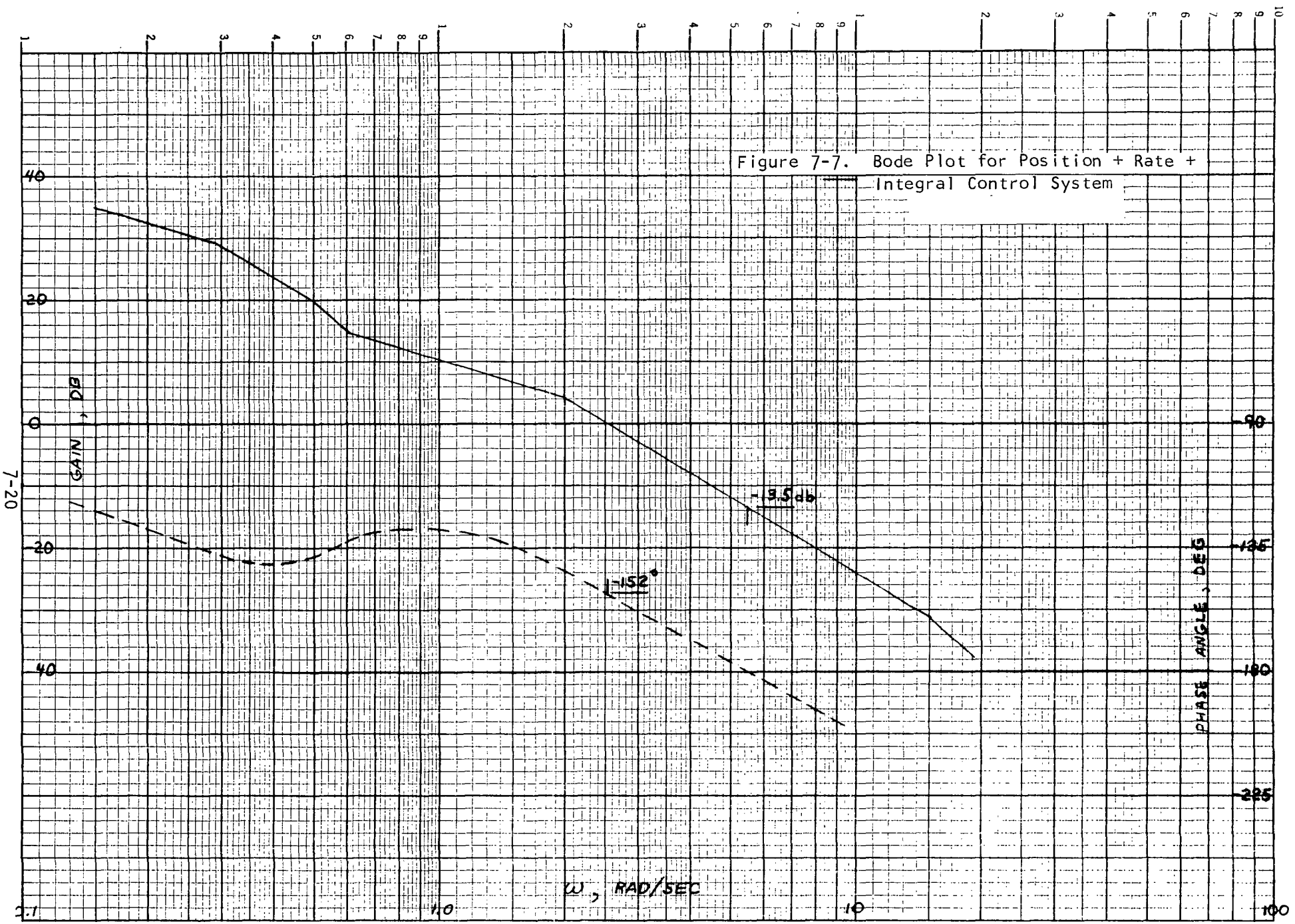

Figure 7-7. Bode Plot for Position + Rate + Integral Control System

The system response, as indicated by the simulation time histories of Figures 7-8 through 7-9 are quite good. The time histories show adequate to excellent response and damping for disturbances on both the hot and cold inlet temperatures to the heat exchanger. The most severe disturbance utilized on the simulated system was the step change from 50°F to 105°F on the hot side of the heat exchanger. This "extreme" disturbance, for a cold side inlet temperature of 0°F, resulted in a brief excursion of the heat exchanger hot fluid outlet temperature of 13°F (to 53°F) from the control point of 40°F. All other system responses to disturbances exhibited less than 10°F excursions as shown in the time histories and tabulated in Table 7-2. For less "extreme" and more realistic disturbances on the hot side (20 second ramps between 50°F and 105°F) the hot fluid exit temperature remains well below 10°F as shown in Figures 7-10 and 7-11. The case of a 20-sec ramp change in cryogen inlet temperature (between 0 and -400°F) is shown in Figures 7-12 and 7-13 and the results are included in Table 7-2.

SUMMARY

As a result of the control system evaluation study performed with the system mathematical models, only the control system with position + rate + integral modes of control provides the stability, damping and high response required. It is this type of controller that is, therefore, recommended. The controller contains as components

1. Liquid (T_H) temperature position sensor
2. Electronic amplifier circuit for processing sensor signal
3. Actuator which can be pneumatic with a torque motor driven valve
4. Cryogen valve with a maximum CA of about 0.08 $in.^2$ for the case of hydrogen

Both the temperature sensor and pneumatic actuator must have a reasonably fast response with lag time constants of about 2 seconds and 0.5 seconds respectively. The electronic amplifier circuit provides the system phase compensation and generates the error signal for the actuator drive. The transfer function of the circuit is

$$\frac{0.5}{S} + \frac{1.333\ S + 1}{0.0667\ S + 1}$$

The amplifier circuit can be designed as shown in the schematic of Figure 7-12. The circuit illustrated involves the use of three amplifiers with various passive elements, and provides all the characteristics, including saturation limits, that were incorporated into the control system of the computer simulation.

To avoid freezing in the heat exchanger in case of warm fluid shutdown, a signal can be fed to the present amplifier causing the control valve to shutdown, thus, eliminating any cryogen flow into the heat exchanger during the absence of warm fluid flow.

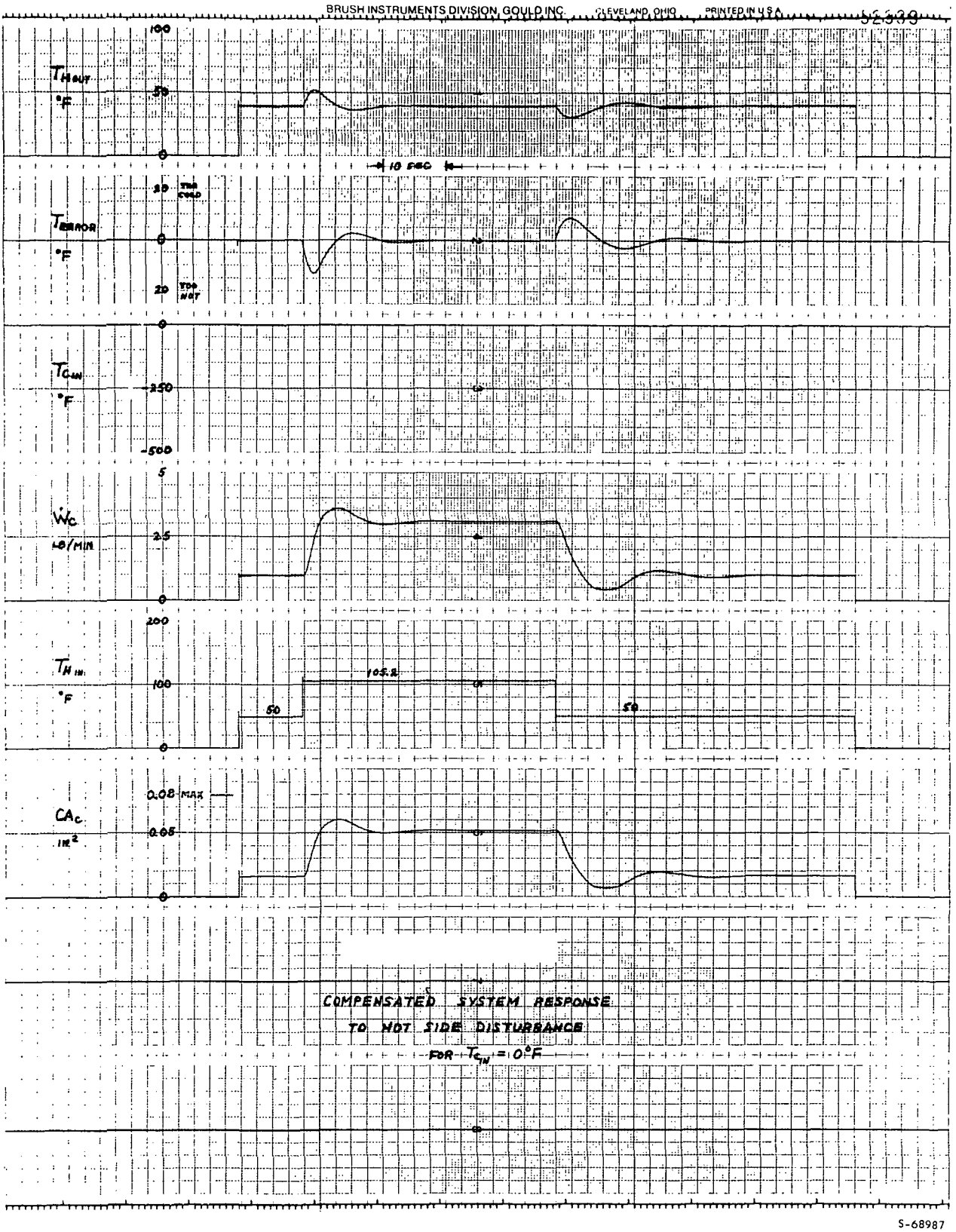

Figure 7-8. Compensated System Response to Hot Side Disturbance for $T_{C_{IN}} = 0^{o}F$

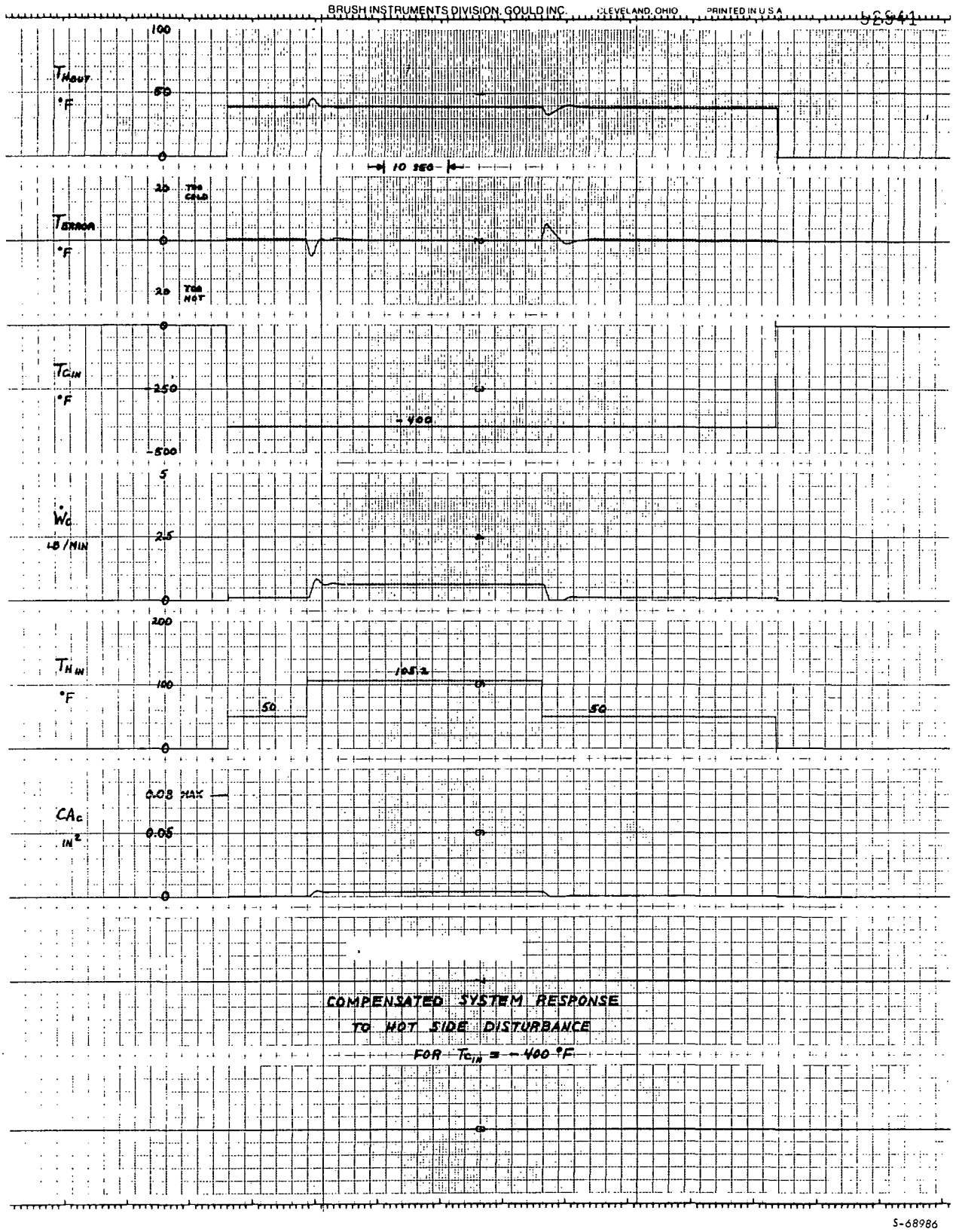

Figure 7-9. Compensated System Response to Hot Side Disturbance for $T_{C_{IN}} = -400^{\circ}F$

TABLE 7-2

TRANSIENT CHARACTERISTICS OF THE SYSTEM

Time Hist. Figure No.	System State		HX Hot Fluid Exit Temp
	Hot Fluid Inlet Temp.	Cold Fluid Inlet Temp.	Max Excursion From 40°F Ref.
7-8	Step from 50°F to 105°F	0°F	+13°F
	Step from 105°F to 50°F	0°F	-8.5°F
7-9	Step from 50°F to 105°F	-400°F	+6°F to 46°F
	Step from 105°F to 50°F	-400°F	-6.5°F to 33.5°F
7-10	20 sec ramp from 50° to 105°F	0°F	+3°F
	20 sec ramp from 105° to 50°F	0°F	-2°F
7-11	20 sec ramp from 50° to 105°F	-400°F	+0.5°F
	20 sec ramp from 105° to 50°F	-400°F	-0.5°F
7-12	50°F	20 sec ramp from 0°F to -400°F	-3°F to 37°F
	50°F	20 sec ramp from -400°F to 0°F	+3°F to 43°F
7-13	105°F	20 sec ramp from 0°F to -400°F	-7°F to 33°F
	105°F	20 sec ramp from -400°F to 0°F	+5.5°F to 45.5°F

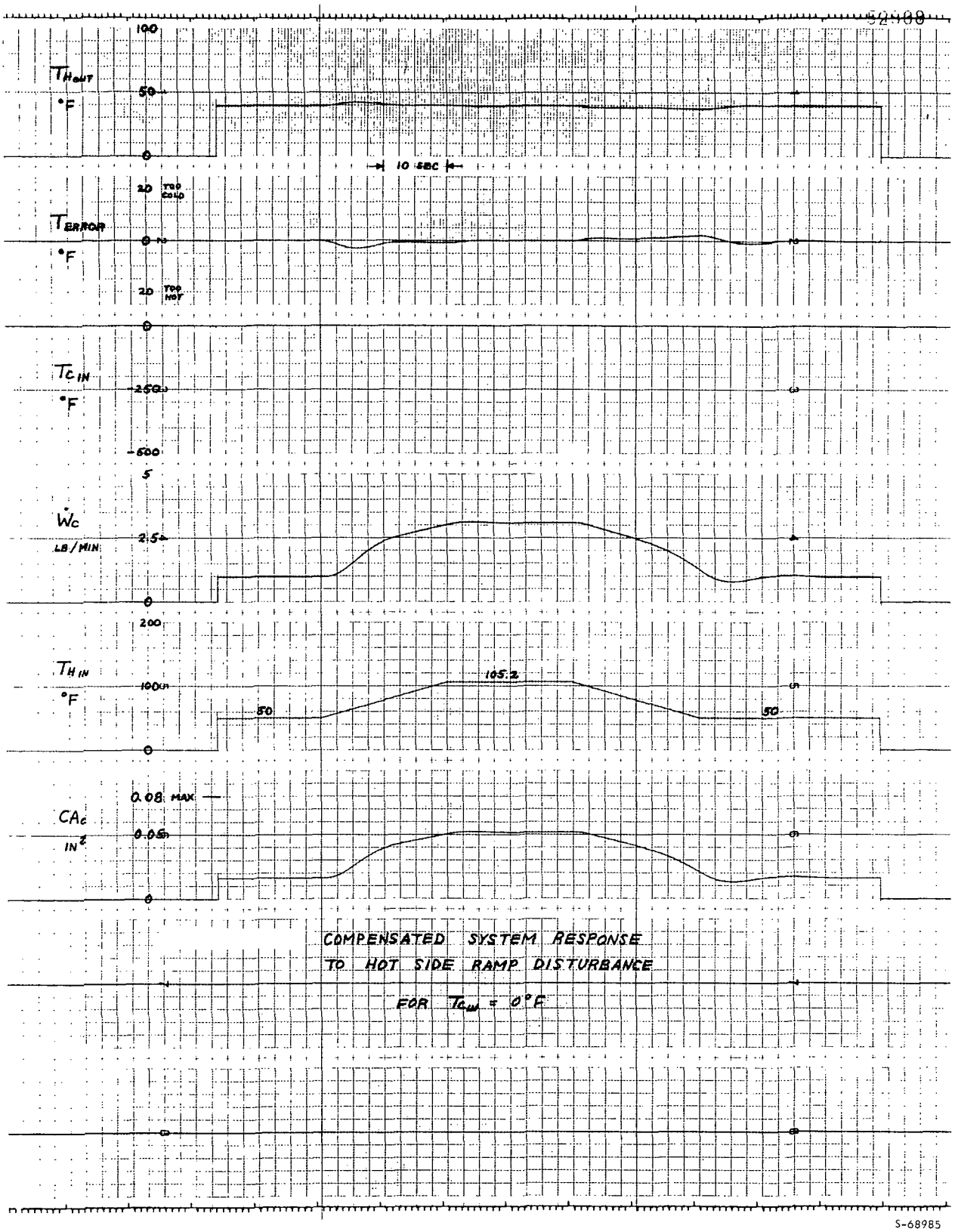

Figure 7-10. Compensated System Response to Hot Side Ramp Disturbance for $T_{C_{IN}} = 0^{o}F$

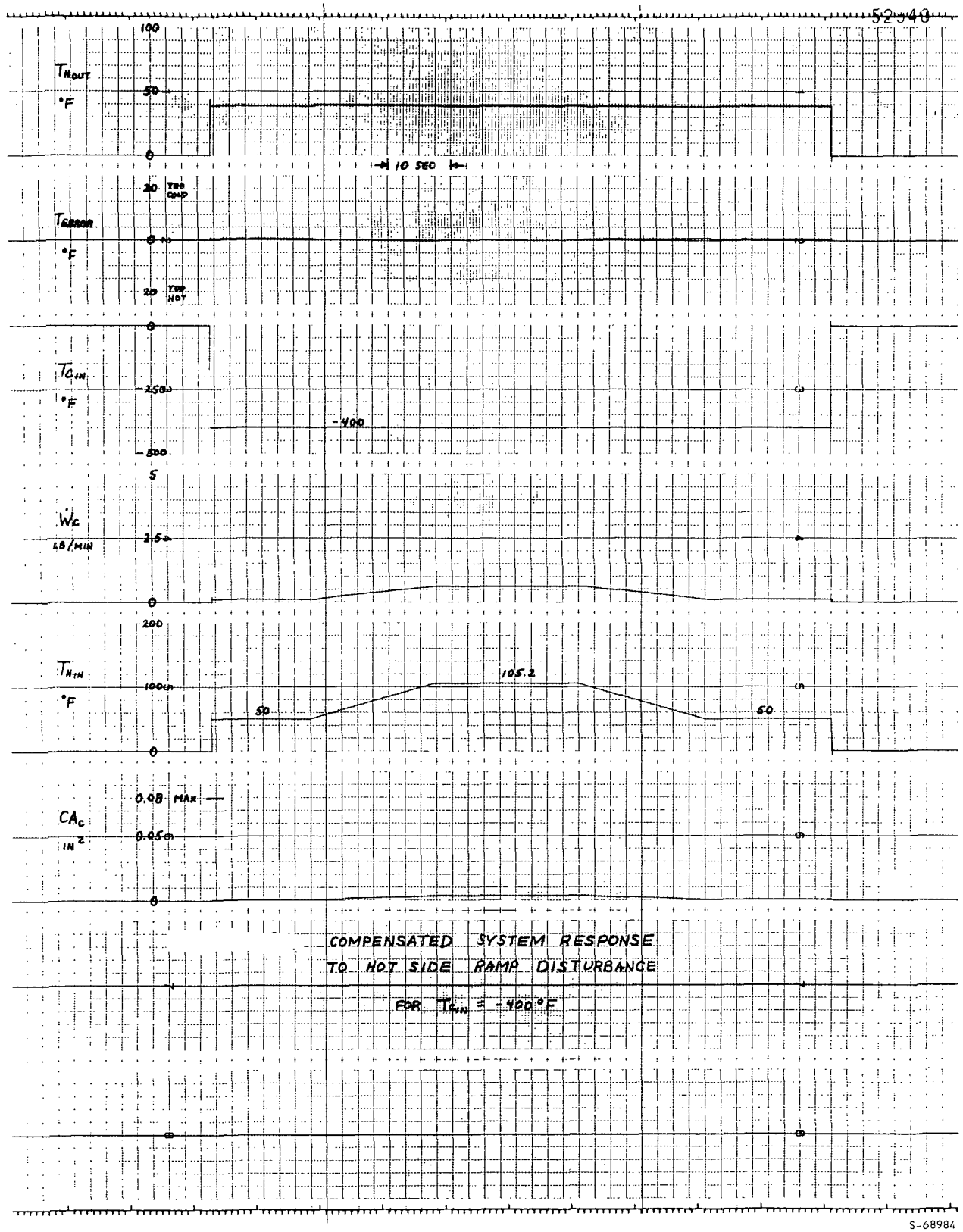

Figure 7-11. Compensated System Response to Hot Side Ramp Disturbance for $T_{C_{IN}} = -400^{o}F$

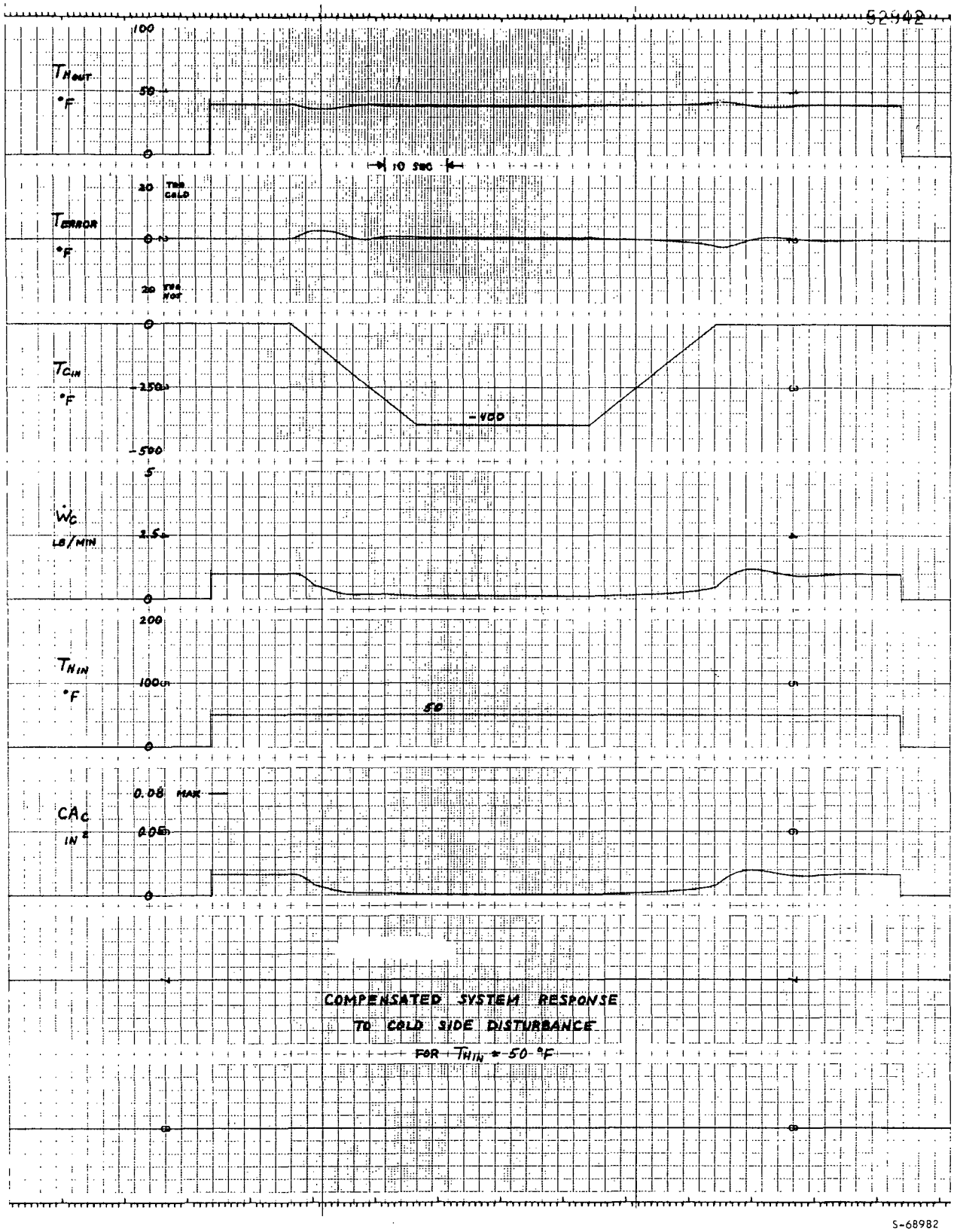

Figure 7-12. Compensated System Response to Cold Side Disturbance for $T_{H_{IN}} = 50^{o}F$

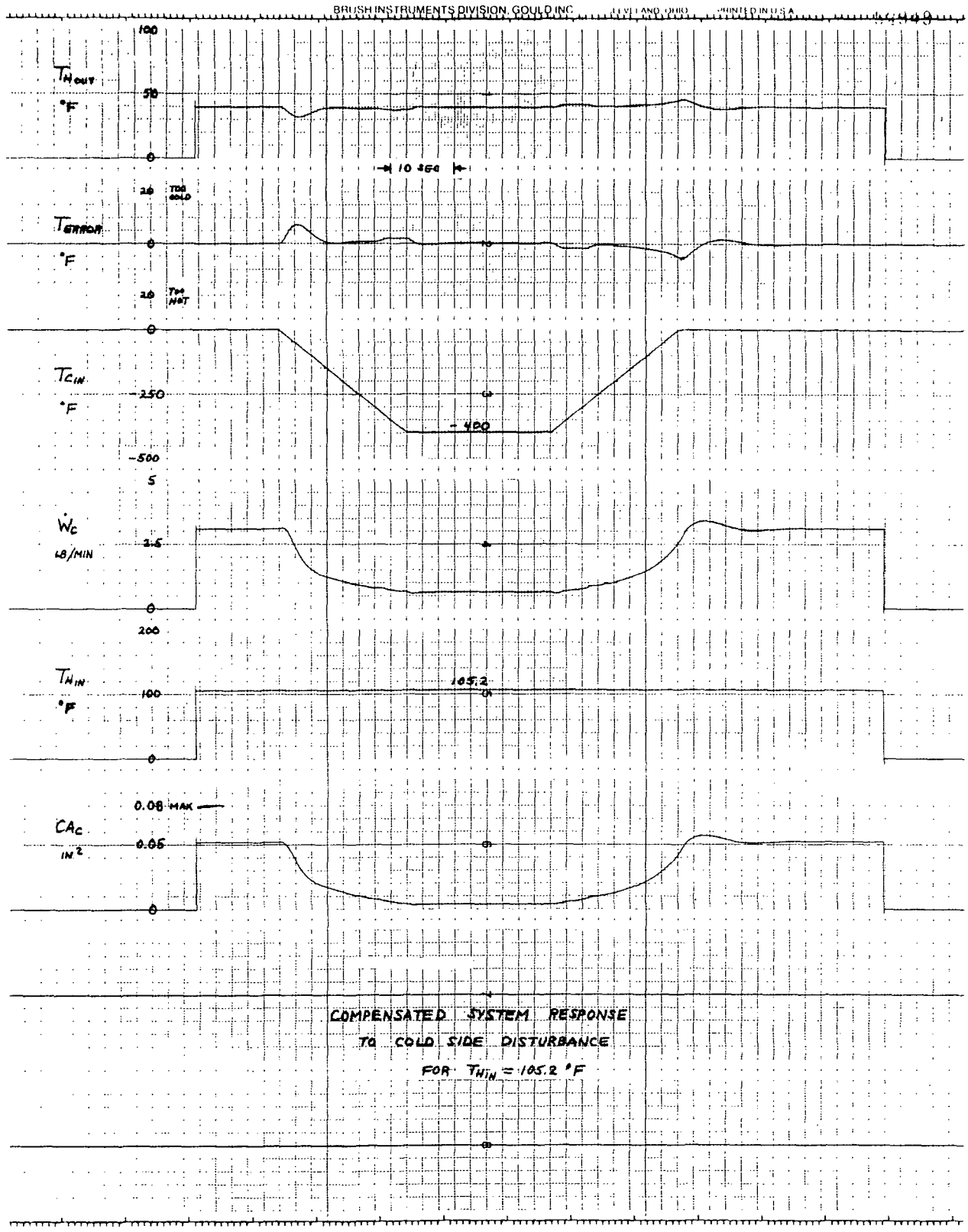

Figure 7-13. Compensated System Response to Cold Side Disturbance for $T_{H_{IN}} = 105.2^{o}F$

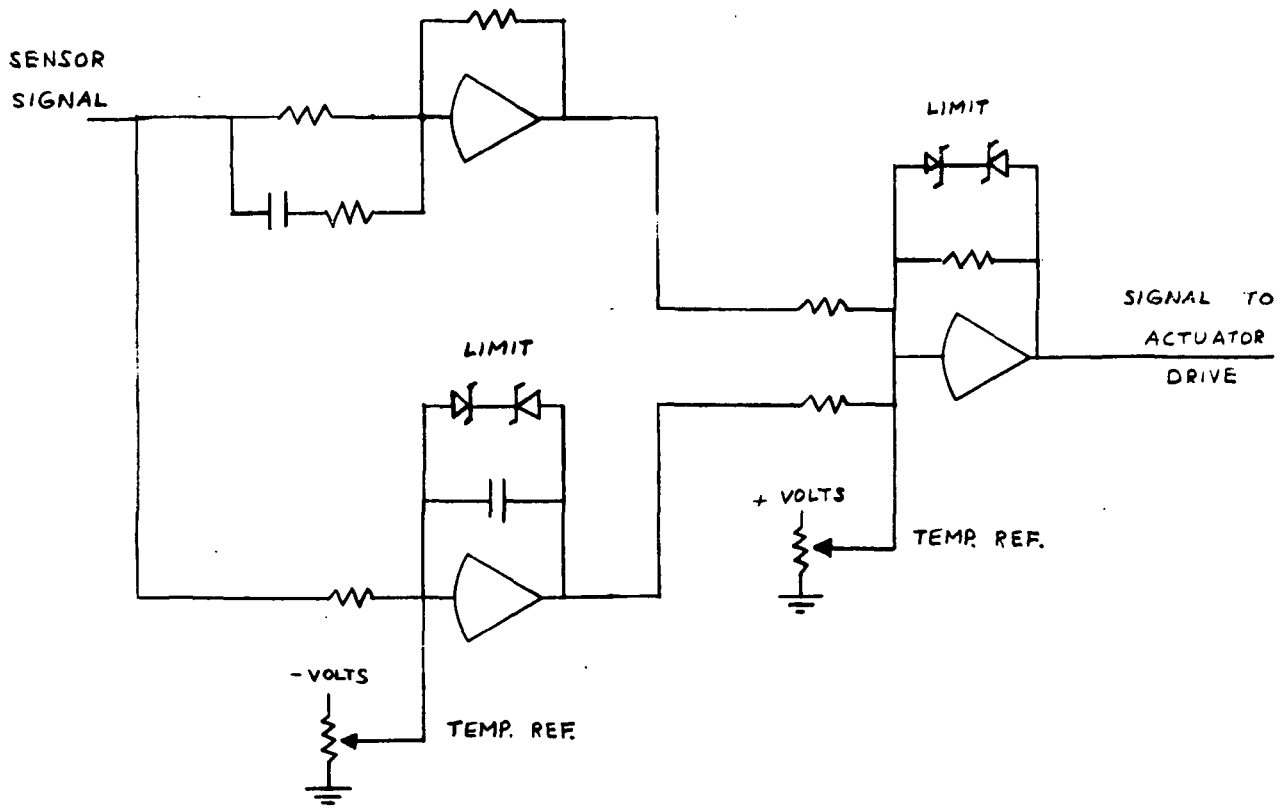

Figure 7-14. Electronic Circuit Schematic for Phase Compensation

SECTION 8

SELECTED HEAT SINK SYSTEM

CANDIDATE SYSTEMS

In the previous sections, a tradeoff study was conducted for the cryogenic heat exchanger and the control system using hydrogen as the heat sink fluid and E-2 as the warm fluid. The results of the study should be valid, as pointed out before, if oxygen is used as the heat sink fluid and also if Freon-21 is used as the warm fluid. Based on this tradeoff study, several systems were selected and are listed below (see Figure 8-1a and 8-1b).

System 1--Tubular Heat Exchanger with Upstream Flow Control

System 2--Plate-fin Heat Exchanger with Upstream Flow Control

System 3--Tubular Heat Exchanger with Downstream Flow Control

System 4--Plate-fin Heat Exchanger with Downstream Flow Control

All the above systems meet the desired performance both at steady state conditions and when subjected to disturbances either in the heat load or in the cryogen inlet conditions. The main variation among these systems is in the heat exchanger design and the location of the flow control valve. All the systems use a position + rate + integral control scheme.

The heat exchanger design is either a tubular, multipass cross-counter flow or a plate-fin multipass cross-counterflow. In the tube and shell design, the cryogen flows in 0.1-in. o.d. ring-dimpled tubes, while the warm fluid makes 10 passes over the tubes' bank in a cross-counter flow pattern. In the plate-fin design, the cryogen makes one pass in a finned passage 0.2-in. high and 20 fins per inch. The warm fluid makes eight passes in passages 0.1-in. high, finned with offset rectangular fins (20 fins per inch). The weights of the two units are comparable.

Although the weights of the tubular and plate-fin heat exchangers are comparable, the tubular unit is favored for the following reasons. In a plate-fin design, and at minimum cryogen inlet temperatures, the increase in warm fluid viscosity close to the wall could create quasi-stagnation areas in the plate-fin narrow passages where freezing could start. An accurate prediction of this phenomenon is quite difficult. Furthermore, an increase of the warm fluid pressure level beyond the selected design value (100 psia) may require heavier material gages in the plate-fin design and, consequently, may result in a weight penalty.

The control valve location, whether upstream or downstream of the heat exchanger, does not affect the control capability as indicated by the control analysis. One advantage of the downstream location is in the fact that the valve is exposed to warm gas and not to two-phase or liquid cryogens. On the

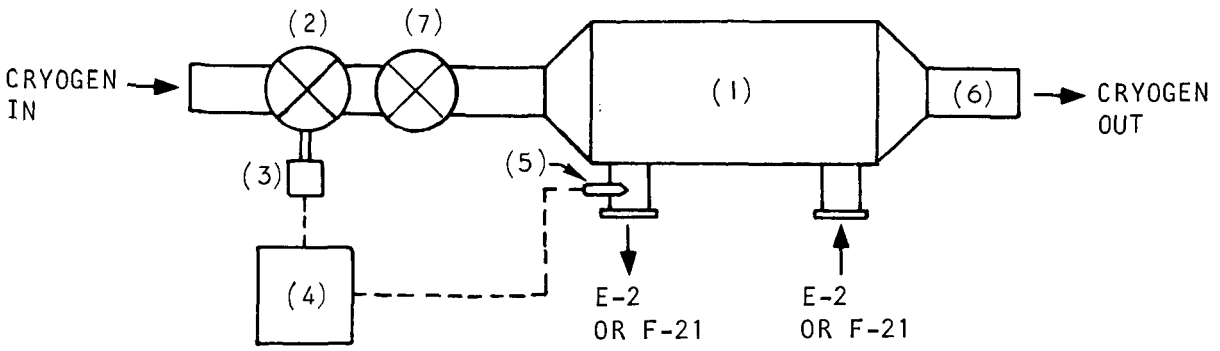

a. Upstream Control Valve

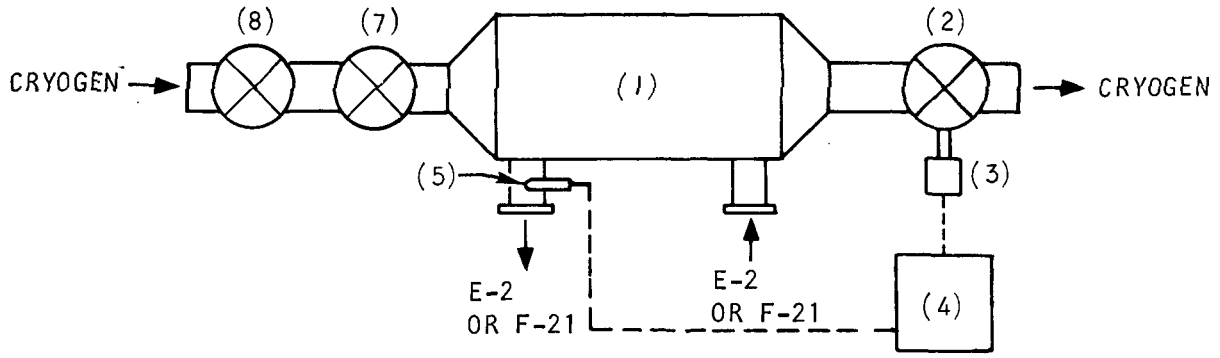

b. Downstream Control Valve

COMPONENTS:

(1) CRYOGENIC HEAT EXCHANGER: EITHER TUBULAR OR PLATE-FIN DESIGN

(2) FLOW CONTROL VALVE = CA ≃ 0.08 SQ IN. (FOR H_2), ZERO LEAKAGE DURING SHUTDOWN

(3) ACTUATOR = PNEUMATIC OR HYDRAULIC, WITH TIME CONSTANT OF 0.5 SEC OR BETTER

(4) CONTROLLER = SEE DETAILS IN FIGURE 8-3

(5) TEMPERATURE SENSOR = LAG TIME CONSTANT OF 2 SEC OR BETTER

(6) VENT DUCT

S-68979-A

(7) CHECK VALVE

(8) SHUTOFF VALVE

Figure 8-1. Recommended Heat Sink Systems

other hand, in case of a warm fluid shutdown, the liquid cryogen will still enter the heat exchanger and may cause heat exchanger freeze-up unless a shut-off valve is provided upstream of the heat exchanger. This valve does not have to be part of the heat sink system if it is provided elsewhere upstream of the heat exchanger.

The two-phase flow stability in the heat exchanger core may be sensitive to the location of the control valve. Upstream location induces a liquid pressure drop and, though not in the individual tubes of the heat exchanger, may still provide a stabilizing effect. Downstream location raises the pressure level in the heat exchanger and, therefore, decreases the density ratio. This was also shown to be a stabilizing effect.

A check valve is included in the system to prevent reverse flow of the cryogen due to pressure fluctuations in the heat exchanger. This valve is located in the cryogen inlet line just upstream of the heat exchanger.

SELECTED SYSTEM

With NASA agreement, a heat sink system consisting of a tubular multi-pass cross-counter flow heat exchanger and a position + rate + integral control scheme was selected. The cryogen flows inside small diameter, ring-dimpled tubes which are arranged in tightly-spaced, staggered rows. The warm fluid makes several cross-flow passes outside the tubes. The control system consists of a flow control valve, an actuator, an electronic amplifier circuit for processing sensor signal and a temperature sensor. AiResearch decided to test with both the upstream and downstream locations of the flow control valve later in the program. The selected heat sink system offers simplicity, reliability and minimum risk from freezing.

The next section describes the cryogenic heat exchanger, the most important component of the system. The rest of the components of the heat sink system are described in the following paragraphs.

Cryogen Flow Modulating Valve and Actuator

The heat exchanger system utilizes a valve either in the cryogen inlet or outlet line to modulate the flow of cryogen as required to maintain the hot fluid outlet temperature at a nominal value of 40°F. The valve must control the hydrogen flow at inlet conditions of -420°F to 0°F and approximately 20 to 40 psia over a flow range of approximately 0 to 3 lb/min. A fast response of the valve is required to prevent large excursions of the hot fluid outlet temperature during transient conditions. A time constant of 0.5 seconds was found to be adequate in the analog simulation analysis.

A valve design which meets these requirements and is suitable for this application is a normally closed electro-pneumatically actuated poppet or plug type shutoff and modulating valve. This valve is shown schematically in Figure 8-2. The poppet is inlet pressure balanced and spring loaded in the closed position. The valve is opened by applying pressure to Chamber "A" and overcoming the spring load.

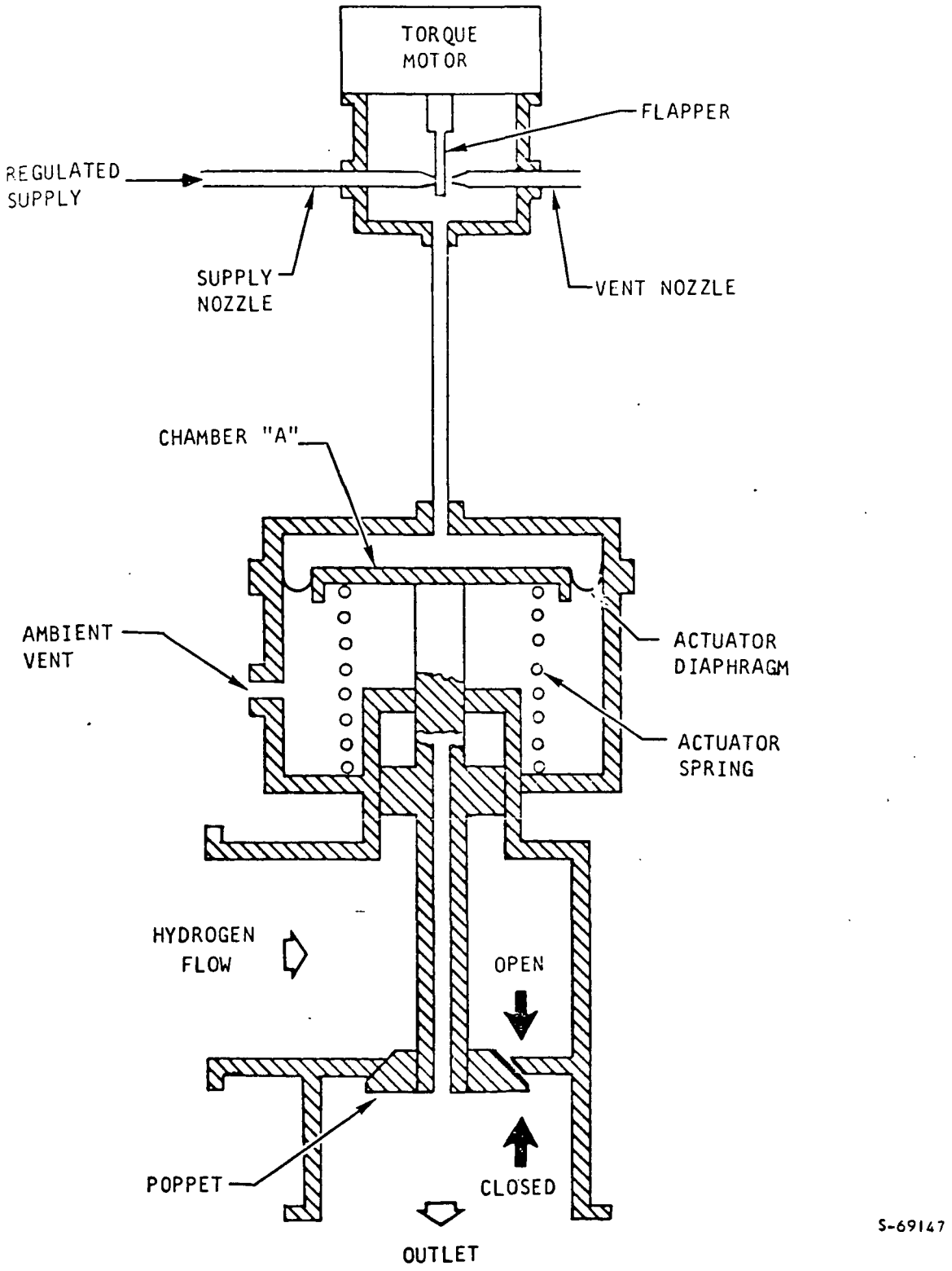

Figure 8-2. Flow Control Valve and Actuator Schematic

A regulated pneumatic supply pressure is ported to the torque motor supply nozzle and with zero electrical signal from the controller, this nozzle is closed. Chamber "A" is then vented through the torque motor vent nozzle. As the electrical signal to the torque motor is increased, the flapper moves to open the supply nozzle and close the vent nozzle, raising the pressure in Chamber "A" and opening the valve. For a given value of input signal there is a predetermined valve position.

Using a plug instead of the poppet shown allows better modulation in the "just open" range. In addition, the plug shape can be tailored to provide an optimum flow area vs stroke curve as required.

Typically, a 15 psig regulated pneumatic pressure source is used for the supply and a 0 to 10 milliamp dc signal provides full valve stroke. This valve can be packaged in an envelope of approximately 3 in. x 3 in. x 4 in. and have a weight of less than 2 lb.

Temperature Sensor

The temperature sensor used in the control system for cryogen flow control senses the heat transport fluid leaving the heat exchanger. To control the fluid temperature to the desired value of $40^{\circ}F$ within a close tolerance, the sensor must accurately sense the bulk fluid temperature and have predictable characteristics and sufficient change in some parameter as a function of temperature. In addition, a fast response to a change in fluid temperature is required to prevent large excursions from the control temperature due to transients in either fluid circuit. In the analog simulation analysis conducted on the system it was found that a sensor time constant of about 2 seconds or less is desirable.

A sensor which meets these requirements and can be used in this application is a glass bead thermistor. The thermistor provides relatively large changes in resistance for small changes in temperature in a predictable and repeatable manner. The thermistor head can be installed in a probe which then can be installed in a port in the fluid line. The sensor probe should be installed immediately downstream of the heat exchanger in a high velocity fluid stream to reduce the lag time of the sensor. This type of sensor and installation is capable of allowing close tolerance steady state control and, having a time constant of 2 seconds or less, should have acceptable transient response. This sensor can be packaged within an envelope of 1 in. diameter by 3 in. long with a weight of less than 0.2 lb.

Check Valve

This valve is located in the cryogen inlet line just upstream of the heat exchanger. The valve can be a simple poppet type with a small spring load to assist valve closing. Pressure drop of the valve at maximum flow should be approximately 1 psi or less. The valve envelope can be approximately 2 in. dia by 4 in. long with a weight of less than 1 lb.

Controller

As indicated by the heat sink system transient analysis, the control system which offers the best stability and response is one that incorporates position, rate and integral modes of control. The rate mode affords the system high response and recovery from disturbances by anticipating temperature excursions. The response is achieved by phase change rather than by gain change and thus does not hurt stability. The position mode provides response when no error rate signal exists. The integral mode eliminates any steady-state error that would otherwise exist.

The rate and position control signals are generated by processing the sensor temperature signal through an electronic lead-lag phase compensation network. The integral control signal is achieved in a parallel signal path by integrating the error between the sensor signal and the reference set point of $40^{\circ}F$.

A controller to provide this position, rate and integral control can be a solid-state electronic unit which accepts a signal from the temperature sensor and outputs a dc control current to the control valve. The electronic circuitry as shown on the block diagram, Figure 8-3, includes

- A sensor bridge circuit
- An amplification and dynamic compensation stage
- A control current output stage
- Power supply and EMI filter circuitry

The electronic circuit components can be mounted on printed circuit cards mounted within a 17 cubic envelope. The weight of the controller can be 0.8 lb max. Including output control power to the valve, the unit power consumption can be 6 watts maximum of power for a 28 vdc power source.

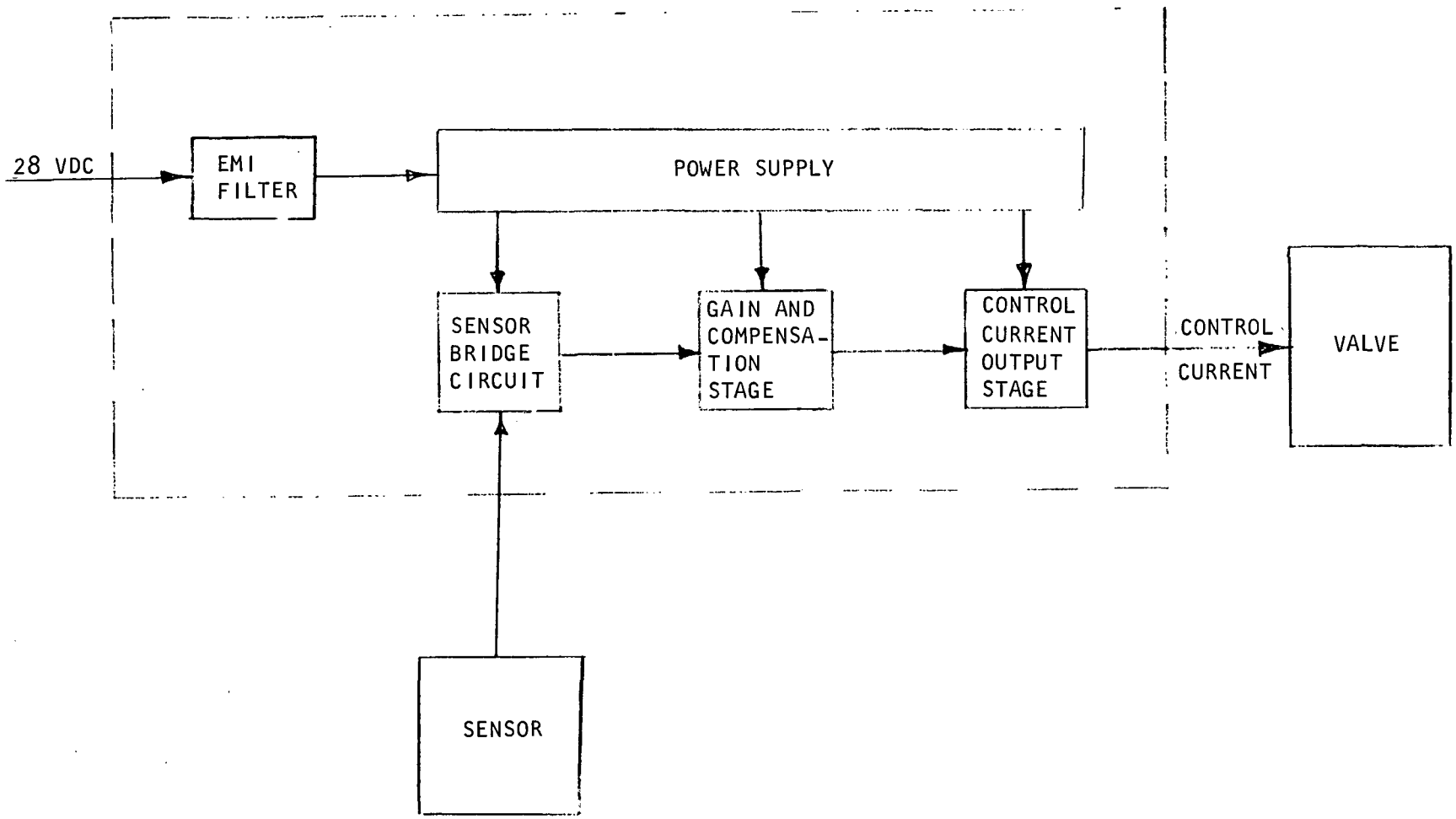

Figure 8-3. Controller Block Diagram

SECTION 9

HEAT EXCHANGER DESIGN

USE OF FREON-21

The tradeoff study of the heat sink system presented in the previous sections was carried out using E-2 (a fluorocarbon compound) which has been selected as the candidate warm fluid. The main factors affecting this selection were the freezing point, boiling point at 1 atmosphere, and liquid density. It was also pointed out that Freon-21 is comparable to E-2, except for a lower boiling point as shown below.

	Specific Heat Btu/lb ^{o}F	Freezing Point ^{o}F	Boiling Point at 1 atm ^{o}F	Density lb/ft^3
E-2	0.242	-190	220	103
Freon-21	0.256	-211	48	85

The lower boiling point of Freon-21 results in a higher system operating pressure and the lower density results in higher system pressure drop. The differences in the other two important properties, i.e., the specific heat and the freezing point are small and actually favor the Freon-21.

Since the use of E-2 would add considerably to the cost of a test program due to fluid cost, and Freon-21 is currently considered on Space Shuttle applications, and since the conclusions reached during the tradeoff study hold for both fluids, it was decided with NASA concurrence to design and test the cryogenic heat exchanger using Freon-21.

DESIGN POINT CONDITIONS

In addition to having an optimum design from weight and volume standpoints, the heat exchanger must maintain a wall temperature sufficiently higher than $-211^{o}F$ to eliminate any freezing problems. The heat exchanger must also provide stable operation, free from any flow instability which could degrade the performance or initiate freezing of the warm fluid. The design point variables for the preliminary design of the heat exchanger are listed in Table 9-1.

The worst design condition for the heat exchanger from the heat load and pressure drop standpoints is at maximum heat load with the inlet temperature of the hydrogen at its maximum value. The thermal conductance ratio is selected in this case such that the wall temperature is maintained appreciably above $-211^{o}F$ when the cryogen inlet temperature drops to its lowest value ($-420^{o}F$) while the heat load is at its maximum value.

TABLE 9-1

DESIGN POINT VARIABLES
FOR THE DESIGN OF THE CRYOGENIC HEAT EXCHANGER

Side	Hydrogen	Freon-21
Flow, lb/hr	148	2810
Inlet temperature, ^{o}F	0	125
Outlet temperature, ^{o}F	112.5	40
Effectiveness	0.9	0.68
Heat load, Btu/hr	60,000	60,000
Inlet pressure, psia	25	150
Pressure drop, psi	up to 10	up to 5

Based on the tradeoff study a heat exchanger effectiveness of 0.9 has been selected which gives the minimum total weight consisting of the weight of the heat exchanger, the weight of consumables, and the penalties weight.

Assuming a minimum hydrogen storage pressure of 40 psia and allowing a pressure drop of 15 psi in the lines and valves leading to the heat exchanger, the inlet pressure of the hydrogen to the heat exchanger is 25 psia. Hence, the overall pressure drop in the heat exchanger including ducting, manifolding, etc. must be less than 10 psi, thus maintaining the outlet pressure slightly above atmospheric pressure.

The inlet pressure of the Freon-21 is specified in Table 9-1 as 150 psia which is sufficiently high to ensure one-phase operation of the warm fluid.

HEAT EXCHANGER DESIGN DETAILS

A schematic of the heat exchanger is shown in Figure 9-1. The heat exchanger is of tube and shell type and has ten-pass, cross-counterflow arrangement with the cryogen flowing inside the tubes and the warm fluid flowing outside the tubes. The tubes contain ring dimples to increase the heat transfer and pressure drop on the hydrogen side. The increase in heat transfer is required to minimize the weight and have a reasonably shaped heat exchanger, and the high pressure drop is desired for good flow distribution on the hydrogen side.

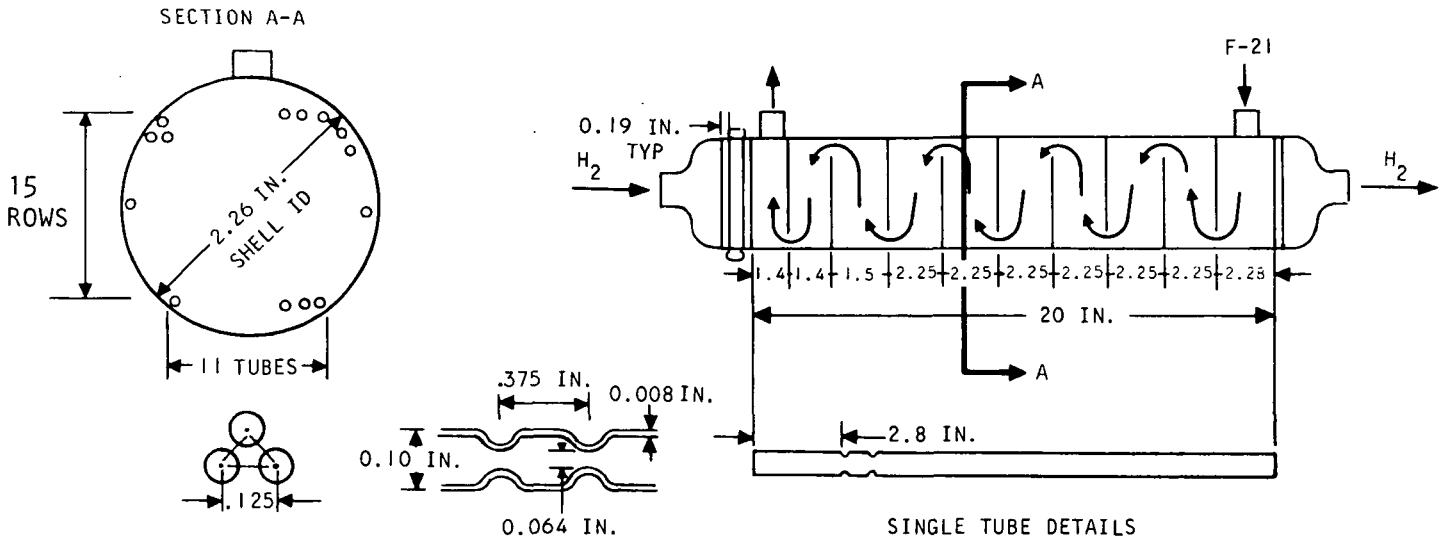

- TUBULAR - TEN-PASS, CROSS COUNTER FLOW ARRANGEMENT WITH CRYOGEN INSIDE TUBES AND WARM FLUID OUTSIDE TUBES
- HEAT EXCHANGER DETAILS

MATERIAL	= STAINLESS STEEL
CONSTRUCTION	= DIMPLED TUBE AND SHELL
NUMBER OF TUBES	= 228
TUBE OUTSIDE DIAMETER	= 0.1 IN.
TUBE WALL THICKNESS	= 0.008 IN.
TUBE LENGTH, ACTIVE	= 20 IN.
TUBE SPACING	= 0.125 IN.
DIMPLE DIMENSIONS	= AS SHOWN ABOVE
NUMBER OF BAFFLES	= 9
TYPE OF BAFFLES	= SEGMENTED
HEAT EXCHANGER WEIGHT	= 7.7 LB.

S-69149

Figure 9-1. Tubular Heat Exchanger Design

The heat exchanger design includes four unique features which ensure against freezing.

The first feature is the reduced baffle spacing close to the cryogen inlet. The spacing of the last two warm fluid passes is reduced from 2.25-in. to 1.4-in. This results in an increase of the heat transfer coefficient on the outside surfaces of the tubes in areas where the cryogen is at its lowest temperature. The increase in the Freon-21 velocity in the last pass also augments heat transfer to the surface of the inner header, thus eliminating freezing in these critical areas.

The second feature is the elimination of the ring dimples in the first portion of the tubes (2.8-in.). This length extends over the last two warm fluid passes. Hence, the increase in heat transfer on the Freon side due to increased velocity and decrease in heat transfer on the hydrogen side act to bring the tube wall temperature closer to the warm fluid temperature. Elimination of the dimples in this portion of the tubes also ensures against disturbing any vapor film in the two-phase regime of the cryogen and hence a low heat transfer coefficient on the cryogen side is maintained.

The third feature is the addition of one more header on the hydrogen inlet side. This causes further separation of the cryogen from the warm fluid. The cryogen impinges on the upstream header and causes it to cool down to the cryogen inlet temperatures while the warm fluid adjacent to the downstream header causes it to remain at a temperature sufficiently above the Freon-21 freezing temperature; thus eliminating freezing on the surfaces of the header.

The fourth feature is the careful control of warm fluid bypassing around the tube bundle by minimizing the spacing between the tube bundle and the shell. A significant bypassing would cause a significant reduction of the warm fluid velocity inside the tube bundle and could initiate freezing.

The two-phase regime of the hydrogen occupies only a small fraction of tube length (less than 1-in.). This is due to the small latent heat of vaporization as compared to the total enthalpy change of the hydrogen and due to the high temperature difference between the hydrogen and the Freon-21 at the hydrogen inlet of the heat exchanger. Hence, the dynamics of the two-phase flow regime have a small effect on the flow dynamics inside the heat exchanger tubes as long as uniform flow distribution is maintained. Uniform flow distribution is achieved by making the pressure drop in the inlet and outlet manifolds small relative to the core pressure drop (less than 20-percent). The high design point pressure drop on the hydrogen side is selected such that the core pressure drop remains appreciable relative to manifold pressure drop during the two-phase operation ($-420^{o}F$) when the hydrogen flow rate is much less than the design point value.

It was pointed out in the previous sections that flow instability on the warm fluid side could occur which would then cause freezing or congealing, even though calculations may show the wall temperature to be above freezing. It was shown that such flow instability is caused by the increased viscosity of the liquid with decreasing temperature which creates a negative slope of the pressure drop--flow rate curve.

Although the warm fluid outlet temperature in the present case is reasonably high (40°F), a very low tube wall temperature could cause this phenomenon to occur locally, i.e., very close to the tube wall. Hence, to overcome this possibility, two features are included in the heat exchanger design. The first feature is to maintain the tube wall at a temperature which does not cause an appreciable increase in the liquid viscosity (tube wall temperatures will be shown under the section dealing with the heat exchanger performance). The second feature is to maintain turbulent flow on the warm fluid side, especially, in the last two passes where the cryogen is at its lowest temperature. As shown in Section 3, turbulent flow reduces the adverse effect of viscosity on the pressure drop.

Drawing 168942 shows the configuration of the cryogenic heat exchanger which was fabricated for performance testing. Some minor changes were made to the test unit from the configuration shown. These changes were limited to the inlet and outlet lines in details such as length and inclusion of instrumentation ports. Figure 9-2 is a photograph of the completed test unit.

The active heat exchanger core is as defined in Figure 9-1. After layout of the tube pattern, a final selection of tube number, pattern and shell size was made which most closely matched the analytical design and minimized the bypass area between the shell and tube bundle. To ensure minimum bypass in this area, the baffle support channels (item 15 on the drawing) were formed in such a manner that excessive gaps between tubes and wall were eliminated.

Series 300 stainless steels were selected over aluminum for this application because of its inherent ductibility at cryogenic temperatures. Since the unit has appreciable thermal and pressure stresses during operation, and since local yielding may occur as a result of local stress concentrations, it is necessary to have a ductile material to ensure adequate fatigue life.

A stress analysis was conducted to define the required material gages and joint configurations in the high stress areas and ensure the adequacy of design. Of particular concern were the imposed stresses in the tubes and shell at the header and baffle interfaces due to combined thermal and pressure loading. The thermal loads were evaluated at the severest temperature conditions of -420°F hydrogen inlet and +125°F F-21 inlet. The pressure loads are based on a F-21 proof pressure level of 200 psig and a cryogen proof pressure level of 100 psig. The shell and header configuration shown on the drawing resulted from this analysis. An expansion joint was incorporated between the two cryogen inlet side headers to accept the differential thermal expansion of the tube bundle and shell.

The heat exchanger is fabricated using brazed and welded construction. Subsequent to fabrication, the heat exchanger was leak-checked to ensure no leakage on each fluid side at proof pressure levels. Prior to shipment to the test facility, thermocouples were installed in the header which forms the interface of the inlet cryogen to outlet F-21 in the last F-21 pass.

The dry weight of the heat exchanger is 7.7 lb. Although the core is close to optimum from a weight standpoint, some weight savings could be realized in the shell, manifold, and lines for a flight configuration design.

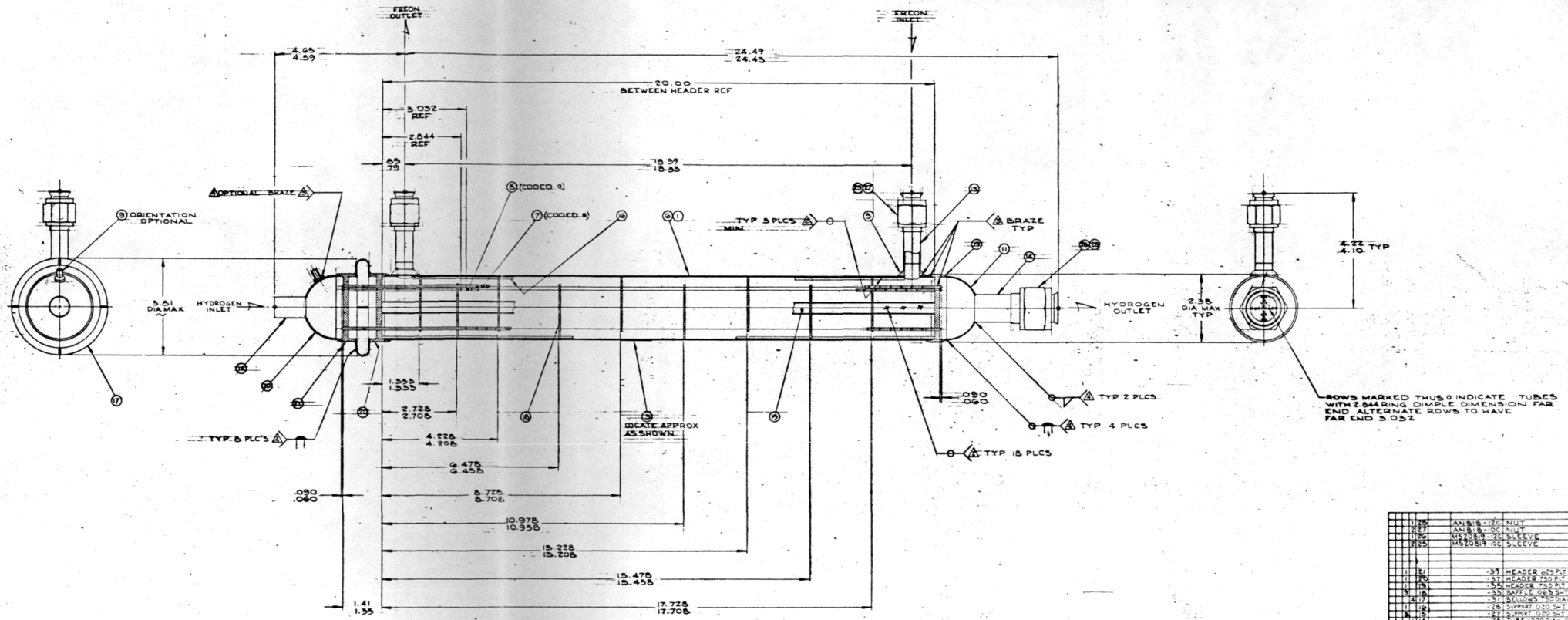

QTY REQD	ITEM NO.	CODE IDENT NO.	PART OR IDENTIFYING NO.	NOMENCLATURE OR DESCRIPTION	SPEC ZONE
2	25		AN816-12C	NUT	2
2	27		AN816-10C	NUT	2
2	26		MS20819-12C	SLEEVE	5
2	25		MS20819-10C	SLEEVE	5
1	21		.39	HEADER .625 PIT CRES 347 MIL-S-6721 COMP Cls	5,12
1	20		.67	HEADER .750 PIT CRES 347 MIL-S-6721 COMP Cls	5,10
1	19		.55	HEADER .750 PIT CRES 347 MIL-S-6721 COMP Cls	5,9
3	18		.55	BAFFLE .065 SHT CRES 321 MIL-S-6721 COMP Cls	5,9
4	17		.91	BELLOWS .750 DIA x .020 WALL MILT-8808	5,9
1	16		.28	SUPPORT .020 SHT CRES 347 MIL-S-6721 COMP Cls	4
1	15		.27	SUPPORT .020 SHT CRES 347 MIL-S-6721 COMP Cls	4
1	14		.25	TUBE .2000 AN .035 WALL MIL-T-8808	3,9
2	13		.25	TUBE .625 DIA x .035 WALL MIL-T-8808	3,9
1	12		.21	TUBE .750 DIA .035 WALL MIL-T-8808	3,9
1	11		.20	DOME .063 SHT CRES 347 MIL-S-6721 COMP Cls	5,7
1	10		.19	DOME .032 SHT CRES 347 MIL-S-6721 COMP Cls	5,7
1	9		.17	BOSS .375 DIA BAR CRES 347 QQ-S-763 CONDA	10,11
4	8		.16	TUBE .500 DIA x .035 WALL CRES 347	14,11
1	7		.15	TUBE .500 DIA x .035 WALL CRES 347	4,11
1	6		.14	SHELL .040 SHT CRES 347 MIL-S-6721 COMP Cls	4,8
2	5		.11	BOSS 1.000 DIA BAR CRES 347 QQ-S-763 CONDA	3,9
1	3		168935-1	IDENTIFICATION PLATE	4
1	1		-3	BRAZED ASSY	4

PARTS LIST

5. PRESSURE TEST HYDROGEN CIRCUIT TO 100 PSIG AND FREON CIRCUIT TO 200 PSIG

△ WELD

△ FURNACE BRAZE USING NICKEL BASE BRAZING ALLOY

△ SPOTWELD

1. ALL MACHINED SURFACES 125 NOTED UNLESS OTHERWISE SPECIFIED

FINAL

AIRESEARCH MANUFACTURING COMPANY

HEAT EXCHANGER ASSY CRYOGENIC

J 70210 168942

SCALE 1/1 SHEET 1 OF 1

168942 F

168942

9-6

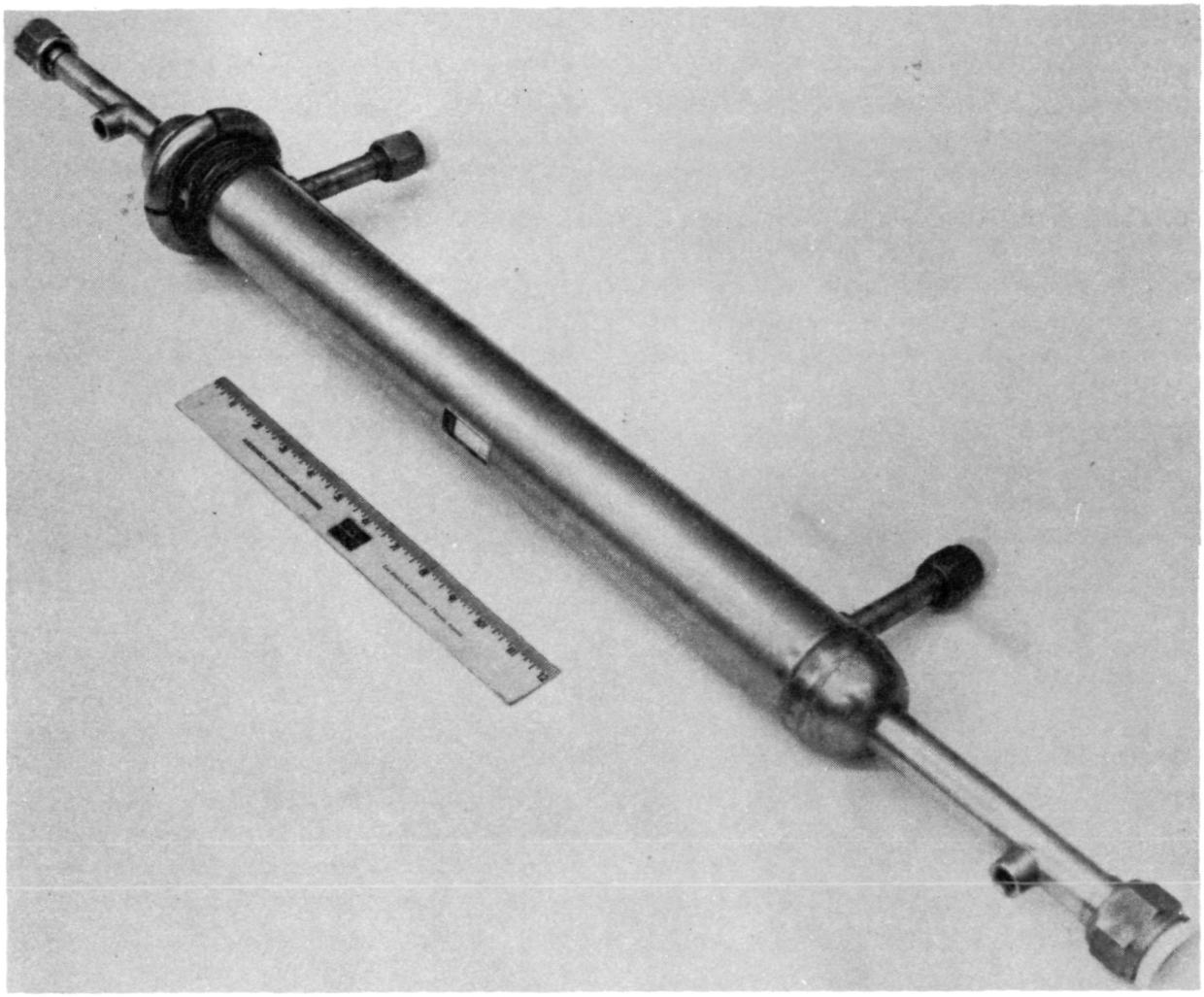

Figure 9-2. Cryogenic Heat Exchanger

SECTION 10

TEST SYSTEM AND TEST PROCEDURE

A schematic and photographs of the test system are shown in Figures 10-1 through 10-4. The system basically consists of two fluid loops. The Freon loop is a closed (recirculating) loop, whereas the hydrogen loop is a single-pass flow system. The hydrogen loop is further subdivided into three arrangements: one to supply $0^{o}F$ gas, a second to supply cryogenic liquid hydrogen, and a third to supply cryogenic hydrogen gas. Each of the three hydrogen arrangements was used in turn to supply appropriately conditioned hydrogen to the heat exchanger. The various loops are described in the following paragraphs.

FREON-21 LOOP

The Freon loop consists of an accumulator, pump, heat exchanger for heat input, temperature control valve, filter, drier, the heat exchanger under test, flow control valve and instrumentation. Thermocouple mixing cans are provided at the inlet and outlet of the test heat exchanger. Shutoff valves are provided to isolate the heat exchanger and thermocouples from the rest of the system. The individual components are described below.

Reservoir

The reservoir provides the liquid/gas separation, allows for thermal expansion of the liquid, and acts as a reservoir for the pump. Provisions for pressurizing, venting and charging the loop with liquid are provided as a part of the accumulator. A sight glass also is provided to determine the liquid level.

Flow and Temperature Control

Flow and temperature control is achieved by control valves which are automatically controlled from remote set points. Both control loops typically consist of e/i or cps/i converters, set point controllers, and i/p converters. Each controller has the typical functions of proportional band, rate and reset controls. The control valves are modulated by pneumatic actuators responding to the i/p converters.

The temperature control valve is a three-way modulated valve that mixes the hot Freon from the heat exchanger with cooler Freon which bypasses the heat exchanger.

The flow control valve is a straight modulating valve that accomplishes its function by throttling off the flow and back-pressurizing the pump. The flow control valve was originally installed between the steam heat exchanger and the test heat exchanger. Some difficulties were encountered and it was felt that they resulted from the pressure drop (approximately 50 psi) across the flow control valve, which induced Freon vaporization. To overcome this difficulty, the flow control valve was relocated to a point downstream of the test heat exchanger and the flow meter.

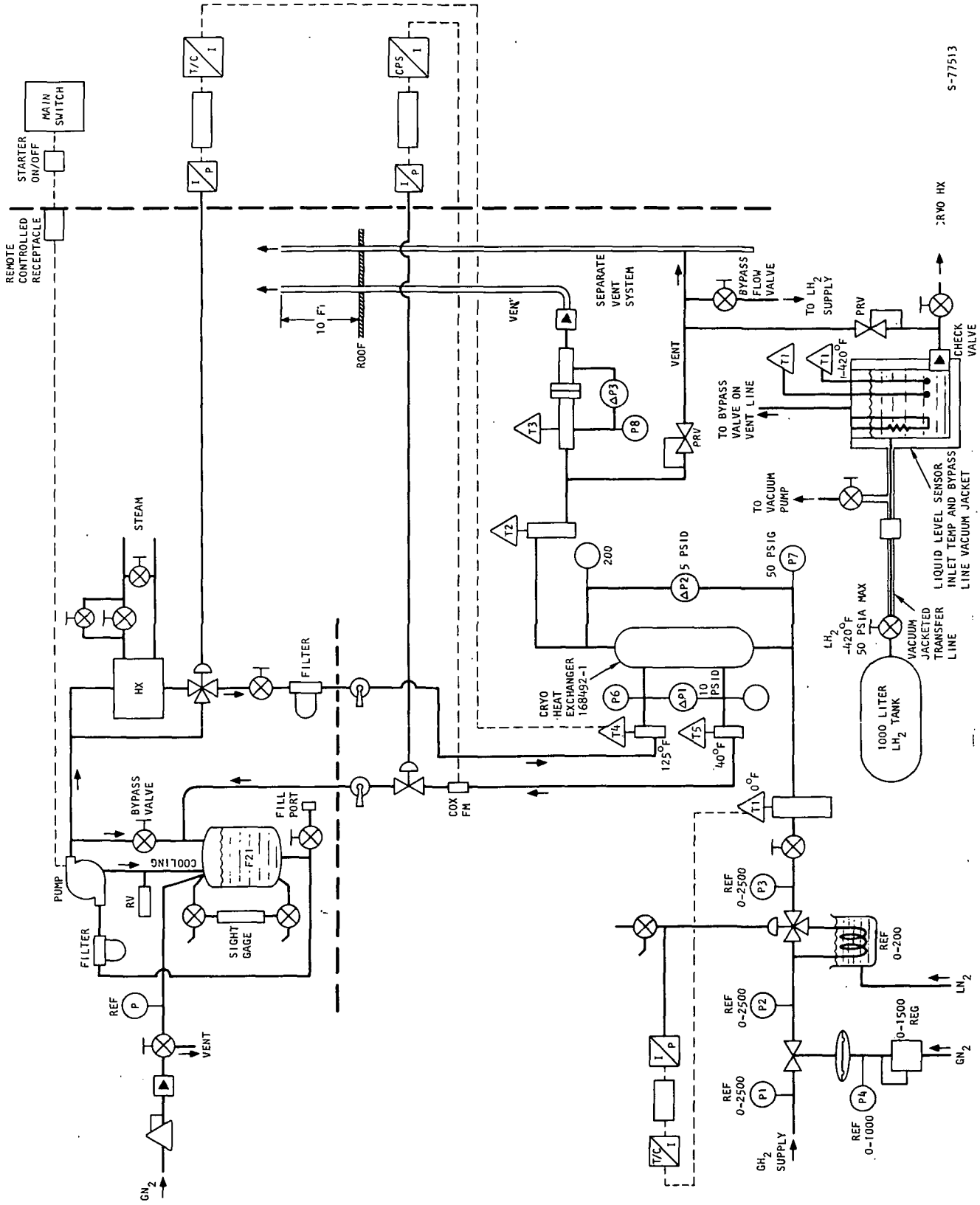

Figure 10-1. Test System Schematic

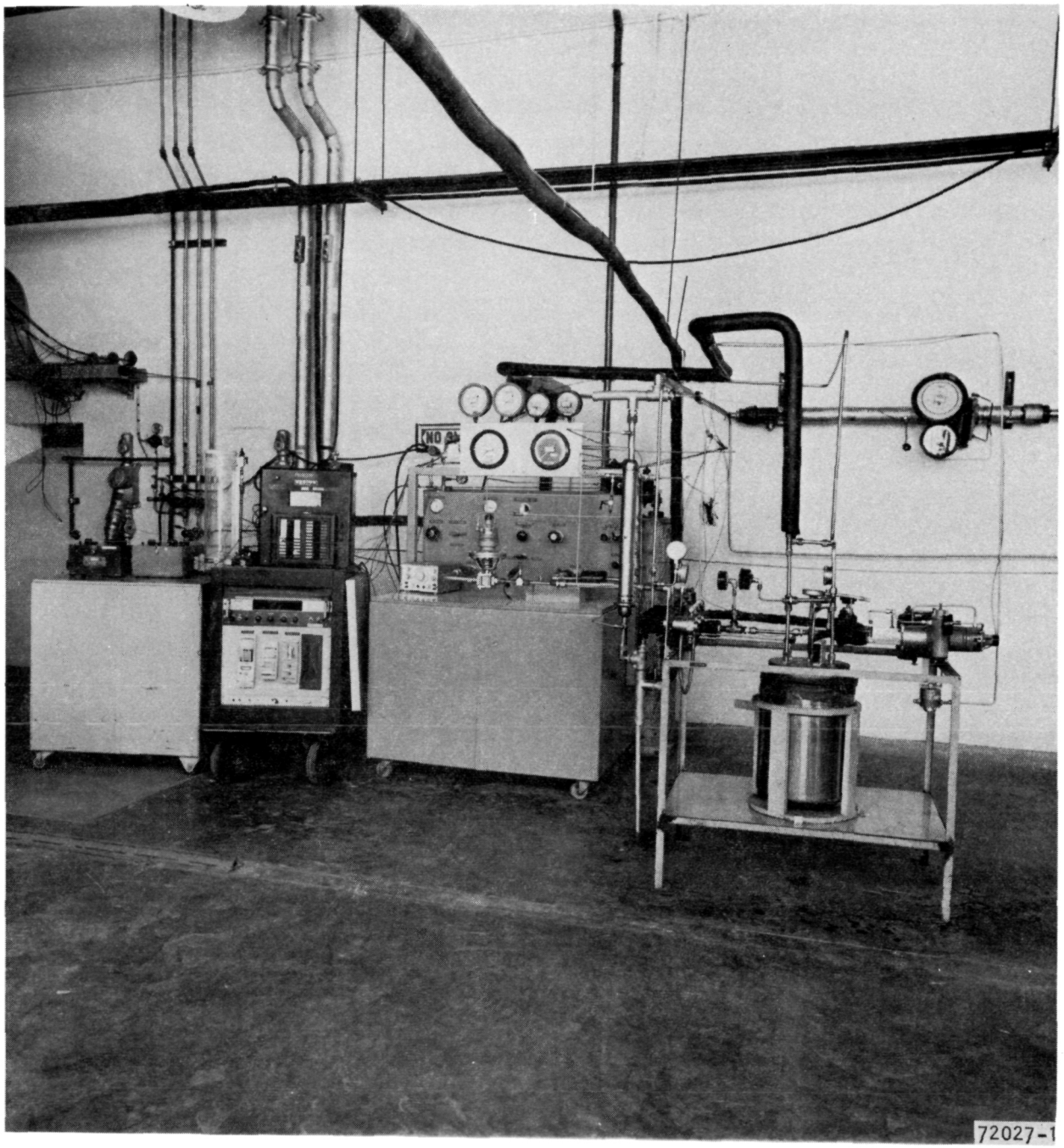

Figure 10-2. Test System Showing Liquid/Gas Separation Tank (Far Right) and Uninsulated Cryogenic Heat Exchanger

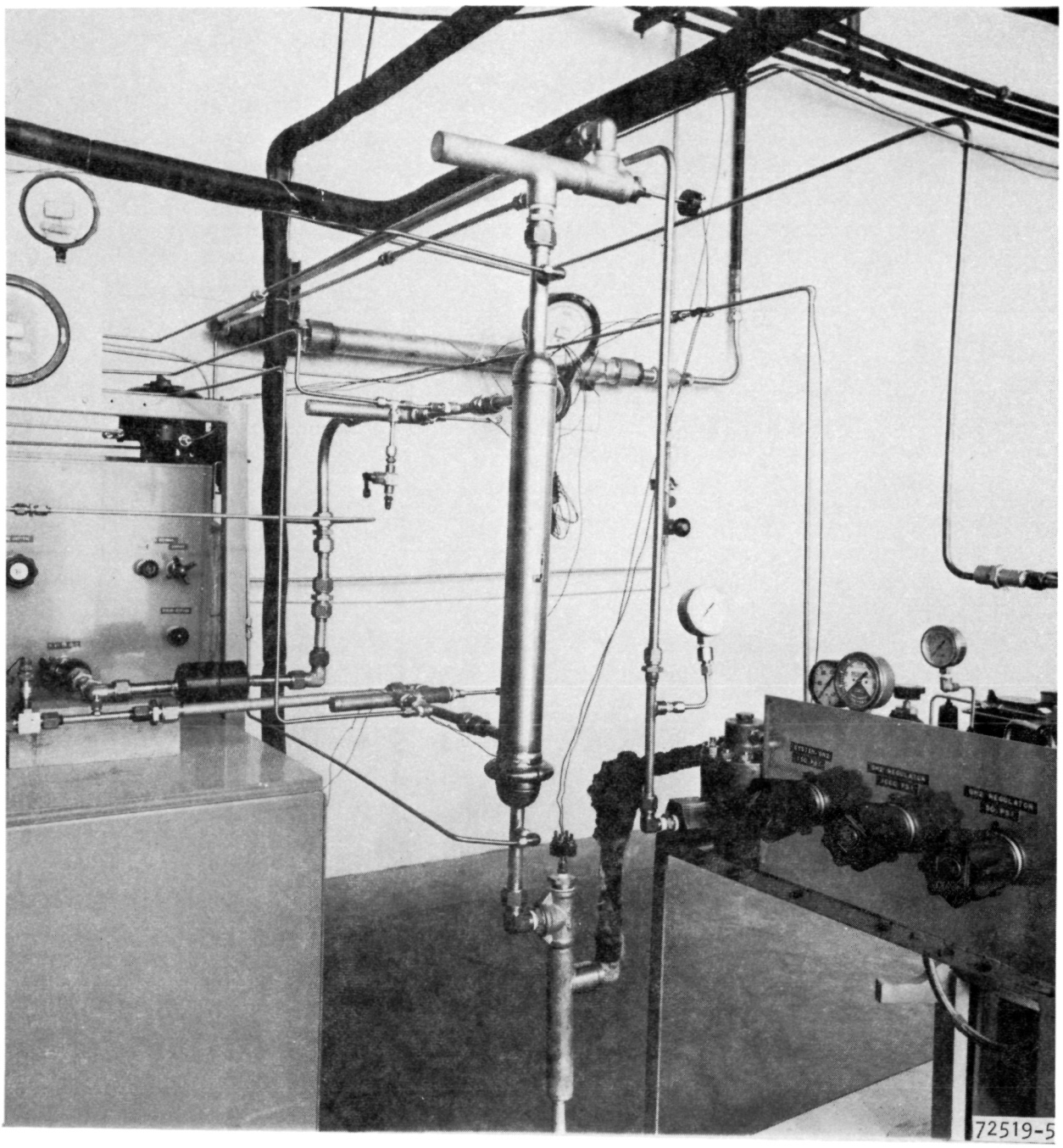

Figure 10-3. Cryogenic Heat Exchanger Mounted in Test System

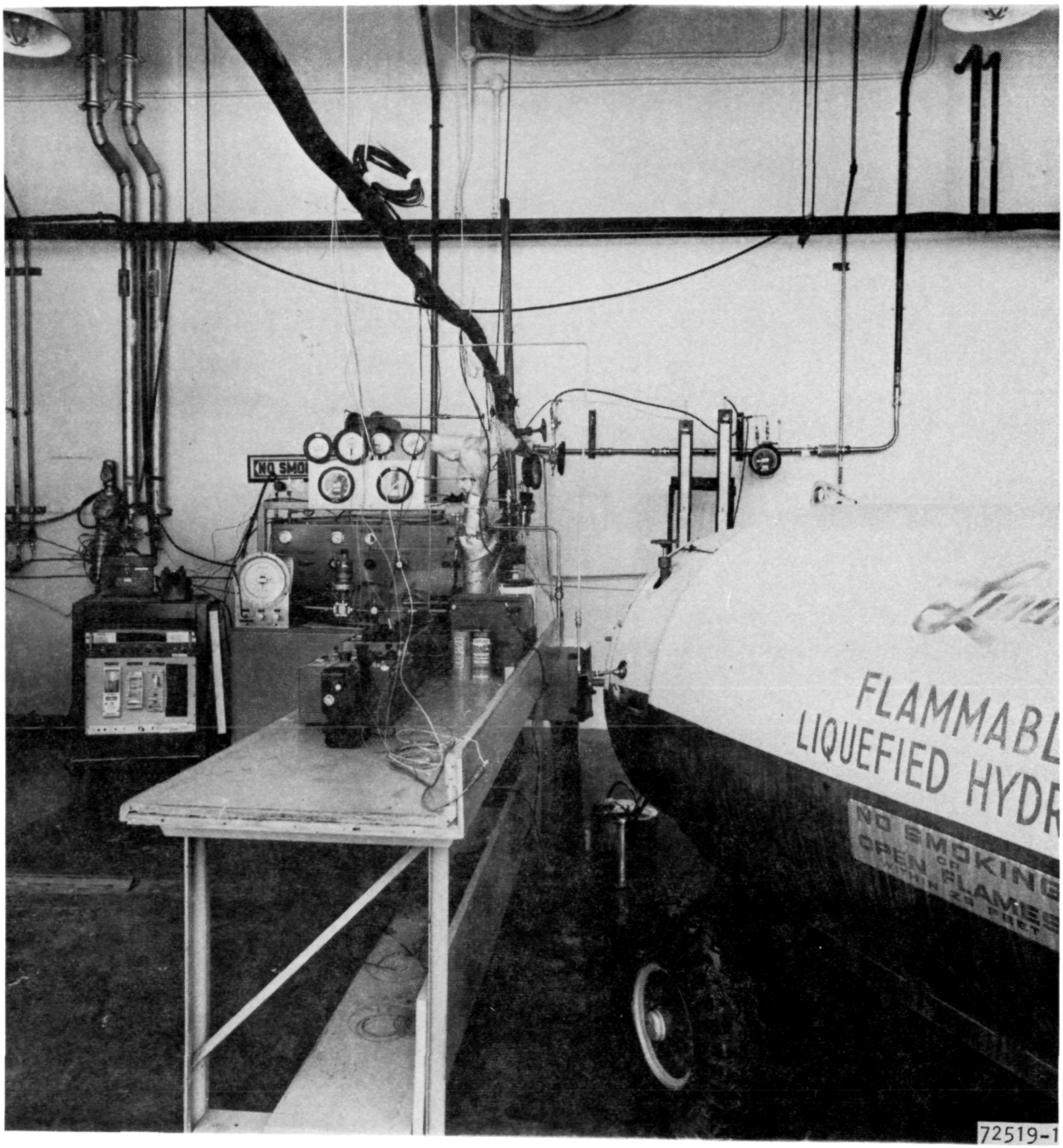

Figure 10-4. Test System Showing Cryogenic Hydrogen Tank, Insulated HX, and Part of Instrumentation

Heat Source Heat Exchanger

Heat is added to the Freon in a heat exchanger using condensing steam as the heat source. The steam is throttled down from the steam generator condition (120 psi and 350°F) to avoid raising the pressure in the Freon loop. A manually operated valving system is incorporated in the steam system to provide control of steam flow rate.

Freon Pump

The pump used for circulation of the Freon is a centrifugal Crane Chempump, Mod GB-3K-751-1S. Its inlet pressure is rated at 150 psi, and it is capable of approximately a 50-psi pressure rise.

Instrumentation

A description of the instrumentation listing the type, brand name, serial number, location, purpose, range and estimated accuracy for each item on the cryogenic HX is given in Table 10-1. A description of the Freon side instrumentation is given below.

1. Temperature Measurement

Both inlet and outlet temperatures of the Freon were measured by copper-constantan thermocouples mounted in fluid mixing chambers at the inlet and outlet of the test heat exchanger, as shown in Figure 10-1. Both thermocouples were read on a dual channel L & N pot. This instrument internally selects either of the two channels and uses internal reference compensation to read out directly in degrees F.

2. Pressure Measurement

The static pressure at inlet and outlet of the heat exchanger was measured by two Ashcroft pressure gauges, as indicated in Table 10-1. The pressure drop across the HX also was measured independently by a Barton pressure gauge.

Two pressure taps were used. The taps were located between the HX manifold and the temperature mixing unit (within 3 inches from the manifolds).

3. Flow Measurement

The Freon flow rate was measured by a Cox Model An-8 turbine type installed in the Freon system just downstream of the test heat exchanger and fluid mixing chamber. This is an ideal location as the temperature at this point is required to be always constant. Therefore, the need for elaborate temperature compensation was eliminated. A suitable K factor vs frequency calibration chart was obtained. From the chart, a K factor of 10233 cycles per gallon was determined and this value was used in all flow calculations.

TABLE 10-1

INSTRUMENTATION LIST

Type and Brand	Serial No.	Location	Purpose	Range	Accuracy	Certification Date
Freon Side Measurements						
L & N temperature pot	43B028	CryoHX	Inlet and outlet temperature	-100 to 1000°F	±0.5°F	11-21-72
Ashcroft pressure gauge	44E522	Freon inlet to HX	Freon inlet static pressure	0 to 200 psig	±0.25-percent FS	1-31-72
Ashcroft pressure gauge	44E581	Freon outlet of HX	Freon outlet static pressure	0 to 200 psig	±0.25-percent FS	11-16-72
Barton pressure gauge	44Q607	Cryo HX	Freon pressure drop	0 to 25 psid	±0.5-percent FS	1- 9-73
Eric digital counter, model 720	41A122	Cryo HX	Freon flow rate	0 to 9999 count	±0.1 percent	10-13-72
Hydrogen Side Measurements						
Rubicon millivolt pot	43D033	Cryo HX	Inlet and outlet hydrogen temperature	0 to 100 mv	±0.2-percent FS	1-30-73
Rubicon millivolt pot	43E041	Inside inlet header	Header temperature	0 to 100 mv	±0.2-percent FS	1-11-73
Minimite temperature pot	43B122	Flow measuring section	Hydrogen flow rate	-340 to 400°F	±0.5°F	10- 7-72
L & N temperature pot	43B077	Liquid/inpot separation tank	Liquid or vapor temperature	-440 to 150°F	±0.5°F	11-10-72
M/D pressure gauge	44Q392	Inlet to HX	Hydrogen inlet static pressure	0 to 200 psig	±0.3-percent FS	11-30-72
Master test pressure gauge	44Q839	Outlet of HX	Hydrogen outlet static pressure	0 to 100 psig	±1.-percent FS	11-14-72
Barton pressure gauge	44Q040	Cryo HX	Warm gaseous hydrogen pressure drop	0 to 50 psid	±0.5-percent FS	1-31-73
Barton pressure gauge	44Q036	Cryo HX	Cryogenic hydrogen pressure drop	0 to 5 psid	±0.5-percent FS	1-25-73
Barton pressure gauge	44Q039	Flow measuring section	Hydrogen flow rate	0 to 30 in. H_2O	±0.5-percent FS	10-30-72
Barton pressure gauge	44Q527	Flow measuring section	Hydrogen flow rate	0 to 100 in. H_2O	±0.5-percent FS	10-30-72
Meriam manometer	44P091	Flow measuring section	Hydrogen flow rate	0 to 60 in. H_2O	±0.5-percent FS	N/A
W & T pressure gauge	44S669	Flow measuring section	Hydrogen flow rate	0 to 120 in. Hg	±0.5-percent FS	1-24-73
Simpson 260 meter	42Q325	Liq./vap. separation tank (up)	Determine hydrogen phase	0 to 250 v	-	N/A
Simpson 270 meter	42Q316	Liq./vap. separation tank (down)	Determine hydrogen phase	0 to 250 v	-	N/A

HYDROGEN LOOPS

Warm Gas Loop

The hydrogen gas was supplied from the facility high-pressure containers, which are plumbed into the test cell and then regulated down to the desired pressure.

The hydrogen flow was split into two paths, as shown in Figure 10-1, one of which went through coils in a liquid nitrogen bath. The second path by-passed the cooler. Just downstream of the cooler the two paths were reunited in a three-way temperature control valve which was modulated to control the hydrogen inlet temperature from a set point controller. Downstream of the three-way valve, the flow passed through a manually modulated flow control valve which regulated the amount of hydrogen to the heat exchanger.

Cryogenic Liquid Loop

Liquid hydrogen was supplied in a 1000-liter trailer-type dewar. The liquid was pressurized to approximately 30 psi for transfer purposes by means of auxiliary facility plumbing. The liquid was transferred to the test plumbing through a dewar shutoff valve and a vacuum jacketed transfer hose.

The cryogen then passed to a vacuum-jacketed separation tank, designed and built by AiResearch (Figures 10-1 and 10-5). The gas phase was then gravity-separated from the liquid and passed through a port in the top and through a manually operated bypass valve to a separate vent system. The liquid passed through a port in the lower portion of the tank and through a check valve. The separation tank also contained dual chromel-constantan thermocouples aligned with the lower liquid discharge port for temperature measurement. Liquid/gas sensors (one in the bottom of the separation tank and another in the gas bypass vent at the top) were also installed. The purpose of these is to determine the phase of the cryogen in the top and bottom of the separation tank, thereby permitting adjustment to assure relatively pure liquid being delivered to the heat exchanger. The hydrogen then passed through a manual cryogenic long stem flow control valve, and then vertically upward through the test heat exchanger.

Downstream of the test heat exchanger, the same mixing container used for warm testing was used, except the thermocouple probes were changed to chromel-constantan. Next, the hydrogen passed through a manually operated flow control valve. This valve was installed to control the flow for cryogenic testing only.

Finally, the hydrogen passed through thin plate orifice measuring section, the check valve and facility vent stack.

Other miscellaneous purge and pressure relief safeguards also were incorporated into the hydrogen loop, but their presence did not affect the performance of the loop while under test, so they will not be further discussed.

(A) - VENT STACK
(B) - TOP PLATE
(C) - FEEDTHROUGH AND TC BOSSES (2)
(D) - LIQUID SENSORS
(E) - INNER SEPARATOR TUBE
(F) - SUPPLY TUBE AND BAYONET
(G) - DELIVERY TUBE
(H) - SEPARATOR BOTTOM
(I) - SEPARATOR JACKET
(J) - SUPPLY TUBE JACKET
(K) - VACUUM TUBE
(L) - VACUUM VALVE
(M) - CHECK VALVE
(N) - CV JACKET
(O) - CV JACKET END PLATE

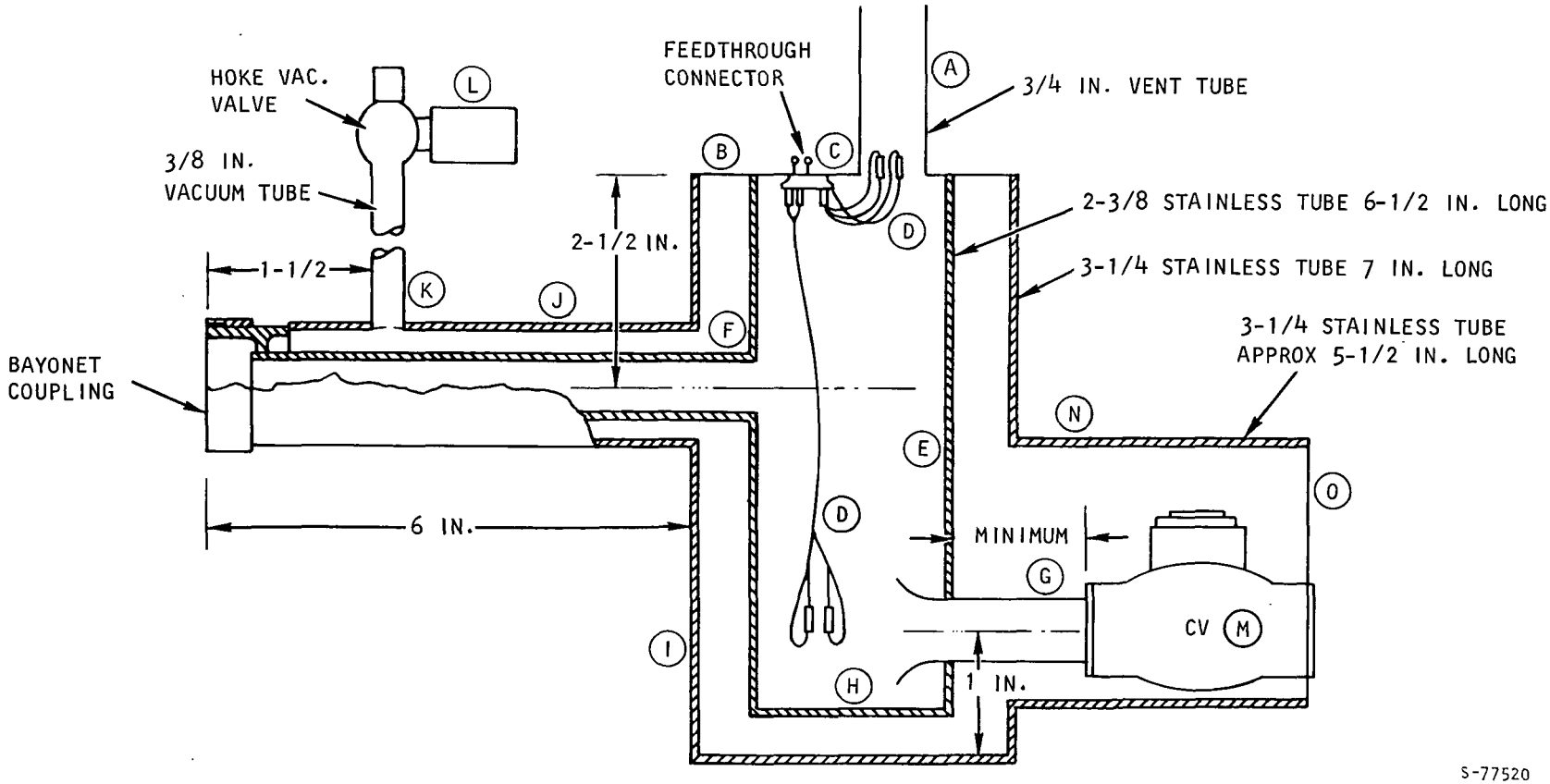

Figure 10-5. Hydrogen Liquid/Vapor Separation Tank

The test heat exchanger H, including all temperature mixing units, were wrapped with strips of fiberglass insulation. The hydrogen inlet between the separation tank and the heat exchanger was encapsulated with foam-in-place polyurethane insulation. The hydrogen plumbing upstream, including the separation tank was all vacuum-jacketed.

Cryogenic Vapor Loop

Cryogenic hydrogen vapor was obtained by drawing the gas phase hydrogen from the 1000-liter hydrogen trailer vent system. The dewar was maintained at pressure by introducing controlled hydrogen gas into what is normally the liquid delivery port. In all other respects the plumbing was identical to that used in cryogenic liquid testing.

Instrumentation

A list of the instrumentation used on the hydrogen side of the heat exchanger is included in Table 10-1. A brief description of these measurements is given below.

1. Temperature Measurement

The inlet and outlet hydrogen temperatures were measured in temperature mixing sections immediately upstream and downstream of the heat exchanger, respectively. Iron-constantan thermocouples were used during warm hydrogen testing (0 to 125°F). Chromel-constantan thermocouples were used during cryogenic testing for its superior millivolt output and lower thermal conductivity at cryogenic temperatures. Boiling liquid nitrogen was used as a reference junction. Both inlet and outlet temperatures were read on the same Rubicon millivolt pot to improve the accuracy of the temperature drop.

Two chromel-constantan thermocouples were mounted on the inside inlet header and were read on a separate Rubican millivolt pot. These temperatures should be representative of the tube wall inlet temperature during cryogenic testing.

2. Pressure Measurement

The inlet and outlet hydrogen static pressures were measured by M/D and Master Test pressure gauges (see Table 10-1). The pressure differential across the same two pressure taps was measured by two Barton pressure gauges depending on the pressure drop range.

During cryogenic testing, the hydrogen inlet pressure tap consisted of a long, 3/32-in. dia. line wrapped loosely several times around the main hydrogen duct. The purpose of this was to minimize the heat leak into the inlet duct.

3. Flow Measurement

The hydrogen flow rate was measured by a thin-plate orifice measuring section located downstream of the HX. As various flow levels were being tested, two sizes of orifices and three ranges of pressure drop gauges were used. This allowed the determination of the hydrogen flow rate with optimum accuracy.

TEST PROCEDURE

Thermocouple Calibration

Prior to any testing, all thermocouples used for temperature measurement were each individually removed and dipped in an ice water bath, and water at 120°F, 160°F, 180°F and 200°F. Water temperature was monitored with a certified mercury in glass thermometer with accuracy of ±0.2°F.

Wherever a reference junction was required for cryogenic temperature measurements, a reference junction of boiling liquid nitrogen was used. Millivolt charts were adjusted for the boiling point of liquid nitrogen at the prevailing altitude of the Mint Canyon Facility.

For cryogenic testing, all pertinent hydrogen thermocouples were changed to chromel-constantan calibration, as mentioned before. Prior to testing, each thermocouple was subjected to an individual test in boiling water, ice water, liquid nitrogen, and finally for the pertinent thermocouples, liquid hydrogen.

Freon Loop Operation

(a) To ensure single-phase liquid, the pressure level in the Freon loop was kept above 150 psi.

(b) As a standard operating procedure the Freon flow was first established before allowing the hydrogen to flow. This was essential during cryogenic testing to prevent any Freon freezing in the heat exchanger.

(c) The Freon flow rate was adjusted to the desired value which was constant during all tests.

(d) A certain amount of hydrogen was introduced to bring the Freon outlet temperature in the range of 40 to 60°F.

(e) The desired inlet Freon temperature was adjusted using the steam heat source heat exchanger and the temperature control system.

(f) Hydrogen flow rate was increased and adjusted to give a Freon outlet temperature of 40°F.

(g) After stable conditions were reached, all temperature, pressure and flow data were recorded.

(h) Freon inlet temperature was adjusted to the next test point conditions.

(i) Shutdown procedures consisted of, first, shutting off the hydrogen flow, then shutting off the steam to the heating heat exchanger. The Freon was allowed to flow until the system was at approximately 60 to 70°F.

Hydrogen Loop Operation

(a) In general, the same test procedures were used in all three types of hydrogen testing. The hydrogen flow was not initiated until the Freon flow was well established.

(b) In the case of the warm hydrogen, the temperature was controlled at 0°F by an automatic temperature control circuit, and the flow was manually adjusted to meet the Freon temperature requirements. In both cryogenic phases, the hydrogen temperature was not controlled but was a resultant of either the saturation temperature in the case of the liquid, or the lowest that could be delivered in the case of the gas testing.

(c) In the cryogenic testing, the set conditions were approximately established with the hydrogen bypass shutoff. This was to conserve the hydrogen test fluid. When conditions approached nominal settings, the bypass valve was opened until the gas phase sensor in the separation tank indicated liquid passing out of the bypass. This assured nearly pure liquid hydrogen being delivered to the heat exchanger. Usually this caused the Freon outlet temperature to drop about another degree. As soon as conditions were stable, data was taken and the bypass flow was shutoff. Flow was then either shutoff to adjust optimum measuring section arrangements, or the Freon temperature adjusted to the next level, and testing continued.

SECTION II

TEST RESULTS AND DISCUSSION

The cryogenic heat exchanger was tested in the vertical position with the hydrogen flowing vertically upward. The testing program consisted of three main phases:

Isothermal pressure-drop measurement

Testing with warm gaseous hydrogen (inlet temperature around $0^{\circ}F$)

Testing with cryogenic hydrogen (liquid and vapor).

The results of each of these test phases will be presented and discussed in the following paragraphs.

ISOTHERMAL PRESSURE-DROP MEASUREMENT

The pressure drop on both the Freon and hydrogen sides of the heat exchanger were measured separately during isothermal operation (no heat transfer). The results are presented in Tables 11-1 and 11-2 for the Freon and hydrogen, respectively.

The isothermal pressure drops of Freon-21 were obtained at a temperature of $105^{\circ}F$, with no hydrogen flowing inside the tubes. The data was obtained over a Freon flow-rate range of 24 to 72 lb/min. The design point was 46.7 lb/min.

The isothermal pressure drops of hydrogen were obtained at a temperature of $0^{\circ}F$, with no Freon flowing outside the tubes. The hydrogen flow rate ranged from 0.85 to 2.85 lb/min. The design point condition was about 2.5 lb/min.

The isothermal pressure-drop data for Freon and hydrogen are also presented in Figures 11-1 and 11-2, respectively, together with theoretical predictions. The data points shown in Figure 11-2, for the case of hydrogen, correspond to the pressure drop from inlet to outlet manifold ΔP, and are related to the measured pressure drop ΔP_m by the following relationship (see Figure 11-3).

$$\Delta P = \Delta P_m - (\Delta P_a + \Delta P_b) \qquad (11\text{-}1)$$

where ΔP_a is the pressure drop in expanding from the inlet duct to inlet manifold and ΔP_b is the pressure drop in contracting from outlet manifold to output duct. Both ΔP_a and ΔP_b would be small if sufficiently large ducts were used. The duct sizes used on the hydrogen side in the present case were dictated by the plumbing of the test loop and resulted in significant values for $(\Delta P_a + \Delta P_b)$ as shown in Table 11-2.

TABLE II-I

ISOTHERMAL PRESSURE DROP OF FREON-21

Run No.	Freon Flow Rate lb/min	Inlet Pressure psig	Inlet Temperature °F	Outlet Pressure psig	Outlet Temperature °F	Pressure Drop psi
1	24.75	145.0	104	144.0	104	1.20
2	27.77	154.0	105	152.5	105	1.40
3	38.5	163.0	105	160.5	105	2.30
4	48.82	167.0	105	164.0	106	3.70
5	54.02	173.0	106	169.5	106	3.70
6	59.21	193.0	108	189	108	4.20
7	62.6	181.0	106	176.5	106	4.70
8	69.11	188.0	107	179.4	107	5.50
9	72.02	194.0	108	188.0	108	5.90

TABLE II-2

ISOTHERMAL PRESSURE DROP OF HYDROGEN

Measured Variables							Calculated Variables			
Run No.	H_2 Flow Rate lb/min	Inlet Press. psig	Inlet Temp. °F	Outlet Press. psig	Outlet Temp. °F	Pressure Drop psi	Inlet & Outlet Ducts ΔP, psi	Core ΔP psi	σ	σ ΔP (Core) psi
1	.85	5.5	0.0	3.4	0.0	2.15	0.81	1.34	1.25	1.82
2	1.340	11.5	0.0	7.3	0.0	4.20	1.75	2.45	1.74	4.26
3	1.8450	18.6	0.0	12.2	0.0	6.30	2.36	3.94	2.20	8.67
4	2.175	23.8	0.0	16.1	0.0	7.70	2.84	4.86	3.06	14.90
5	2.650	30.2	0.0	20.7	0.0	9.55	3.57	6.0	2.95	17.7
6	2.850	34.5	8.0	24	8.0	10.40	3.77	6.63	3.28	21.8

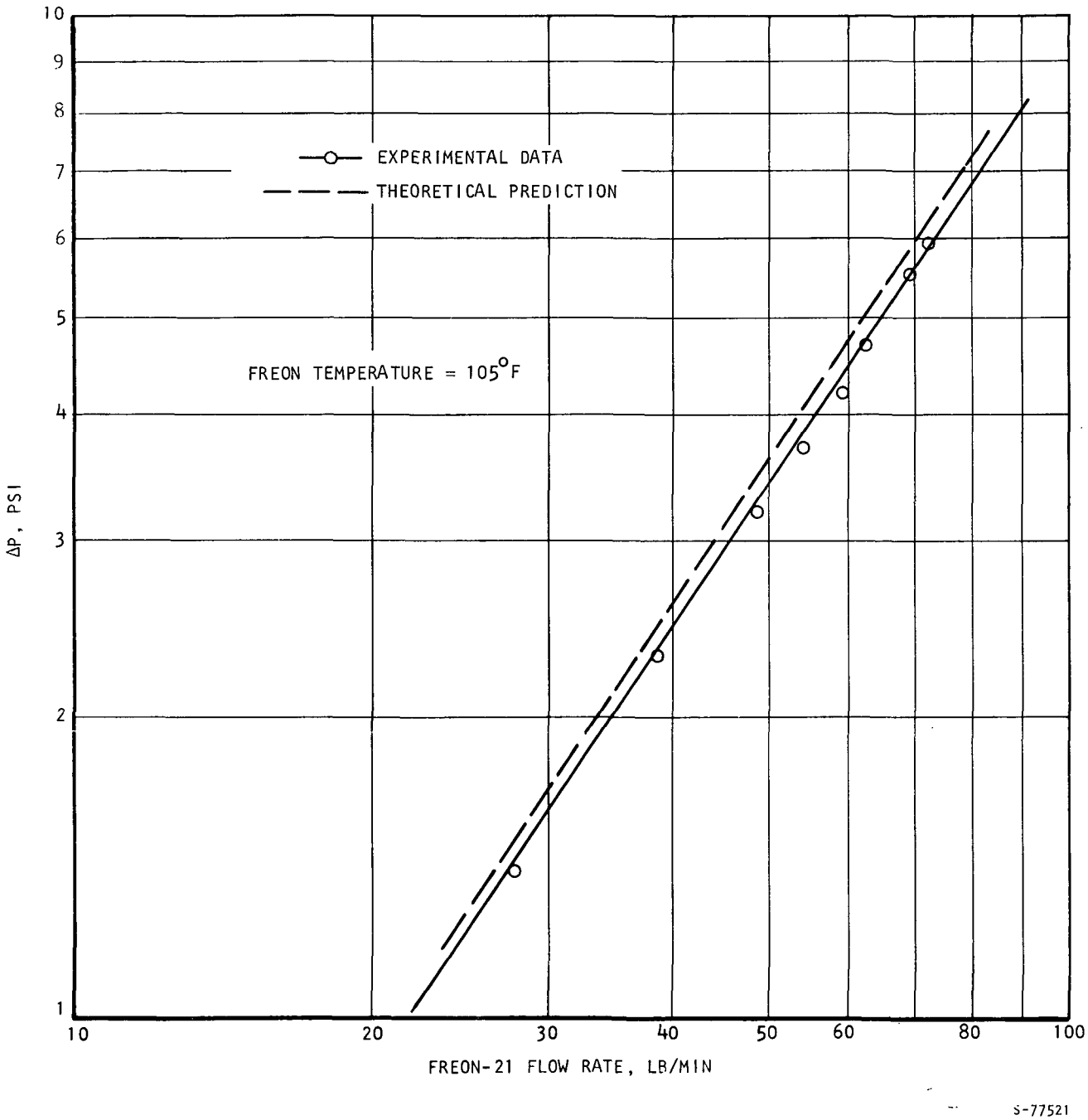

Figure 11-1. Isothermal Pressure Drop of Freon-21

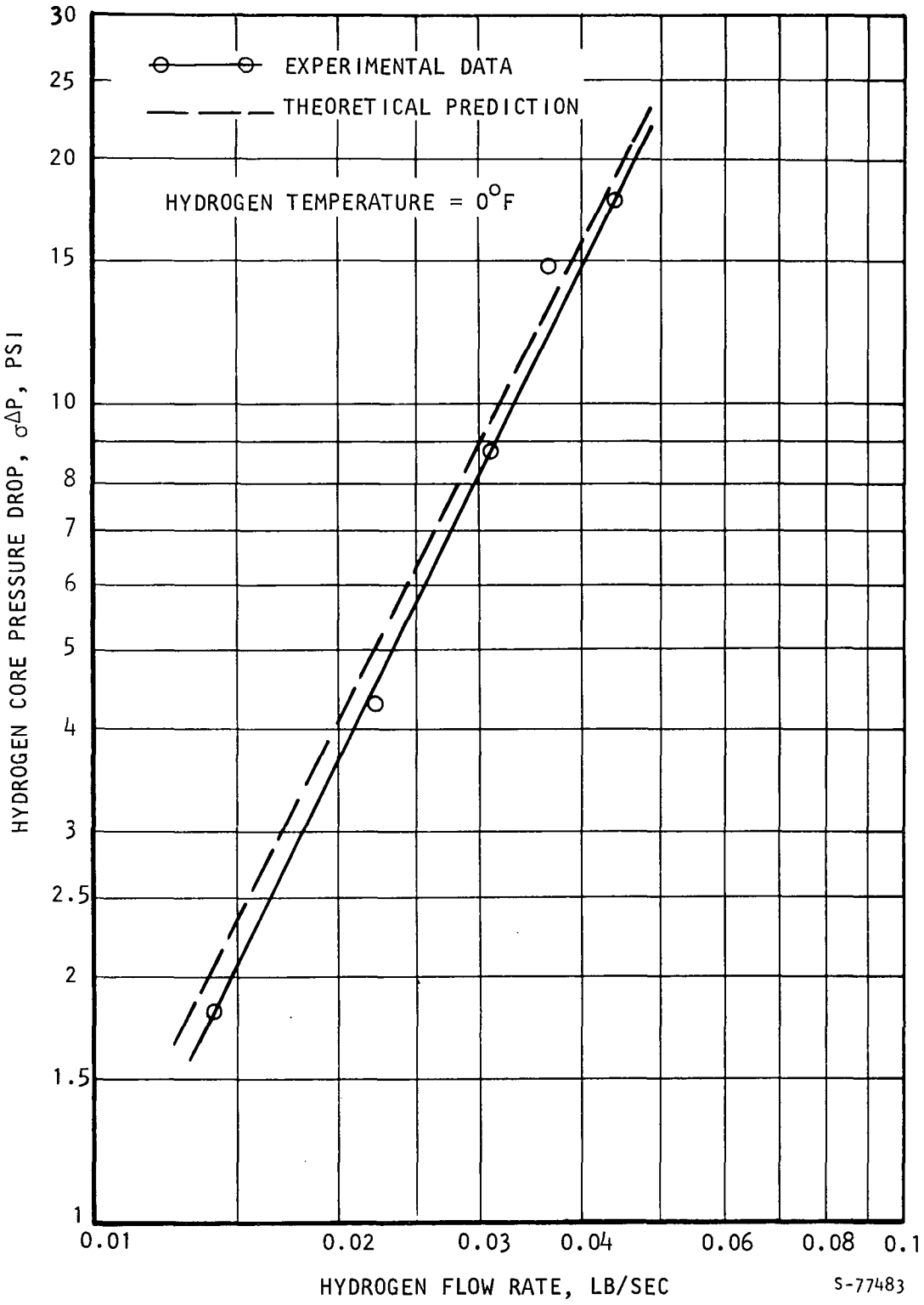

Figure 11-2. Isothermal Hydrogen Pressure Drop

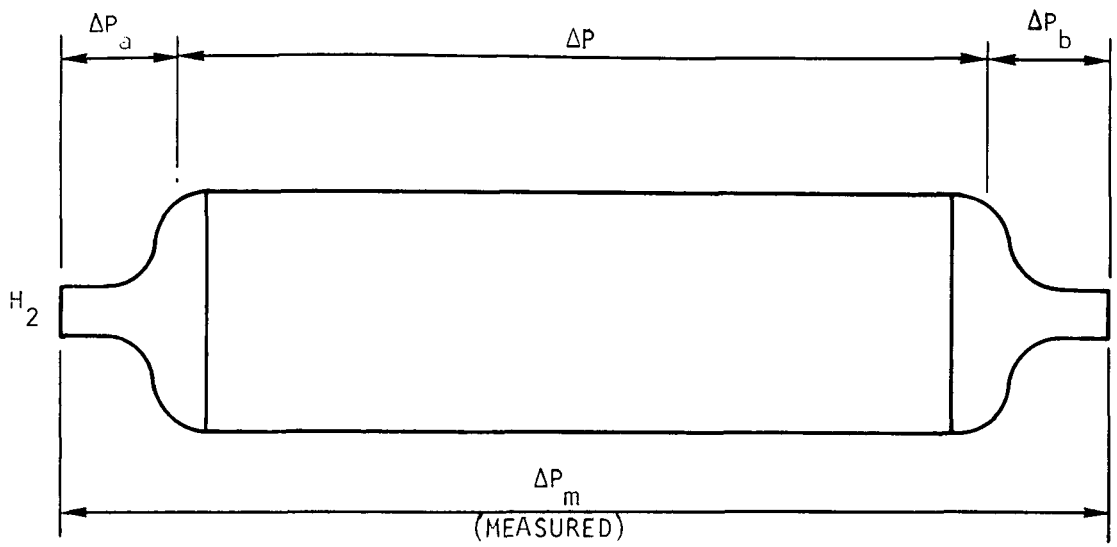

ΔP_a = INLET DUCT TO MANIFOLD PRESSURE DROP

ΔP_b = MANIFOLD TO OUTLET DUCT PRESSURE DROP

S-77517

Figure 11-3. Schematic of ΔP_m Versus ΔP for Hydrogen Warm Gas

The agreement between theoretical predictions and experimental data is good with a deviation of about six percent in case of the Freon flowing outside the tube bank and of eight percent in case of hydrogen gas flowing inside the tubes. The predictions were in general higher than the data, and should yield conservative designs.

TESTING WITH WARM GASEOUS HYDROGEN (INLET TEMPERATURE AROUND $0^{\circ}F$)

The second phase of testing was directed towards warm gaseous hydrogen. The test data for this case is summarized in Table 11-3. The controlled variables during this testing are:

Freon-21 inlet temperature

Freon-21 flow rate (constant during all runs)

Freon-21 inlet static pressure

Hydrogen inlet temperature (approximately constant during all runs)

Hydrogen flow rate

Hydrogen inlet pressure

The measured variables are:

Freon-21 outlet temperature

Freon-21 outlet static pressure

Freon-21 pressure drop

Hydrogen outlet temperature

Hydrogen outlet static pressure

Hydrogen pressure drop

The heat load was calculated from the data on either side of the heat exchanger by the following equation

$$Q = W\ Cp\ (T_1 - T_2) \qquad (11\text{-}2)$$

where W is the flow rate, Cp is the specific heat, T_1 and T_2 are the inlet and outlet temperatures.

The hydrogen flow adjustment was done manually to meet the heat load requirement as dictated by the Freon-21 inlet temperature. The objective was always, except for two runs, to adjust the hydrogen flow rate to maintain the Freon-21 around $40^{\circ}F$.

TABLE II-3

TEST DATA FOR HYDROGEN INLET TEMPERATURE AROUND 0°F

Run No.	Hydrogen Conditions							Freon-21 Conditions						
	Flow Rate lbs/min	Inlet Temp. °F	Outlet Temp. °F	Inlet Press. psia	Outlet Press. psia	Press. Drop psi	Heat Load BTU/hr	Flow Rate lbs/min	Inlet Temp. °F	Outlet Temp. °F	Inlet Press. psia	Outlet Press. psia	Press. Drop psi	Heat Load BTU/hr
1	0.904	1.	55	19.07	17.2	1.87	10,500	46.76	56	41	115.9	113.4	2.75	10,400
2	0.99	0.	68	21.1	17.7	3.	14,500	46.26	68	48.5	176.4	172.9	3.	13,500
3	1.018	2.	123	21.8	18.3	3.4	26,500	44.72	125	86	164.4	161.4	3.	27,400
4	1.3	0.	59.5	21.9	18.4	3.5	16,700	46.92	61	44	139.4	134.9	4.5	11,900
5	1.530	2.5	77	29.4	23.4	5.2	24,500	46.88	77	40	150.9	147.7	3.25	26,000
6	1.71	2.	78	31.9	25.4	6.15	28,000	46.77	82.5	41	201.4	197.9	3.4	30,000
7	1.71	-2.	82	31.6	25.4	6.10	30,800	46.6	82	40	194.4	191.4	3.25	29,300
8	2.08	1.	95	37.4	29.9	7.65	41,600	46.8	102	41.5	183.4	179.9	3.2	43,400
9	2.2	6.	103	39.4	31.4	8.1	47,600	46.77	108	41	119.9	107.4	3.4	47,500
10	2.55	3.	113	45.4	35.4	9.4	64,000	46.67	125	40	109.4	106.6	3.75	60,000

The reduced data is summarized in Table 11-4. The Freon-21 side and the hydrogen side temperature effectivenesses are calculated from the raw data by the following equations

$$\text{Freon Effectiveness} = \frac{T_{F1} - T_{F2}}{T_{F1} - T_{H1}} \tag{11-3}$$

$$\text{Hydrogen Effectiveness} = \frac{T_{H2} - T_{H1}}{T_{F1} - T_{H1}} \tag{11-4}$$

where T_{F1} = inlet Freon temperature

T_{F2} = outlet Freon temperature

T_{H1} = inlet hydrogen temperature

and

T_{H2} = outlet hydrogen temperature

The heat exchanger UA was calculated on the basis of the heat load and the log mean temperature difference, ΔT_m, i.e.

$$UA = \frac{Q}{\Delta T_m} \tag{11-5}$$

The ΔT_m was based on pure counter flow charts which is a good approximation for the present 10 pass cross-counter flow HX. The value of UA was determined on the basis of the heat loads shown in Table 11-3 for both the hydrogen and Freon sides which resulted, for some runs, in the two UA values listed in Table 11-4.

The parameter σ is

$$\sigma = \frac{\rho}{\rho_s} \tag{11-6}$$

where ρ is the average hydrogen gas density in the HX and ρ_s is the standard density for air.

The HX core $\sigma\Delta P$ on the hydrogen side corresponds to the pressure drop from inlet to outlet manifold and excludes the pressure drops in the inlet and outlet ducts as explained before.

TABLE II-4

REDUCED DATA FOR HYDROGEN INLET TEMPERATURE AROUND 0°F

Run No.	Hydrogen Flow Rate, lbs/sec	Freon Side Effectiveness	Hydrogen Side Effectiveness	UA BTU/hr °F	Inlet & Outlet Duct Pressure Drop, psi	Hydrogen Core Pressure Drop, psi	σ	σΔP (Core) psi
1	.015	.273	.98	1000	1.	0.87	1.30	1.13
2	.0165	.25	~1.	1230 to 1320	1.02	1.98	1.36	2.7
3	.017	.317	.984	1230	1.1	2.3	1.33	3.06
4	.0217	.278	.975	1340	1.7	1.8	1.42	2.56
5	.0255	.495	~1.0	2950	1.8	3.4	1.87	5.35
6	.0285	.515	.943	1780 to 1910	2.1	4.05	2.02	8.2
7	.0285	.5	~1.	2790	2.1	4.	2.02	8.08
8	.0347	.6	.932	2100 to 2280	2.65	5.	2.35	11.75
9	.036	.656	.95	3120	2.6	5.5	2.45	13.50
10	.0425	.69	.9	2500 to 2690	3.4	6.	2.79	16.7

The test data is presented in Figures 11-4 to 11-7 together with the theoretical predictions.

Figure 11-4 shows the heat rejection rate, (heat load) versus the hydrogen flow rate. The experimental results show that, to meet the desired maximum heat rejection rate of 60,000 BTU/hr, a hydrogen flow rate of about 0.041 lb/sec (248 lb/hr) is required. This is in excellent agreement with the predicted results.

The hydrogen core pressure drop versus hydrogen flow rate is shown in Figure 11-5. At maximum heat load conditions, i.e., at a hydrogen flow rate of 0.041 lb/sec, the hydrogen core pressure drop is about 6 psi.

The hydrogen side effectiveness is shown in Figure 11-6 at different flow rates. At a flow rate of 0.041 lb/sec the hydrogen side effectiveness is 0.91 which exceeds the design value of 0.9. At lower hydrogen flow rates the hydrogen side effectiveness was quite high and in some cases very close to one.

The heat exchanger UA is presented in Figure 11-7. The scatter of the data points in this case is significant. This is due to the inaccuracy in calculating the ΔT_m for cases where the hydrogen effectiveness is close to one. The rest of the data, however, are in good agreement with the theoretical prediction.

TESTING WITH CRYOGENIC HYDROGEN

The test data for this case is summarized in Table 11-5. The inlet hydrogen conditions range from 37°R liquid to 95°R vapor. The controlled and measured variables were essentially the same as for the case of warm gaseous hydrogen tests. The hydrogen liquid phase condition was determined by the liquid/vapor separation tank described previously.

An additional measured variable in this case is the inside inner header temperature. This temperature was measured at two locations in the header and it should be representative of the inlet tubes' wall temperature in areas which are in contact with the Freon-21.

The reduced data is given in Table 11-6. The Freon-21 and hydrogen side effectiveness were calculated using equations 11-3 and 11-4. This includes a certain approximation in case of liquid hydrogen at the inlet because of the two-phase portion shown in Figure 11-8. However, since the hydrogen latent heat of vaporization is a small fraction of the total enthalpy change in the HX (less than ten percent), equation 11-4 should be a good approximation.

The hydrogen core pressure drop is determined from the measured ΔP in the same manner explained before.

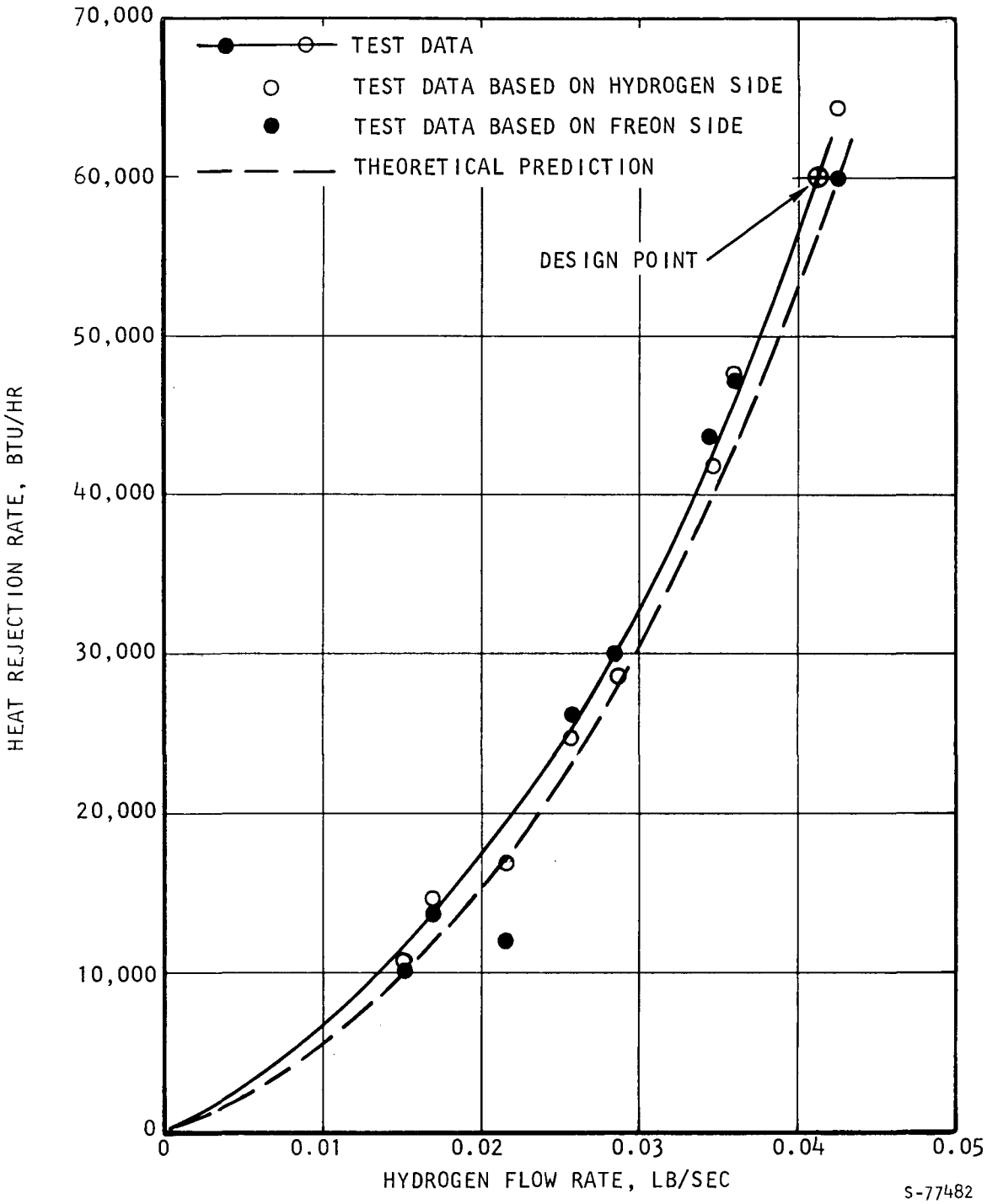

Figure 11-4. Heat Rejection Rate vs Hydrogen Flow Rate
Hydrogen Inlet Temperature Is $0^{\circ}F$

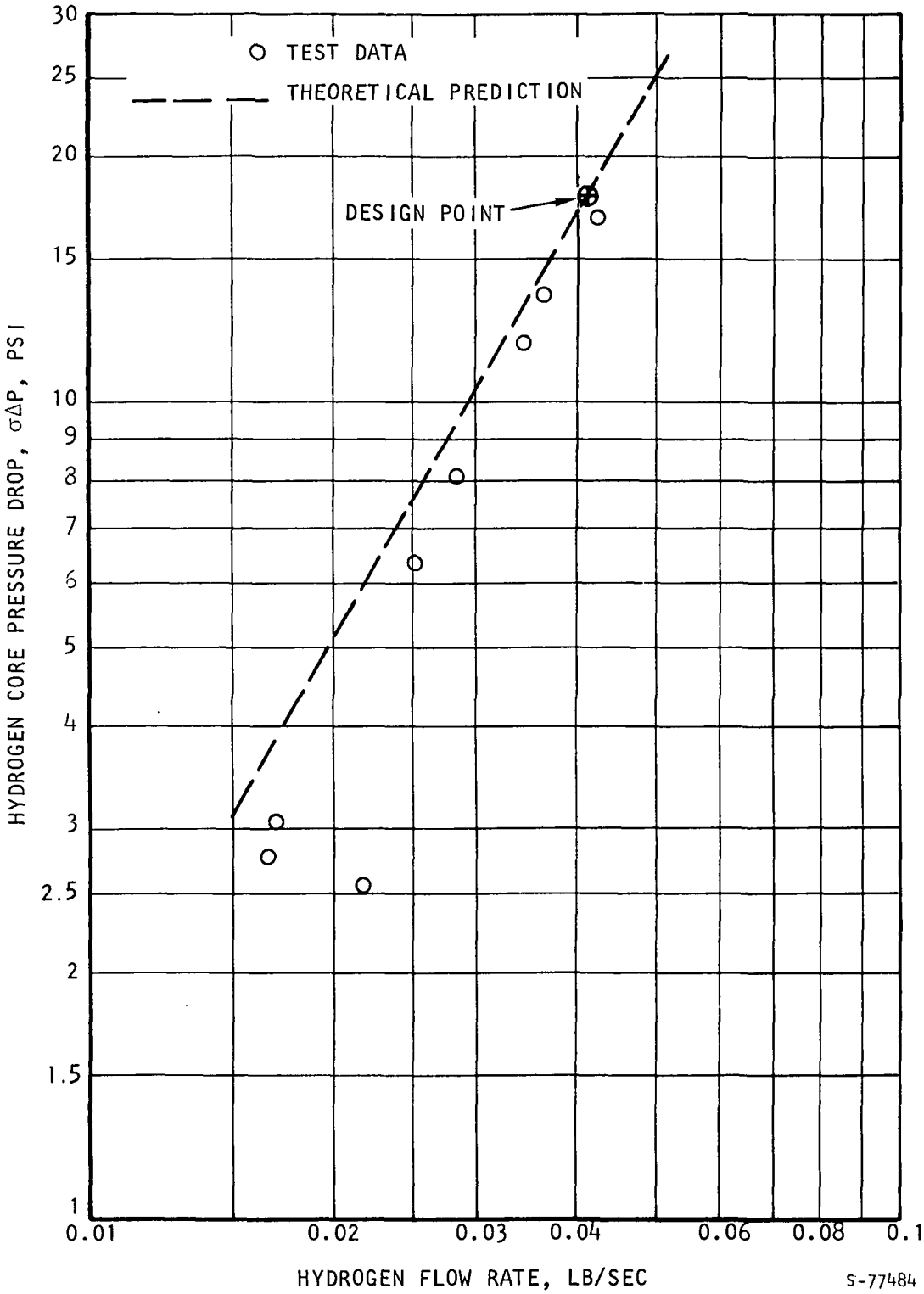

Figure 11-5. Hydrogen Pressure Drop Versus Hydrogen Flow Rate (Hydrogen Inlet Temperature Is 0°F)

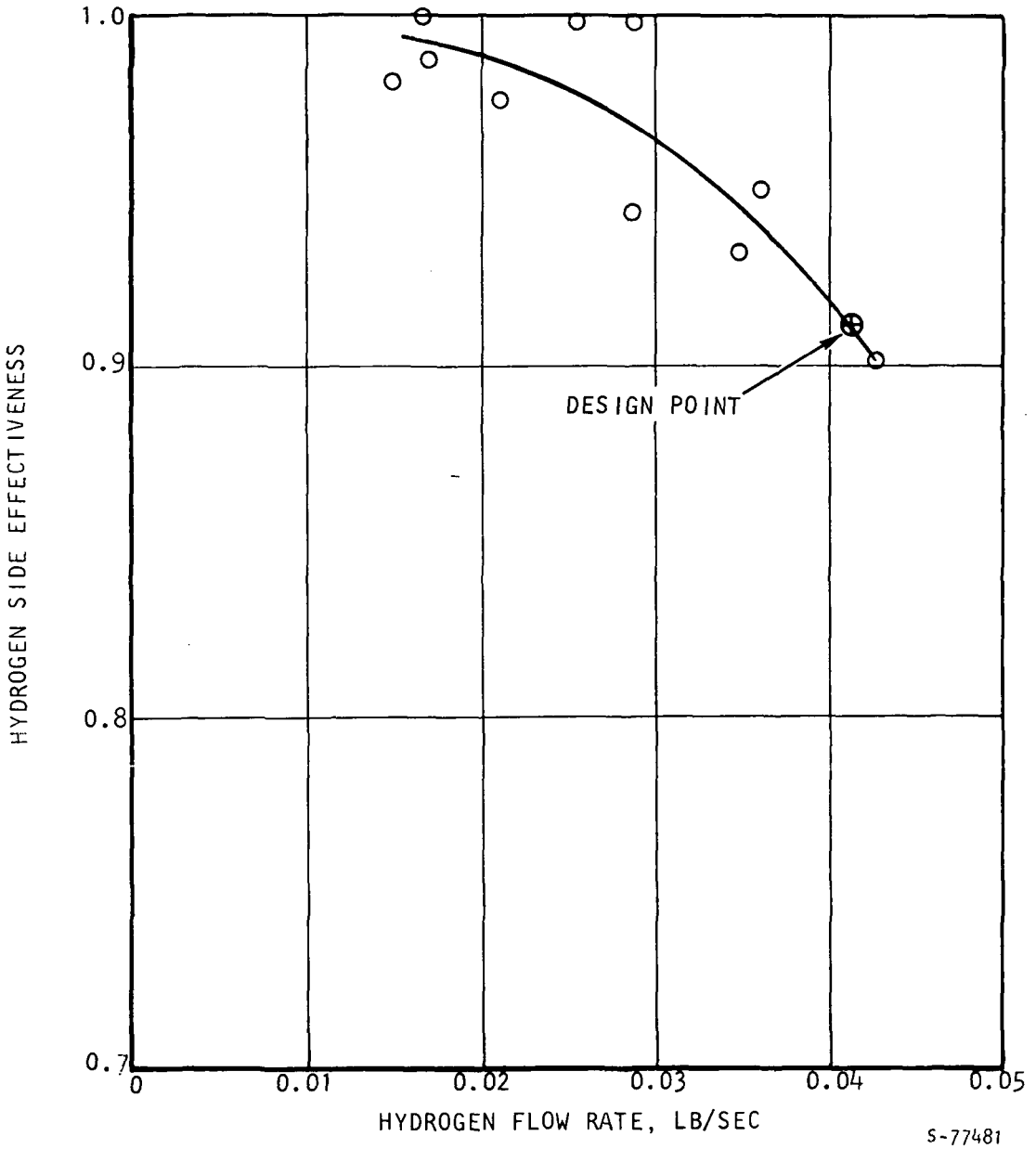

Figure 11-6. Hydrogen Side Effectiveness Versus Hydrogen Flow Rate (Hydrogen Inlet Temperature Is 0°F)

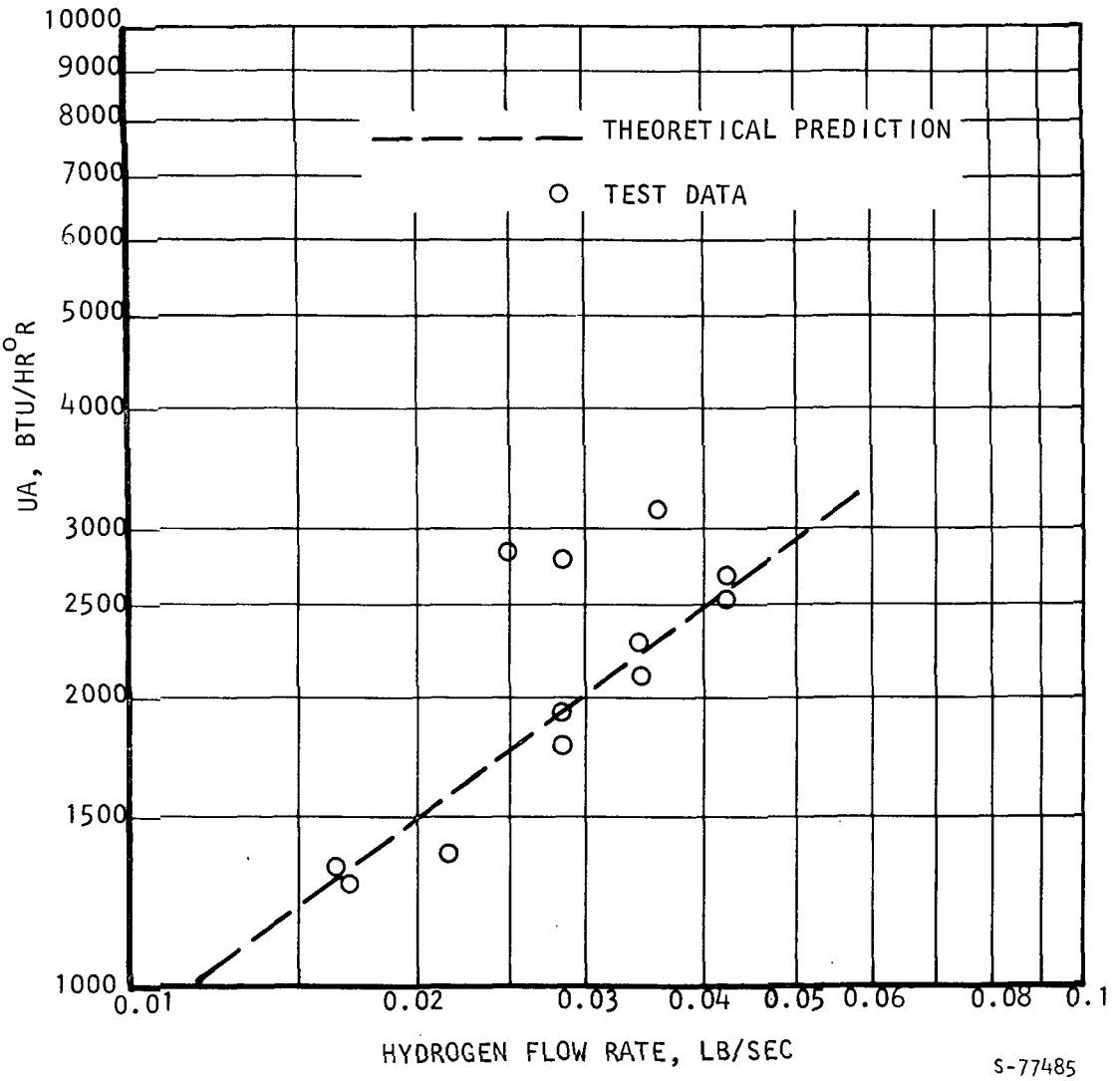

Figure 11-7. Available UA Versus Hydrogen Flow Rate (Hydrogen Inlet Temperature Is 0°F)

TABLE II-5

TEST DATA FOR HYDROGEN AT CRYOGENIC INLET TEMPERATURES

Run No.	Hydrogen Conditions								Freon-21 Conditions						
	Flow Rate lbs/min	Inlet Temp. °R	Outlet Temp. °R	Inlet Press. psia	Outlet Press. psia	Press Drop psi	Heat Load BTU/hr	Header Temp. °R	Flow Rate lbs/min	Inlet Temp. °R	Outlet Temp. °R	Inlet Press. psia	Outlet Press. psia	Press. Drop psi	Heat Load BTU/hr
1	.118	37.3[1]	499	26.85	26.85	-	12,500	-	46.86	516	499	135.65	131.35	3.2	12,000
2	.177	95.[2]	522.75	37.15	35.35	.06	16,100	408-427	46.88	523.	500	184.9	180.4	3.2	16,500
3	.248	51.[2]	541.5	27.1	24.8	-	28,300		46.98	542.	501	131.3	125.3	3.25	28,900
4	.31	82.[2]	541	35.5	34.45	.13	29,600	395-419	46.88	542.5	500	192.4	187.9	3.2	30,000
5	.38	43.[1]	562.5	25.3	24.3	.2	45,500		46.84	563.	501	160.	156.	3.2	44,000
6	.425	55.[2]	561	28.48	25.8	.3	43,400	388-416	46.74	561.5	500	184.4	181.4	3.	43,600
7	.47	40.[1]	585	25.6	24.2	.6	58,200	380-414	46.84	585.5	501	163.	157.5	3.4	60,000
8	.56	72.[2]	584	27.95	25.4	.67	60,000	384-416	46.87	586.	502	181.4	175.9	3.4	60,000

[1] Liquid
[2] Vapor

TABLE II-6

REDUCED DATA FOR HYDROGEN AT CRYOGENIC INLET TEMPERATURES

Run No.	Hydrogen Flow Rate lbs/sec	Freon Side Effectiveness	Hydrogen Side Effectiveness	UA BTU/hr °F	Inlet and Outlet Duct Pressure Drop, psi	Core Pressure Drop psi	σ	σΔP (Core) psi
1	.00197[1]	.0357	.967	135	-	-	-	-
2	.00297[2]	.054	.999	275	.015	.045	4.15	.187
3	.00413[2]	.084	.998	350	-	-	-	-
4	.00515[2]	.092	.992	365	.045	.085	4.	.33
5	.0064[1]	.12	.998	530	.068	.132	2.86	.38
6	.0071[2]	.12	.999	600	.1	.2	3.14	.628
7	.0078[1]	.155	.999	710	.107	.493	3.	1.48
8	.00935[2]	.164	.995	790	.2	.47	2.88	1.36

[1] Liquid

[2] Vapor

The values of the HX UA were calculated from the raw data using equation 11-5. These values may not be very meaningful in this case because of the non-linearity of the hydrogen specific heat over the range of the temperature in the HX and because of the very steep temperatures rise in the first portion of the tubes as shown in Figure 11-8.

The performance of the HX at cryogenic temperatures is depicted in Figures 11-9 to 11-11, both by experimental data and theoretical predictions.

The predicted performance was obtained by dividing the HX into three sections along the hydrogen path in case of liquid hydrogen as shown in Figure 11-8. In case of vapor H_2 the HX was divided into two sections only. This procedure represented an approximate method to account for the non-linearity of the specific heat over the hydrogen temperature range in the HX.

The first section of the HX for liquid hydrogen corresponds to the two-phase portion and this is a small fraction of the overall length. The hydrogen temperature in this section is nearly uniform. The second section is assumed to occupy about twenty percent of the overall length of the HX and the third section corresponds to the rest of the HX.

The results for the heat rejection rate versus the hydrogen flow rate are shown in Figure 11-9. The analytical prediction was carried out assuming liquid hydrogen at $40^{\circ}R$ at inlet to the heat exchanger. The liquid data is in agreement with the prediction. The vapor data is included in the figure for comparison purposes and is generally lower than the prediction as expected. To meet the maximum heat load condition (60,000 Btu/hr) a liquid hydrogen at $40^{\circ}R$ and a flow rate of 0.0085 lb/sec (30.7 lb/hr) is required.

The hydrogen core pressure drop ($\sigma\Delta P$) is presented in Figure 11-10. The data in most cases are below the theoretical predictions. The pressure drop in this case is considerably lower than the available pressure drop due to the small hydrogen flow rates required. The scatter in the data is attributed to an experimental inaccuracy due to observed pressure fluctuations which, in some cases, were comparable to the pressure drop in the heat exchanger.

Finally, the UA versus hydrogen flow rate is shown in Figure 11-11. The predictions shown were based on hydrogen vapor at the inlet, i.e., it neglected the two-phase portion. This should not constitute any appreciable error because the two-phase portion is only a small fraction of the HX.

DISCUSSION

The performance of the HX was shown to meet the desired performance at all operating conditions from $0^{\circ}F$ gaseous hydrogen at inlet to $40^{\circ}R$ liquid (or vapor hydrogen) at inlet. In all cases the test data agreed with the predicted performance, which gives confidence in the analytical techniques used in the design and performance prediction of cryogenic heat exchangers.

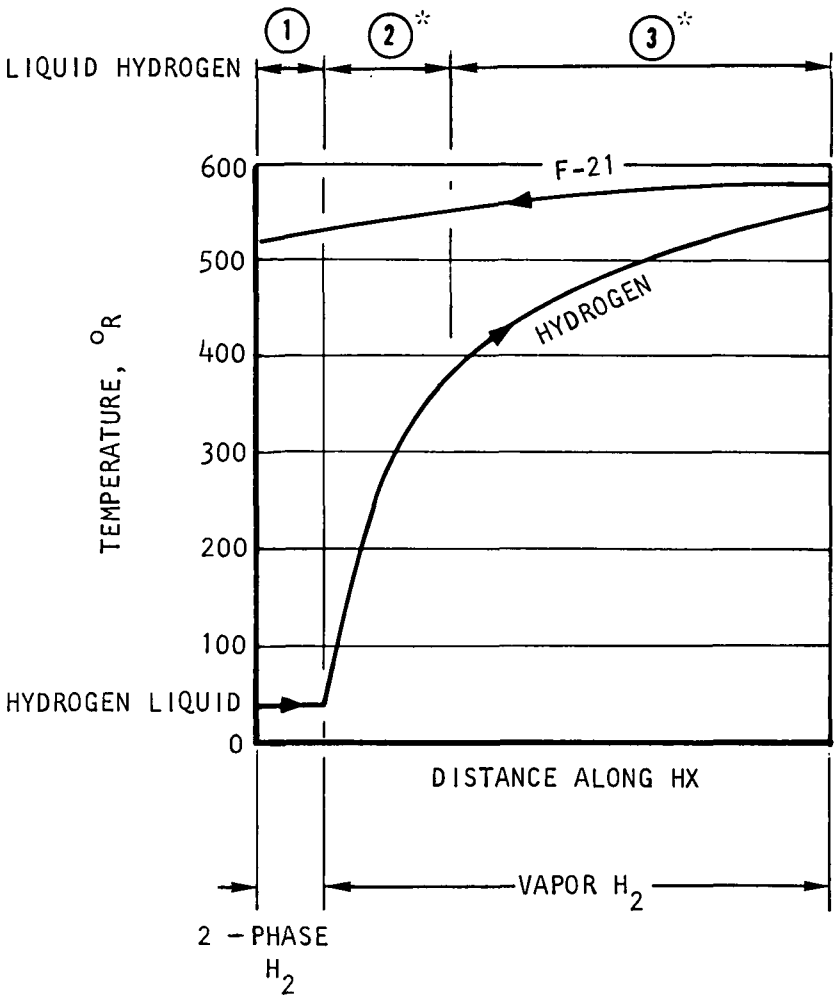

S-77514

*SPECIFIC HEAT IS ASSUMED CONSTANT AT ITS AVERAGE VALUE OVER SECTIONS 2 AND 3 FOR PERFORMANCE PREDICTIONS

Figure 11-8. Temperature Profiles Along HX

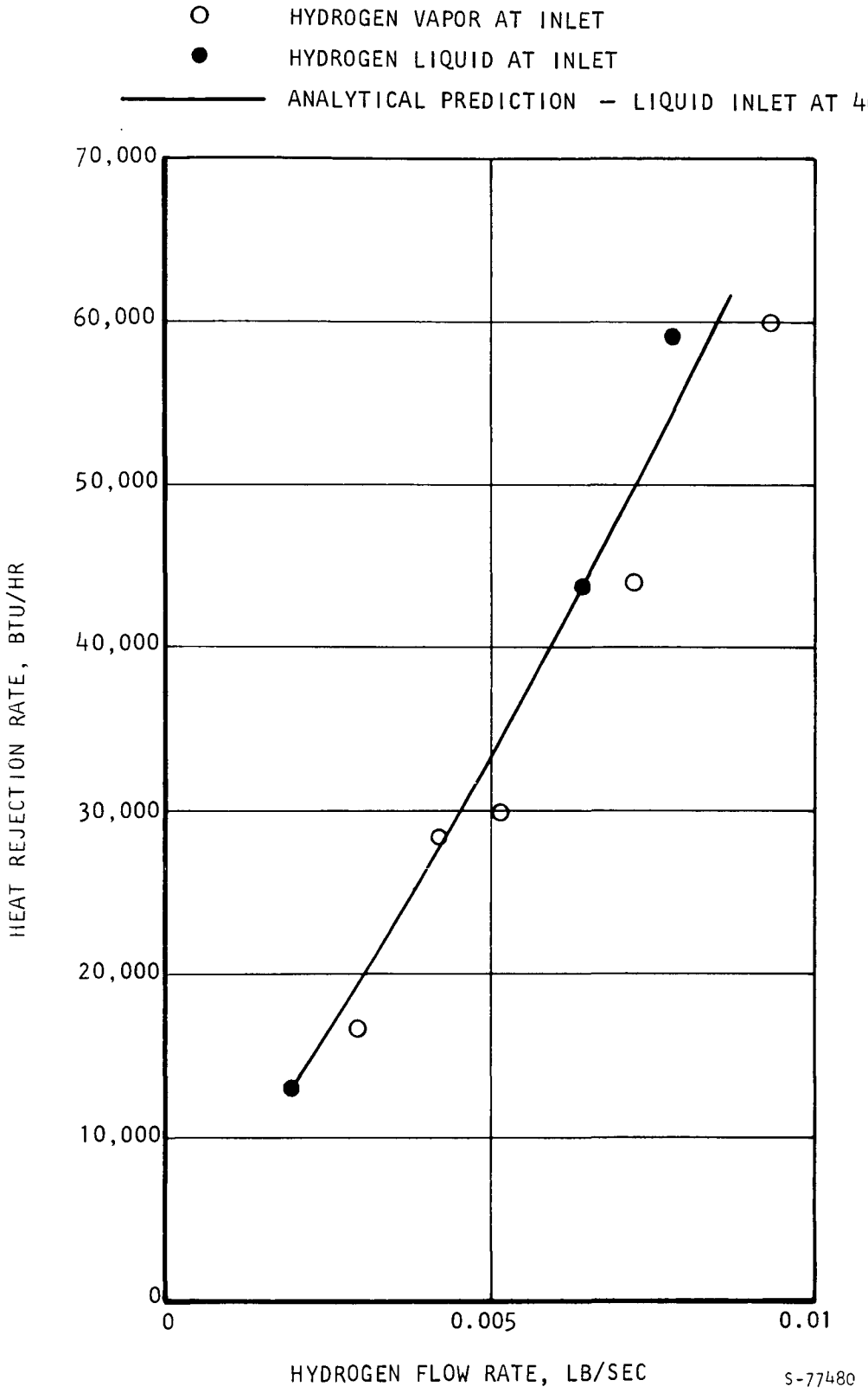

Figure 11-9. Heat Rejection Rate Versus Hydrogen Flow Rate at Cryogenic Inlet Conditions

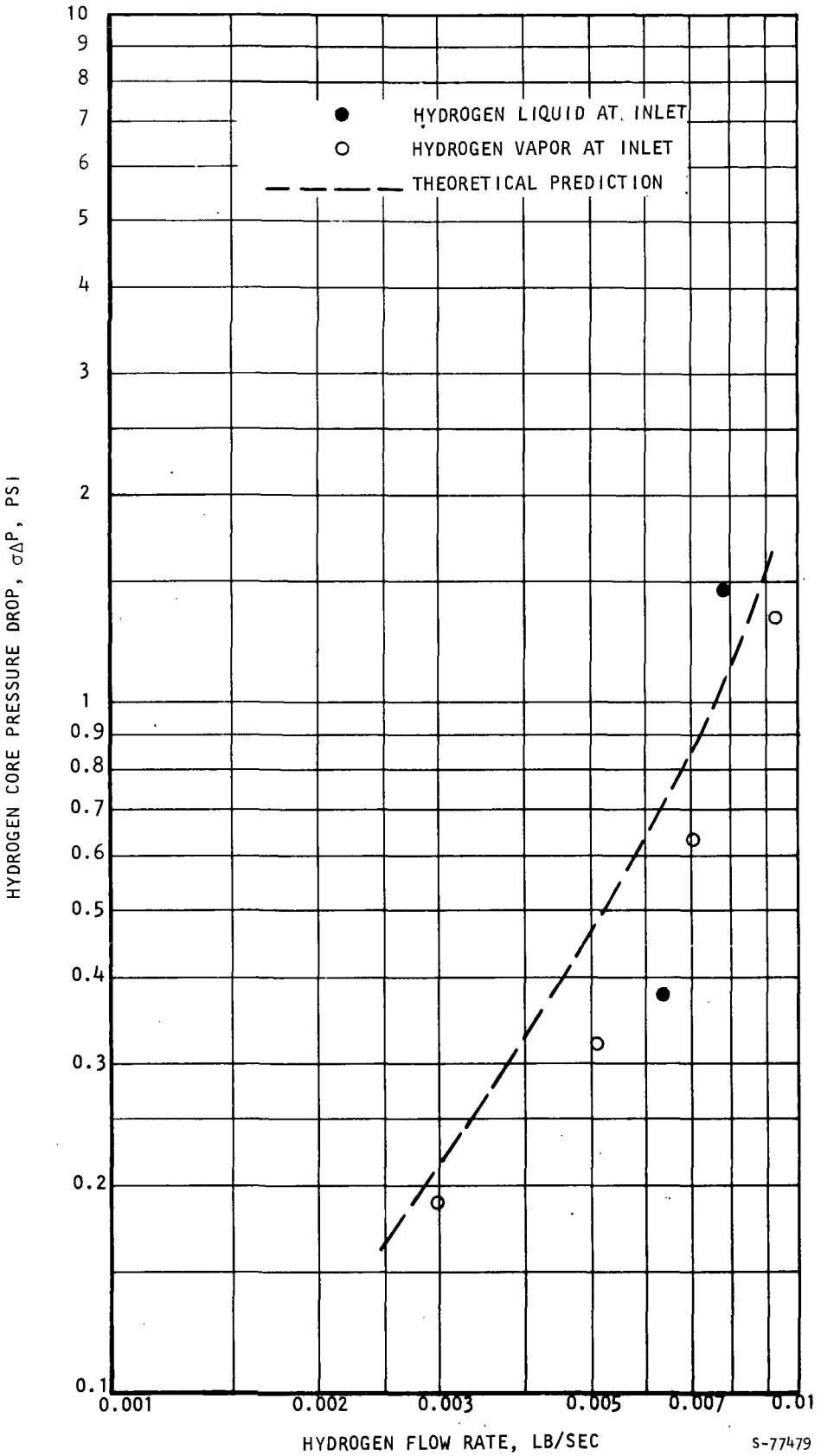

Figure 11-10. Hydrogen Core Pressure Drop at Cryogenic Inlet Conditions

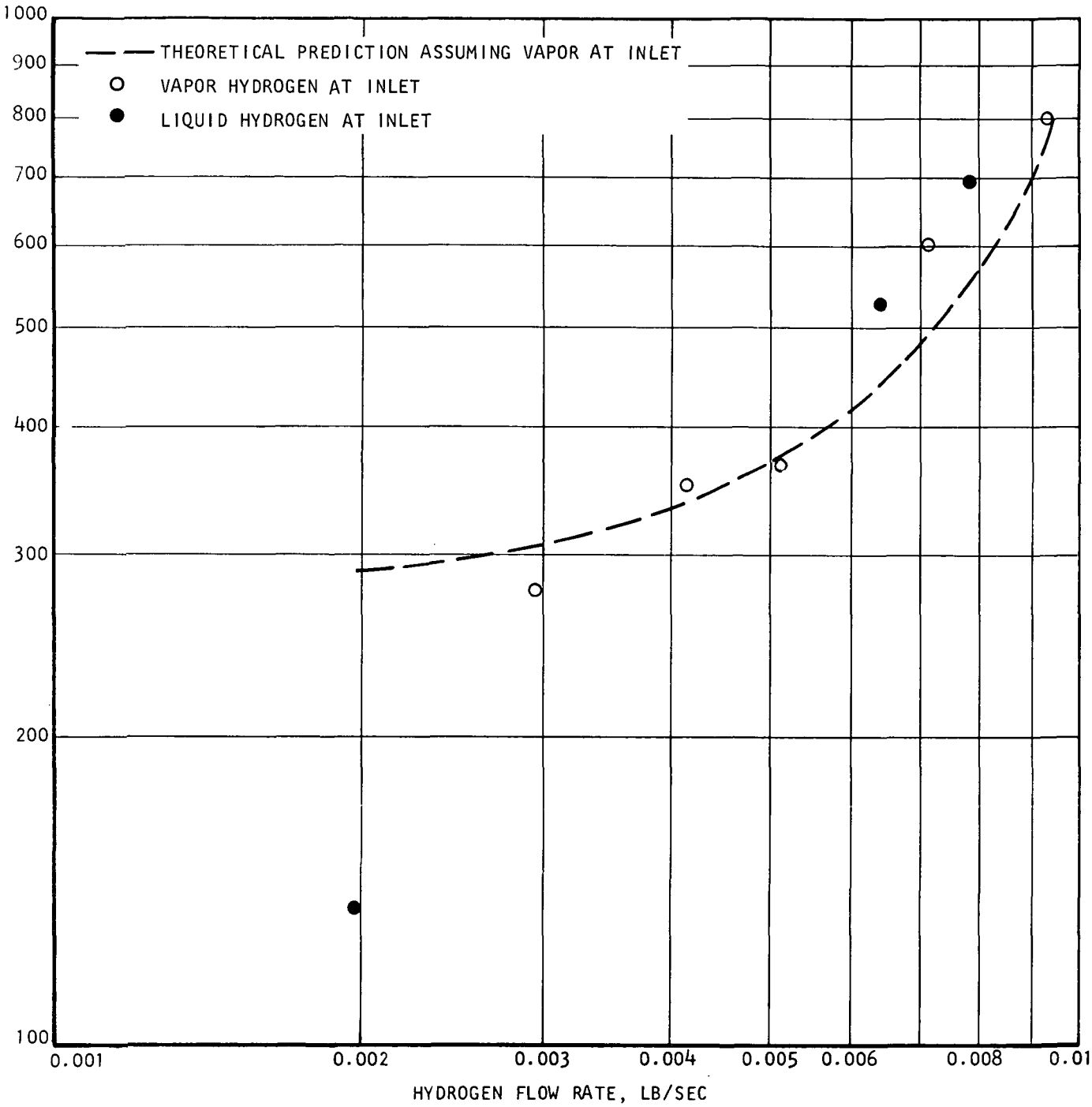

Figure 11-11. Overall Heat Transfer, UA, Versus Hydrogen Flow Rate at Cryogenic Inlet Conditions

In addition to meeting the heat load and pressure drop requirements, the heat exchanger operated above the warm fluid freezing point with a wide margin. Figure 11-12 depicts the estimated temperature distribution along the HX for Run 7, Table 11-5, which is one of the worst conditions from the standpoint of freezing. The measured minimum inside header temperature, which should be approximately equal to the minimum tube wall temperature, also is shown in the figure. This temperature is about 130°F above the warm fluid freezing point.

These results demonstrate the effectiveness of the design features included in the present design and indicate that the present design can be used for warm fluids with higher freezing points, such as Coolanol 15 or glycol-water solution. Such fluids possess higher specific heats than Freon-21, and their use should result in significant power and weight saving of a spacecraft environmental control system.

During liquid hydrogen testing, pressure fluctuations were observed at the inlet and outlet of the heat exchanger. The amplitudes of these pressure fluctuations were small compared to the absolute pressure level in the system but were comparable to the pressure drop across the heat exchanger. For example, in Run No. 5, Table 11-5, the amplitudes were about 0.1 psi as compared to the 0.2 psi pressure drop and 25.3 psia pressure level. These pressure fluctuations, were repetitive in nature and never resulted in any performance degradation.

Since the pressure fluctuations were only observed during liquid hydrogen testing, they must be caused by the two-phase flow. Modulating the cryogen flow with the flow control valve downstream of the heat exchanger resulted in dampening of these fluctuations. This dampening can be attributed to the decrease in the liquid-to-vapor density ratio due to the increase in static pressure level when the downstream valve was used.

It is recommended that cryogen flow modulation be accomplished through a flow control valve downstream of the cryogenic heat exchanger. This also simplifies the valve design since it is located in warm gas area and not in a cryogenic liquid flow stream. This scheme, however, would require a shutoff valve upstream of the heat exchanger to isolate the heat exchanger in case of failure in the warm fluid loop.

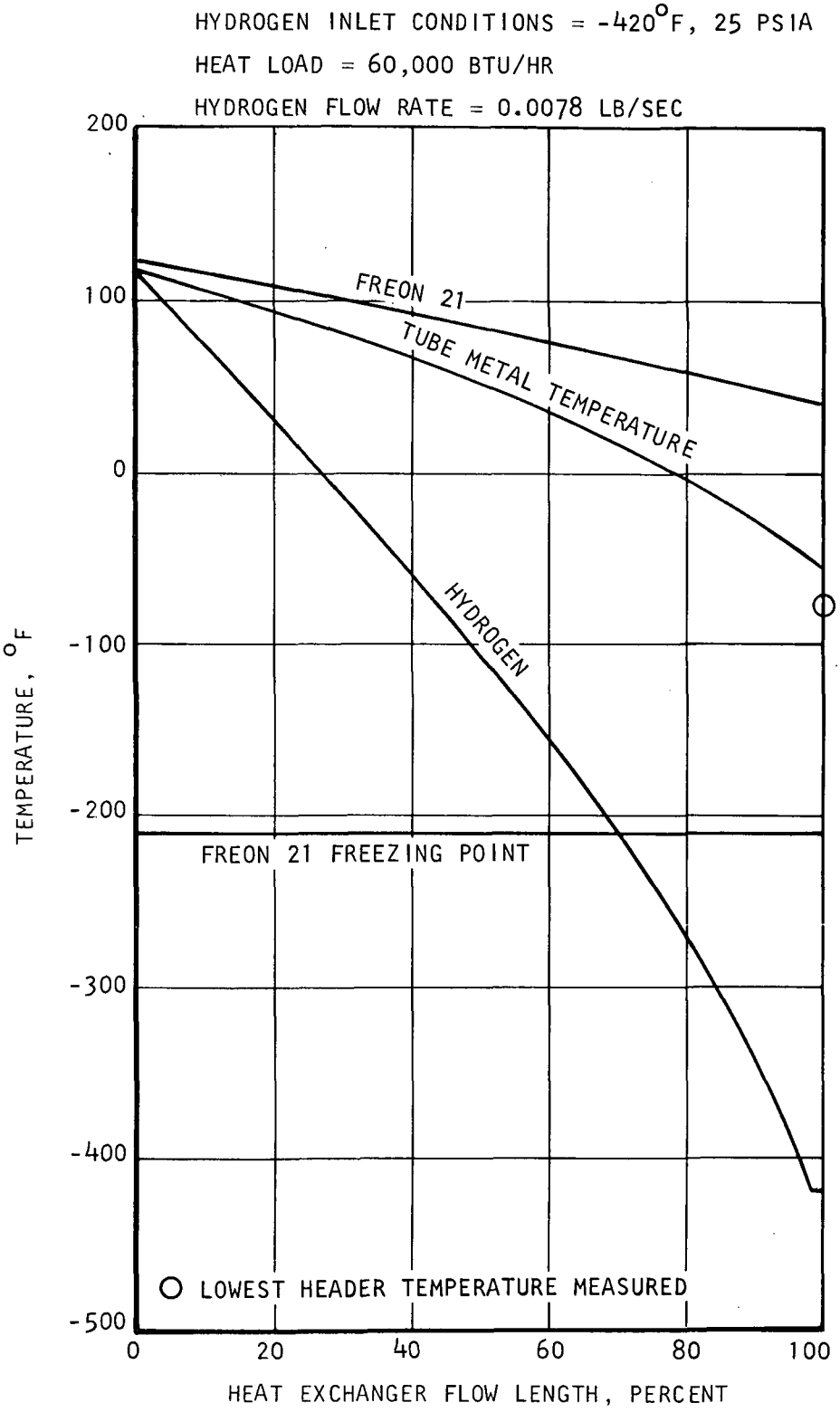

Figure 11-12. Estimated Temperature Distribution Along the Heat Exchanger for Run 7, Table 11-5

SECTION 12

OXYGEN HEAT SINK SYSTEM

WEIGHT OF CONSUMABLES

The heat sink system tradeoff study presented in Section 6, which was based on hydrogen as the heat sink fluid, demonstrated that the cryogen weight and the penalties attached to it constitute the major weight penalty in a cryogenic heat sink system. The heat exchanger weight and the weight penalty attached to the warm fluid pressure drop were shown to be relatively small. Thus, it was concluded that a heat exchanger effectiveness of at least 0.9 is necessary to minimize the cryogen weight consumed.

A system utilizing oxygen as the heat sink fluid was investigated analytically. Figure 12-1 shows the total weight of consumables if oxygen is used as the heat sink fluid, for different periods of operation. The heat load is assumed at its maximum value of 60,000 Btu/hr and the heat exchanger effectiveness is assumed to be 0.9. The two curves shown represent the two limiting operating conditions: from liquid oxygen at 182°R to gaseous oxygen at 0°F.

A comparison between oxygen and hydrogen as expendable fluids is depicted in Figure 12-2. The oxygen and hydrogen inlet conditions to the HX are taken from the typical subcritical propellant tank conditions. Over a period of operation of 4 hr at maximum heat load the total weight of consumables is 17,000 lb, in the case of oxygen, as compared with about 1200 lb for hydrogen. Therefore, the HX weight is even a smaller fraction of the total weight in an oxygen heat sink system.

HEAT SINK SYSTEM DESIGN

The oxygen heat sink system shown in Figure 12-3 was selected on the basis of the tradeoff study conducted for hydrogen and on the basis of the results of the hydrogen heat exchanger testing. The flow modulating valve is located downstream of the HX. A check valve upstream of the HX helps preventing any reverse flow of cryogen due to pressure fluctuations in the HX. Again a shutoff valve may not have to be a part of the heat sink system if it is provided elsewhere upstream of the system.

The various components of the heat sink system have the same design as those described in Section 8 for the hydrogen system. Due to the much higher oxygen flow rates relative to hydrogen, particularly at 0°F inlet condition, the sizes of the heat exchanger and the valves have to be different. For example, the hydrogen HX can accommodate the oxygen flow rate at the 182°R inlet condition while meeting the desired performance. On the other hand, at 0°F inlet condition the HX pressure drop is far in excess of the allowable 10 psi.

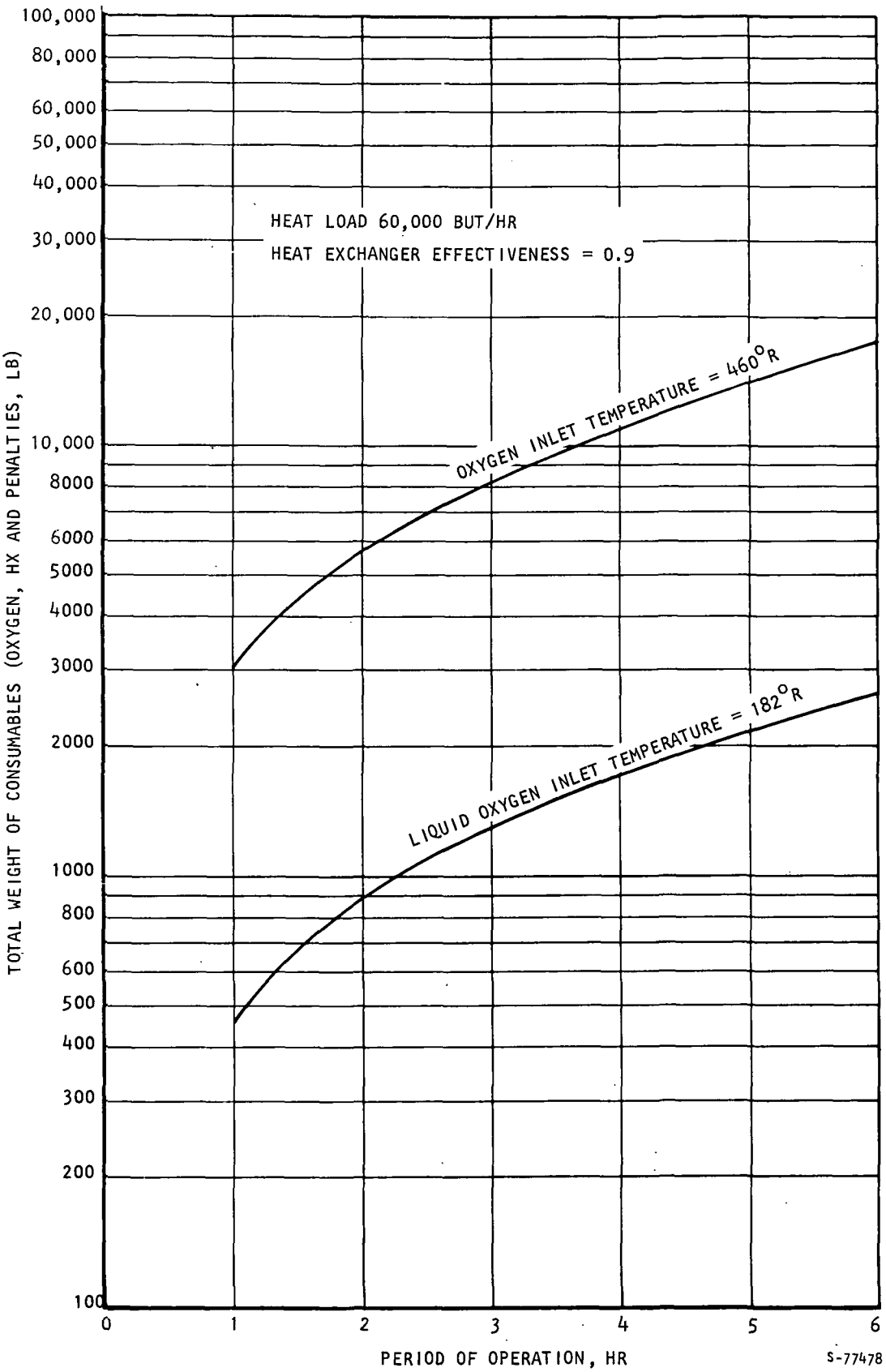

Figure 12-1. Total Weight of Consumables with Oxygen as Expendable Heat Sink

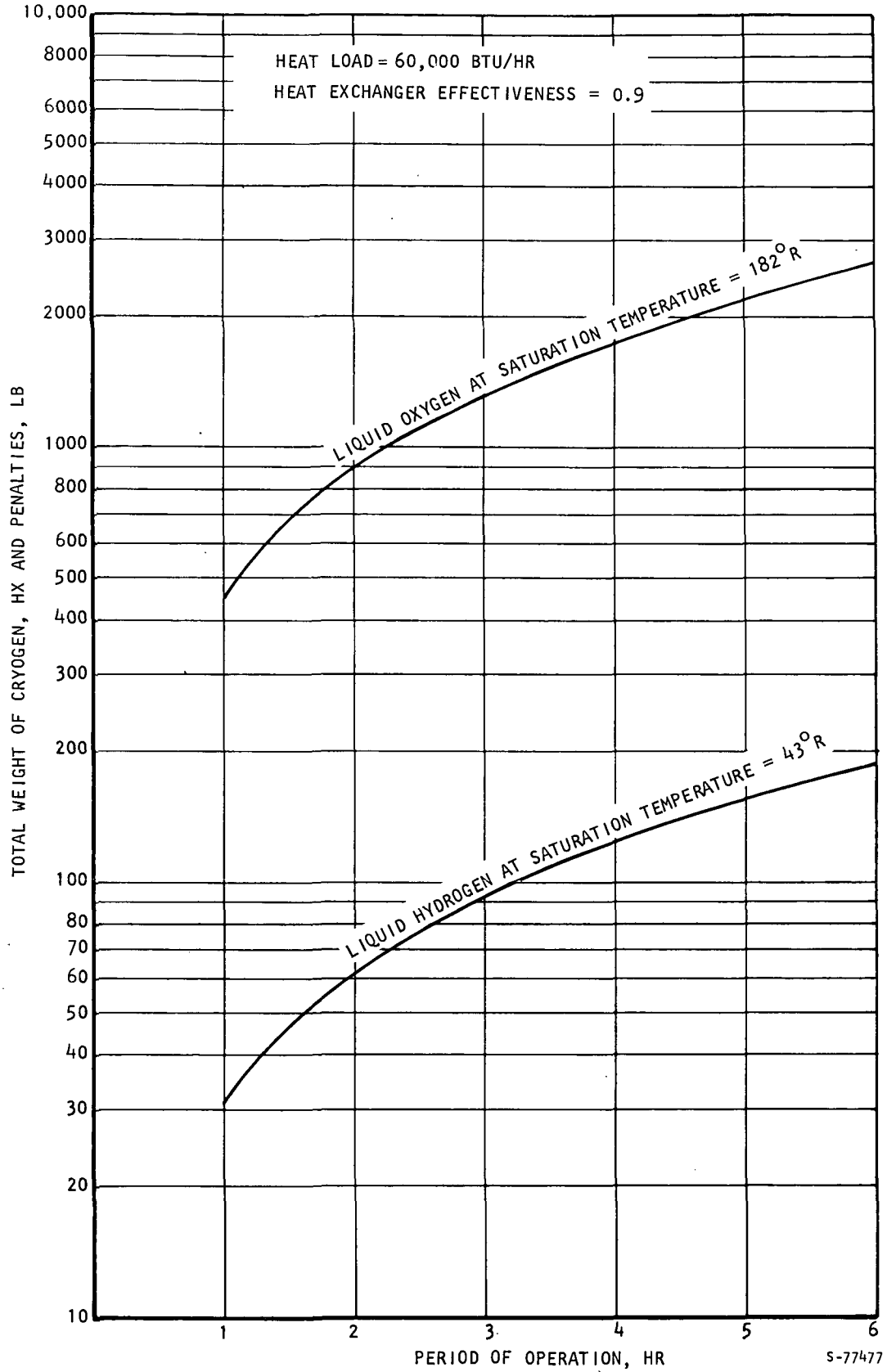

Figure 12-2. Comparison Between Oxygen and Hydrogen as Expendable Heat Sink Fluids

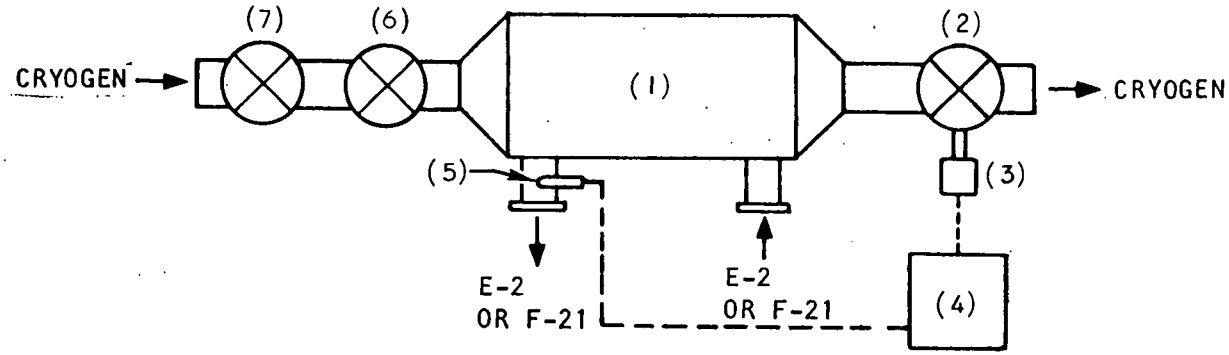

b. Downstream Control Valve

COMPONENTS:

(1) CRYOGENIC HEAT EXCHANGER: EITHER TUBULAR OR PLATE-FIN DESIGN
(2) FLOW CONTROL VALVE
(3) ACTUATOR = PNEUMATIC OR HYDRAULIC, WITH TIME CONSTANT OF 0.5 SEC OR BETTER
(4) CONTROLLER
(5) TEMPERATURE SENSOR
(6) CHECK VALVE
(7) SHUTOFF VALVE

S-68979 -B

Figure 12-3. Oxygen Heat Sink System

The oxygen heat exchanger design is shown in Figure 12-4. The design incorporates all the features developed and tested in the hydrogen HX. The main difference is in the number of tubes required in the oxygen flow path to meet an allowable pressure drop of 10 psi.

The design point performance of the HX also is shown in Figure 12-4.

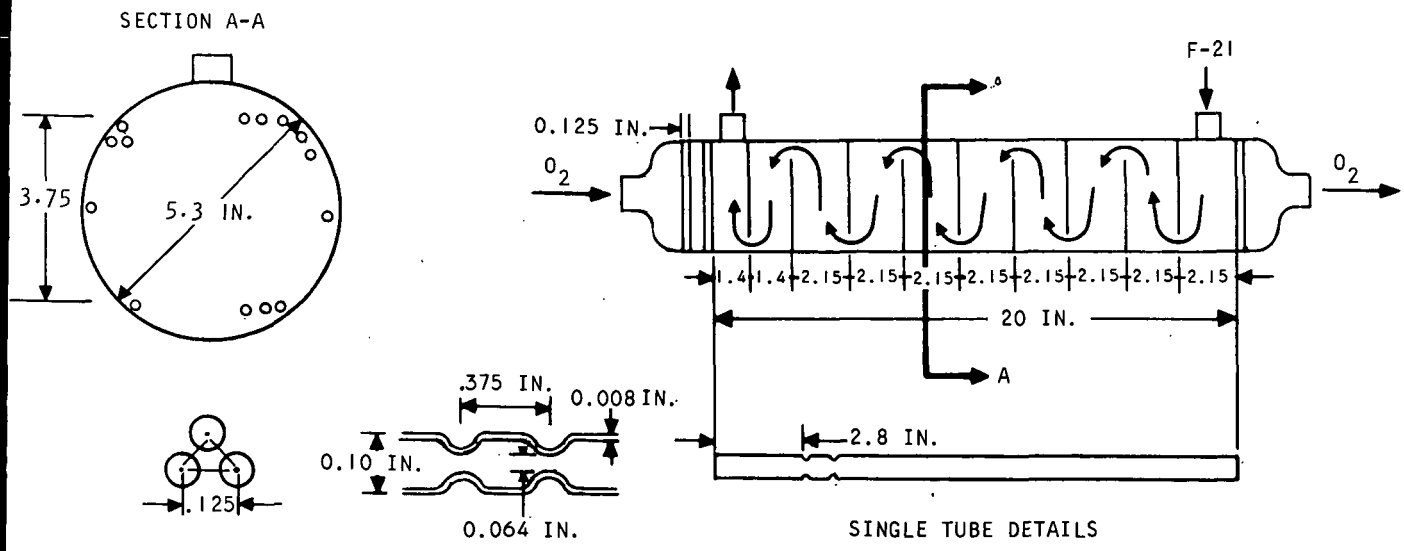

- TUBULAR - TEN-PASS, CROSS COUNTER FLOW ARRANGEMENT WITH CRYOGEN INSIDE TUBES AND WARM FLUID OUTSIDE TUBES
- HEAT EXCHANGER DETAILS

MATERIAL	= STAINLESS STEEL
CONSTRUCTION	= DIMPLED TUBE AND SHELL
NUMBER OF TUBES	= 900
TUBE OUTSIDE DIAMETER	= 0.1 IN.
TUBE WALL THICKNESS	= 0.008 IN.
TUBE LENGTH	= 20 IN.
TUBE SPACING	= 0.125 IN.
DIMPLE DIMENSIONS	= AS SHOWN ABOVE
NUMBER OF BAFFLES	= 9
TYPE OF BAFFLES	= SEGMENTED
HEAT EXCHANGER WEIGHT	= 27 LBS

- DESIGN POINT PERFORMANCE

HEAT REJECTION	= 60,000 BTU/HR
FREON-21 FLOW	= 2810 LB/HR
FREON-21 INLET TEMPERATURE	= 125°F
FREON-21 OUTLET TEMPERATURE	= 40°F
FREON-21 PRESSURE DROP	= 5 PSI
OXYGEN FLOW	= 2400 LB/HR
OXYGEN INLET TEMPERATURE	= 0°F
OXYGEN SIDE EFFECTIVENESS	= 0.9
OXYGEN PRESSURE DROP	= 10 PSI

S-69149-B

Figure 12-4. Oxygen Heat Exchanger Design

SECTION 13

CONCLUSIONS AND RECOMMENDATIONS FOR FUTURE WORK

CONCLUSIONS

A survey of candidate warm fluids resulted in the selection of E-2, a fluorocarbon compound, because of its low freezing point and high boiling point. The final design and testing of the heat exchanger was carried out, however, using Freon -21, which is similar to E-2 except for its low boiling point. This change was motivated by the desire to minimize the cost of the experimental program.

Based on a tradeoff study of the heat sink system, a heat exchanger effectiveness of 0.9 was selected, which resulted in the minimum total weight consisting of the weight of the heat exchanger, the weight of consumables, and the penalties weight.

Based on the HX design study, a tube and shell type was selected with ten-pass cross-counter flow arrangement. The cryogen flows inside ring-dimpled, small-diameter (0.1 in. OD) tubes and the warm fluid flows outside the tubes. The entire heat exchanger is made of stainless steel. Certain unique features were included in the design to prevent any warm fluid freezing during all operating conditions.

Based on a control system tradeoff study, a position + rate + integral control scheme was selected. The control system consists of a flow control valve, an actuator, an electronic amplifier circuit for processing sensor signal, and a temperature sensor. Both upstream and downstream locations of the flow control valve were tested.

The cryogenic heat exchanger was optimally designed and tested using hydrogen as the heat sink fluid since it presents the most optimum solution from a system standpoint.

The heat exchanger was tested in one orientation with $0^{\circ}F$ gaseous hydrogen and cryogenic gaseous and liquid hydrogen and met the desired performance over the entire range of hydrogen inlet conditions.

The hydrogen side effectiveness was found to be higher than the design value (0.9) at all operating conditions, which would result in cryogen-saving during the mission.

The agreement between the test data and the predicted performance gives confidence in the analytical techniques used in the design and performance prediction of cryogenic heat exchangers.

Minimum tube wall temperatures measured were about $130^{\circ}F$ above the Freon -21 freezing point, and $110^{\circ}F$ above the E-2 freezing point. The effectiveness of the design features included in the present design indicates that

the present design can be used for warm fluids with higher freezing points such as Coolanol 25 or even a glycol-water solution. Such fluids possess higher specific heats than Freon-21 and E-2, and their use should result in significant power and weight savings on spacecraft environmental control systems.

During liquid hydrogen testing, pressure fluctuations were observed at the inlet and outlet of the heat exchanger. These fluctuations, however, were repetitive in nautre and never resulted in any performance degradation, or any freezing of the warm fluid. These fluctuations were dampened by placing the cryogen flow modulating valve downstream of the heat exchanger.

The transient performance of the heat exchanger was demonstrated by an analog simulation of the heat sink system. Under the realistic transient heat load conditions (20 sec ramp from minimum to maximum Freon-21 inlet temperature, the control system was able to maintain the warm fluid outlet temperature within $\pm 3^{\circ}F$.

Due to the much higher oxygen flow rates relative to hydrogen at the $0^{\circ}F$ inlet condition, the sizes of the heat exchanger and the valves have to be different for the oxygen heat sink system. The tested hydrogen heat exchanger could have accommodated the oxygen flow rate at the $182^{\circ}R$ inlet condition while meeting the desired performance but the heat exchanger pressure drop would have been far in excess of the allowable 10 psi at the $0^{\circ}F$ inlet condition. Because of this, a separate oxygen heat sink system, that incorporates all the design features of the hydrogen system is presented for comparison purposes.

RECOMMENDED FUTURE WORK

AiResearch believes that the existing cryogenic heat exchanger and test loop offer a good opportunity for gathering additional useful information that will help in the future design and determine the suitability of cryogenic heat sink systems for similar applications. The following future work is recommended to NASA.

Testing With Different Warm Fluids

The success of the various unique design features included in the present heat exchanger design (in maintaining the tube wall temperature above the freezing point of Freon-21 by a wide margin), indicate that the present design can be used for warm fluids with higher freezing points. The candidate fluids of interest in this category include Coolanol 15 and Glycol-water mixtures. Such fluids possess higher specific heats that Freon-21 and E-2; therefore, their use should result in significant power and weight savings on spacecraft environmental control systems.

It is recommended that testing with these and possibly other promising fluids be carried out using liquid hydrogen at about $43^{\circ}R$, as the heat sink fluid, since this constitutes the worst operating condition from the standpoint of warm fluid freezing.

The operating conditions of the warm fluids, such as the flow rate and inlet temperature, would be adjusted to compensate for the fact that the present heat exchanger design was optimized using Freon-21.

Testing the Heat Exchanger in Different Orientations

The heat exchanger should be tested in at least one more orientation. One recommended orientation is the horizontal one (cryogen flowing horizontally). This testing should initially be conducted with Freon-21 as the warm fluid and liquid cryogen as the heat sink fluid. Operation in this orientation may induce liquid stratification, where more liquid cryogen flows in the lower tubes. The purpose of the testing is to demonstrate the effect of liquid stratification on both the freezing problem and the observed pressure fluctuations.

Transient Performance Testing

Transient performance of the cryogenic heat exchanger system has been analyzed in an analog computer simulation but testing has been limited to steady state conditions. It is recommended that the predicted transient performance be verified in test by simulating the selected control system with laboratory or similar available hardware installed in the test setup with the existing heat exchanger. Programmed temperature transients would be imposed on each fluid to simulate anticipated heat load and heat sink transient conditions. Response, stability and control temperature range of the heat transport fluid would be evaluated and the optimum control system design would be established.

During the testing conducted to date, more stable conditions were found to exist when the cryogen flow was controlled by a valve downstream of the heat exchanger. It is usually more desirable to control heat sink fluid flow at the inlet to the heat exchanger for more precise temperature control. As a part of this recommended program a further experimental evaluation of upstream versus downstream control can be conducted. A part of this would be to determine flow stability effects of the valve location.

Testing With Supercritical Cryogen

Generally, if a cryogen is to be stored and periodically used in a zero g environment, storage has been at supercritical pressure. This assures withdrawal of a fluid of known state conditions from the tank. If supercritical cryogens (particularly hydrogen) are to be utilized as a heat sink, the performance of the heat exchanger with this heat sink should be determined.

Hydrogen at pressures slightly above the critical undergoes drastic physical property changes as it is heated through the critical temperature. The heat transfer coefficient also experiences wide variations in this region. Therefore, the performance capabilities of the heat exchanger, particularly the ability to avoid local freezing of the hot fluid, should be demonstrated.

The proposed testing would be accomplished utilizing existing AiResearch owned supercritical cryogen storage tanks designed for space applications. The hydrogen inlet pressure would be varied from 200 to 250 psia and the inlet temperatures varied from approximately 40 to 60°R. The ranges of acceptable cryogen flow rates for the stated inlet conditions and resulting heat exchanger performance would be determined.

Flow Stability Evaluation

Pressure fluctuations were observed during liquid cryogen testing. These fluctuations were found to be very small compared to the system pressure, as described before, but comparable in magnitude to the pressure drop in the heat exchanger.

The objective of this recommended experimental evaluation is to identify the conditions which may result in flow instability. The instability is characterized by a sudden increase in the amplitude of the pressure fluctuations and a subsequent degradation in the heat exchanger performance.

Examples of conditions which may stimulate flow instability are:

(a) Decrease in the pressure level of the cryogen inside the heat exchanger tubes which increases the density ratio, ρ_l/ρ_v

(b) Change the operating conditions such that the boiling regime occupies a larger portion of the heat exchanger tubes, and consequently, would have a more significant effect on the overall performance of the unit

(c) Test the heat exchanger with the hydrogen liquid flowing downwards.

The above conditions can be imposed by varying the test parameters in the present test setup with minimum modifications.

REFERENCES

1. Hendricks, R. C., R. W. Graham, Y. Y. Hsu and A. A. Medeiros, "Correlation of Hydrogen Heat Transfer in Boiling and Supercritical Pressure States," ARS Journal, p. 244, Feb, 1962

2. McCarthy, J. R. and H. Wolf, Forced Convection Heat Transfer to Gaseous Hydrogen at High Heat Flux and High Pressure in a Smooth, Round, Electrically-Heated Tube, ARS Journal, April 1960, p. 423.

3. Hendricks, R. C., R. W. Graham, Y. Y. Hsu and R. Friedman, "Experimental Heat Transfer and Pressure Drop of Liquid Hydrogen Flowing Through a Heated Tube," NASA TND-765, May 1961.

4. Wright, C. C., and H. H. Walters, "Single Tube Heat Transfer Tests Gaseous and Liquid Hydrogen," WADC Technical Report 59-423, August, 1959.

5. Brentari, E. G., etal, "Boiling Heat Transfer For Oxygen, Nitrogen, Hydrogen, and Helium," National Bureau of Standards. Technical Note 317, Sept, 1965.

6. Cryogenic Heat Exchanger, AiResearch Proposal to NASA/MSFC, Oct 1, 1971.

7. Martinelli, R. C., and D. B. Nelson, Trans. ASME, Vol. 170, 1948, p. 695.

8. Ho, D., and M. M. Soliman, AiResearch Internal Memo.

9. P. J. Berenson, "An Experimental Investigation of Flow Stability in Multitube Forced-Convection Vaporizers," ASME Paper No. 65-HT-61, August 1965.

10. J. R. Schuster and P. J. Berenson, "Multitube Forced-Convection Boiler Flow Stability," Garrett-AiResearch Report No. HT-66-0845, Contract AF 33(615)-2289, July 19, 1966.

11. A. P. Fraas, "Flow Stability in Heat Transfer Matrices Under Boiling Conditions," Addendum No. 1, ORNL 59-11-1, March 1961.

12. W. H. Lowermilk, C. D. Lanzo and R. L. Siegel, "Investigation of Boiling Burnout and Flow Stability for Water Flowing in Tubes," NACA TN 4382, September 1958.

13. N. Zuber, "Analysis of Thermally Induced Flow Oscillations in the Near Critical and Supercritical Thermodynamic Region," Final Report NAS 8-11422, NASA Marshall Space Flight Center, Huntsville, Ala. (May 1966).

14. Friedly, J. C., et al., Advances in Cryogenic Engineering, Vol. 14, p. 258, 1968.

15. J. C. Friedly, J. L. Manganaro, and P. G. Kroeger, "Stability Investigation of Thermally Induced Flow Oscillations in Cryogenic Heat Exchangers," Final Rept. NAS 8-21014, NASA Marshall Space Flight Center, Huntsville, Ala. (Oct. 1967).

16. Stone, R. A., "Instability and Freezing in Liquid Heat Exchangers," AiResearch Report No. L-9529, April 1965.

17. Ledinegg, M., Die Wärme, 61, (48), 891-8 (1938).

APPENDIX A

FLOW STABILITY CRITERION

The stability criterion established by Friedly, etal, reference 14, has been considerably modified and is presented in this appendix. For the present application the criterion can be written in the form, see Figure A-1

$$\psi > \sigma \tag{1}$$

Stabilizing to destabilizing pressure drop ratio > Expansion factor for the system.

Neglecting entrance and exit losses, i.e., ΔP_{12} and ΔP_{34}, the parameter ψ reduces to, see Figure 3-7

$$\psi = \frac{\Delta P_{\ell} + \Delta P_{TP} + A\,\Delta P_{fv} + B\,\Delta P_{a}}{C\,\Delta P_{a} + D\,\Delta P_{fv}} \tag{2}$$

where ΔP_{ℓ} = pressure drop across orifice valve

ΔP_{TP} = pressure drop in the two-phase region

ΔP_{fv} = frictional pressure drop in the vapor region

ΔP_{a} = acceleration pressure drop

and A, B, C and D are weighting factors defined below. Knowing that $\frac{u_4}{u_1} = \frac{\rho_{\ell}}{\rho_v}$ (where u is velocity, ρ_{ℓ} is the liquid density and ρ_v is the vapor density) the expressions for the weighting factors are

$$A = \frac{\ln \rho_{\ell}/\rho_v}{1 + (\rho_{\ell}/\rho_v - 1)} \tag{3}$$

$$B = \frac{2}{1 + \rho_{\ell}/\rho_v} \tag{4}$$

$$C \cong \frac{1}{2(\rho_{\ell}/\rho_v - 1)} \left\{ \frac{1 + \left(\frac{2}{3\pi}\right)^2 (\rho_{\ell}/\rho_v)^4}{1 + \frac{1}{4}\left[\frac{2}{3\pi}(\rho_{\ell}/\rho_v)^2 - \frac{3\pi}{2}(\rho_v/\rho_{\ell})^2\right]^2} \right\}^{1/2} \tag{5}$$

$$D \simeq \frac{2(\rho_{\ell}/\rho_v)}{3[(\rho_{\ell}/\rho_v)^2 - 1]} \left\{ \frac{1 + \left(\frac{2}{3\pi}\right)^2 (\rho_{\ell}/\rho_v)^4}{1 + \frac{1}{9}\left[\frac{3\pi}{2}(\rho_v/\rho_{\ell})^2 - \frac{4}{3\pi}(\rho_{\ell}/\rho_v)^2\right]^2} \right\}^{1/2} \tag{6}$$

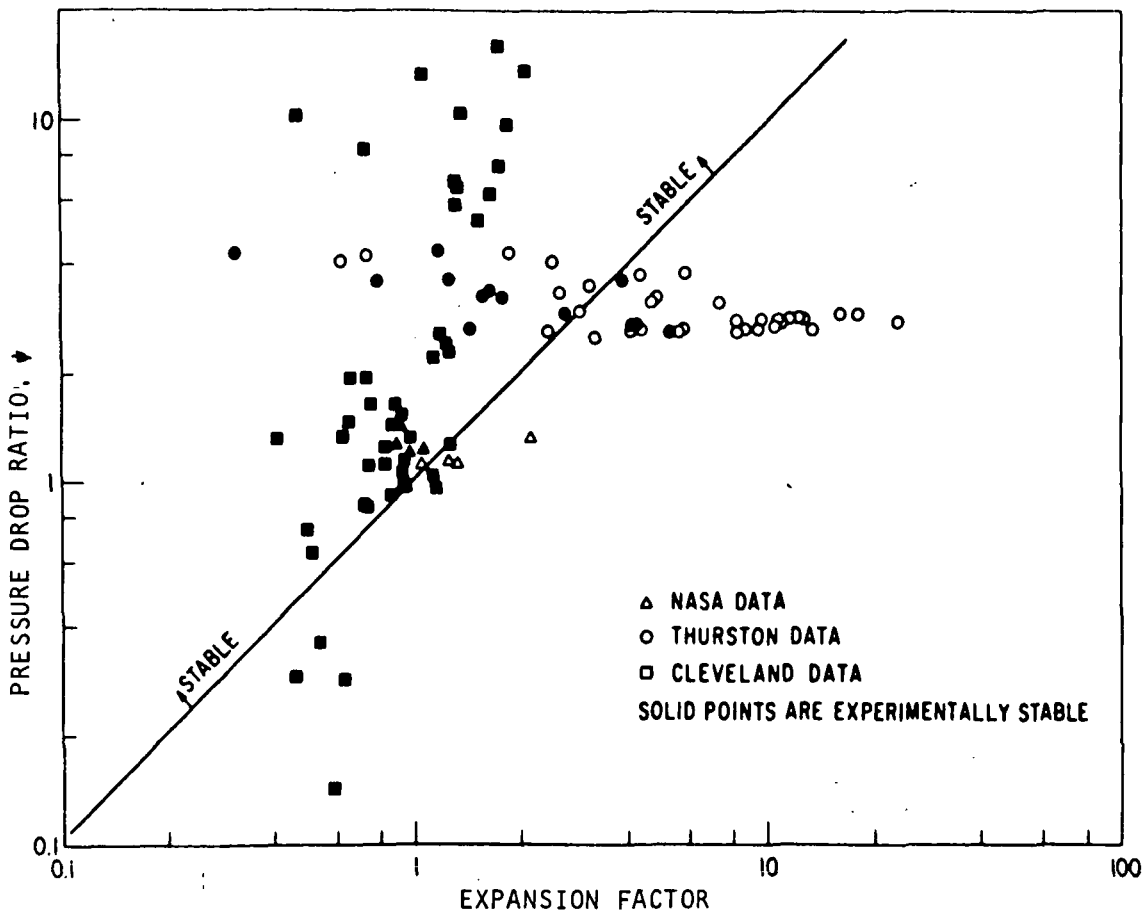

S-68256

Figure A-1. Comparison of Stability Criterion and Experimental Data

Using the approximation that

$$\rho_\ell/\rho_v \gg 1 \gg \rho_v/\rho_\ell$$

equations (3) to (6) reduce to

$$A \cong 2(\rho_v/\rho_\ell) \tag{7}$$

$$B \cong 0.5\,(\rho_v/\rho_\ell)\,\ln(\rho_\ell/\rho_v) \tag{8}$$

$$C \cong (\rho_v/\rho_\ell) \tag{9}$$

$$D \cong (\rho_v/\rho_\ell) \tag{10}$$

The expression for the expansion factor σ can also be reduced to the following form

$$\sigma \cong \frac{\rho_\ell}{\rho_v} \exp - [H \ln \rho_\ell/\rho_v]$$

$$= (\rho_\ell/\rho_v)^{1-H} \tag{11}$$

where $H = \dfrac{h\,A_H}{A_c \rho_\ell Cp}$, (12)

h is heat transfer coefficient, A_H is heat transfer area, A_c is flow area and Cp is specific heat of the fluid.

Using equations 1, 2 and 7 to 11, the stability criterion reduces to

$$\frac{\Delta P_\ell + \Delta P_{TP} + 2(\rho_v/\rho_\ell)\,\Delta P_{fv} + 0.5\,(\rho_v/\rho_\ell)\,\ln(\rho_\ell/\rho_v)\,\Delta P_a}{(\rho_v/\rho_\ell)\,\Delta P_a + (\rho_v/\rho_\ell)\,\Delta P_{fv}} > (\rho_\ell/\rho_v)^{1-H} \tag{13}$$

According to Figure A-1 the larger the left hand side of equation (13) the better change the system has in stable operation. An upper bound of the right hand side of equation 13 is obtained by equaling H=0. Hence

$$\left(\frac{\Delta P_{\ell} + \Delta P_{TP}}{\Delta P_a + \Delta P_{fv}}\right) + \frac{P_v}{P_{\ell}}\left(\frac{2\Delta P_{fv} + 0.5 \ln \rho_{\ell}/\rho_v \, \Delta P_a}{\Delta P_{fv} + \Delta P_a}\right) > 1$$

For $\frac{\rho_v}{\rho_{\ell}} \ll 1$

$$\frac{\Delta P_{\ell} + \Delta P_{TP}}{\Delta P_a + \Delta P_{fv}} > 1 \qquad (14)$$

To ensure stability ΔP_{TP} and/or ΔP_{ℓ} have to be sufficiently large. The stability criterion is discussed further in the text.

APPENDIX B

OPTIMUM THERMAL CONDUCTANCE RATIO ϕ FOR MINIMUM HEAT EXCHANGER VOLUME

The thermal conductance ratio ϕ may be written as

$$\phi = \frac{(\eta hA)_H}{(\eta hA)_c} \tag{1}$$

Also, the overall thermal conductance (U) can be written in terms of ϕ and the thermal conductance on either the hot or cold side

$$\frac{(\eta hA)_H}{UA} = 1 + \phi$$

or $$(hA)_H = \frac{UA}{\eta_H}(1+\phi)$$

and $$(hA)_c = \frac{UA}{\eta_c}\left(1+\frac{1}{\phi}\right)$$

Hence,

$$(hA)_x = \frac{UA}{\eta_x}(1+\phi^{\pm 1}) \tag{2}$$

where for $x = H$ or $x = c$, the positive or negative sign is considered, respectively.

The heat transfer coefficient h is related to the colburn factor j and the core geometry by the following relationship

$$j_x = \left(\frac{ha}{w}\right)_x \alpha_x \tag{3}$$

where a is the free flow area, w is the flow rate and

$$\alpha_x = \frac{Pr_x^{2/3}}{Cp}$$

The hydraulic radius of either side of the heat exchanger is defined as

$$r_x = \left(\frac{aL}{A}\right)_x \tag{4}$$

Combining equations (1), (3) and (4), one gets

$$\left(\frac{L}{r}\right)_x = \frac{\alpha_x \, UA \, (1 + \phi^{\pm 1})}{\eta_x \, (jw)_x} \qquad (5)$$

where L_H and L_c are the flow lengths of the hot and cold fluid, respectively. (See Figure B-1.)

The pressure drop in the heat exchanger core is predicted by the following correlation:

$$\Delta P_x = \frac{W_x^2}{2\rho_x g a_x^2} \, f_x \left(\frac{L}{r}\right)_x \qquad (6)$$

where ρ_x is the density and f_x is the friction factor which is a function of the Reynolds number.

Eliminating $(L/r)_x$ between equations (5) and (6) one gets the minimum required free flow area to meet a specific heat exchanger problem statement

$$a_x = \sqrt{\frac{\alpha_x}{2g} \left(\frac{f}{j}\right)_x \frac{W_x \, UA \, (1 + \phi^{\pm 1})}{(\rho \Delta P)_x \, \eta_x}} \qquad (7)$$

The volume of the heat exchanger can now be written in terms of the core dimensions as, (see Figure C-1)

$$V = \frac{a_H \, L_H}{\beta_H} + \frac{a_c \, L_c}{\beta_c} \qquad (8)$$

where β is the ratio of free flow area to frontal area, i.e., $\beta_H = \left(\frac{a}{a_F}\right)_H$

Combining equations (5), (7), and (8) one gets

$$V = K_H \, (1+\phi)^{3/2} + K_c \, (1+ \frac{1}{\phi} \,)^{3/2} \qquad (9)$$

where

$$K_x = \frac{1}{\beta_x} \sqrt{\frac{\alpha_x^3}{2g} \left(\frac{f}{j}\right)_x \frac{1}{W_x \, (\rho \Delta P)_x}} \; \frac{(UA)^{3/2}}{J_x \, \eta_x^{3/2}} \, , \quad x = H \text{ or } c \qquad (10)$$

and $$J_x = \frac{j_x}{r_x}$$

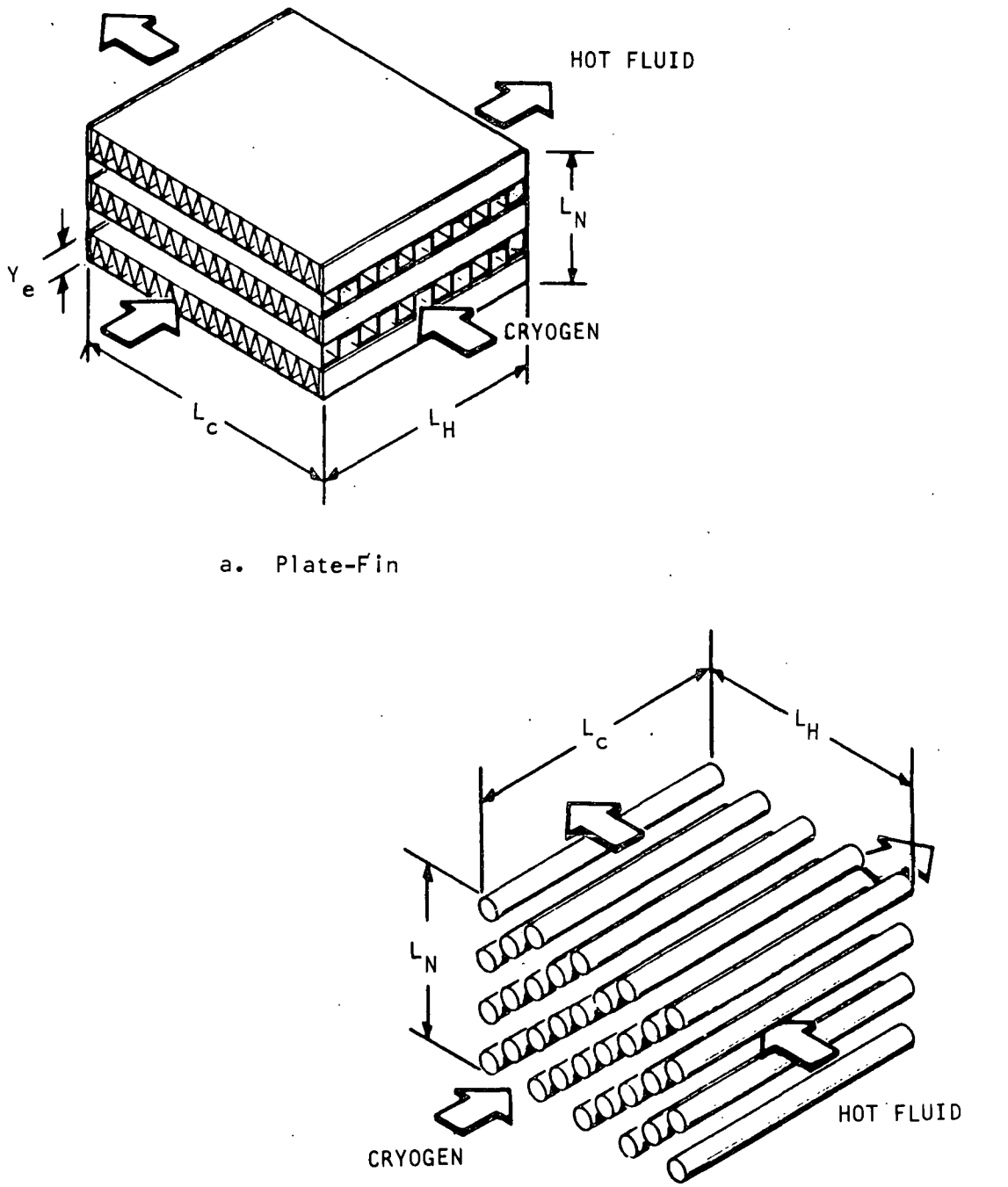

Figure B-1. Heat Exchanger Geometry

A minimum heat exchanger volume is obtained by differentiating equation (9) with respect to ϕ

$$\frac{dV}{d\phi} = 0$$

which gives

$$\phi = \left(\frac{K_c}{K_H}\right)^{0.4}$$

Hence, for a minimum heat exchanger volume the following relationship for ϕ must be satisfied

$$\phi = \left(\frac{\alpha_c}{\alpha_H}\right)^{0.6}\left[\frac{(f/j)_c}{(f/j)_H}\ \frac{W_H(p\Delta P)_H}{W_c(p\Delta P)_c}\right]^{0.2}\left(\frac{\beta_H}{\beta_c}\right)^{0.4}\left(\frac{J_H}{J_c}\right)^{0.4}\left(\frac{\eta_H}{\eta_c}\right)^{0.6} \qquad (11)$$

Figure B-2 shows typical values of f and j for compact fin surfaces. Both f and j vary appreciably with the Reynolds number. However, the ratio f/j is approximately constant. For flow inside tubes, $f/j \simeq 2/Pr^{2/3}$, while for finned surfaces, $f/j \simeq 4$ is a good mean value. A range of 3 to 5 would include most surfaces. Hence, it can be assumed that $(f/j)_c \equiv (f/j)_H$.

Furthermore, the fin effectiveness η is usually close to unity, particularly, for aluminum or copper heat exchangers and hence $\eta_H = \eta_c$ is a good assumption.

Finally, β which is the ratio of free flow area to frontal area is also close to unity and it can be safely assumed that $\beta_H = \beta_c$.

Hence, equation A11 reduces to

$$\phi = \left(\frac{\alpha_c}{\alpha_H}\right)^{0.6}\left[\frac{W_H\,(p\Delta P)_H}{W_c\,(p\Delta P)_c}\right]^{0.2}\left(\frac{J_H}{J_c}\right)^{0.4} \qquad (12)$$

Equation 12 is discussed in the text.

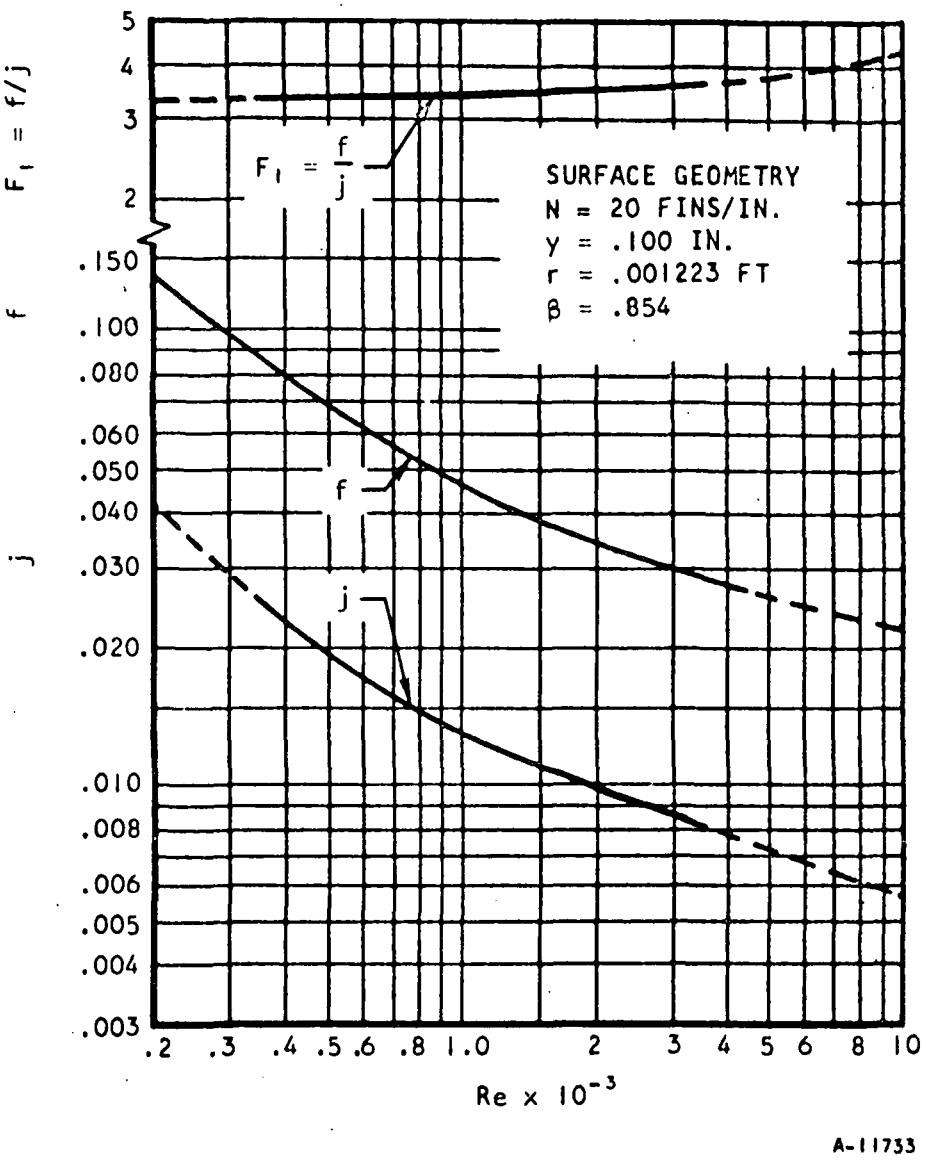

Figure B-2. f, j, and F_1 vs Reynolds Number for an Offset Fin Surface

APPENDIX C

CONTROL SYSTEM MATHEMATICAL MODELS

In order to analyze the dynamic characteristics of the basic cryogenic heat exchanger system and to subsequently synthesize a control system for it, both a linear and a nonlinear mathematical model of the heat exchanger system were generated. Both system models were used to evaluate the candidate control systems at the critical operating conditions. The linear system model, shown in Figure C-1, was utilized in conjunction with transfer function and frequency domain techniques of analysis to evaluate control system stability. This model, however, was of a simplified nature and was used mainly as a preliminary design tool. The nonlinear system model was incorporated into a detailed analog computer simulation which was used to evaluate system stability as well as system response and to finalize control system design. The nonlinear model is described in Figure C-2.

LINEAR SYSTEM MODEL

As indicated in Figure C-1, the linear model of the basic heat exchanger system consists of a single open loop path containing simplified representations of the cryogen flow valve and the heat exchanger. The valve is described by a single gain ($d W_c/dCA_c$), and the heat exchanger is described by two gains ($\partial E_H/\partial W_c$ and $\partial T_{H\,out}/\partial E_H$) with a fixed first order lag time constant of 3.5 seconds. This value of the time constant, which varies between 2.25 and 3.75 seconds over the range of system operating conditions, is representative of the "worst" operating condition for system stability.

NONLINEAR SYSTEM MODEL

The nonlinear model contains a more sophisticated description of all system elements. Limits are imposed on the sensed temperature error as well as the cryogen valve effective area CA_c that the error generates. The CA_c function is nonlinear as described in Figure C-3 with a lower gain at the closed and wide open positions than at midstroke. The heat exchanger time constant is considered a nonlinear function of both fluid flow rates and fluid temperatures. The nonlinearity of the heat exchanger effectiveness, E_H, with respect to hydrogen flow rate, Wc, as well as that of hydrogen specific heat, C_p, with respect to temperature were incorporated in the analysis.

CRITICAL OPERATING CONDITION

In order to utilize the linear system model, a "worst" case operating condition must be determined for evaluation of the model's linear gains. This "worst" case was selected as follows

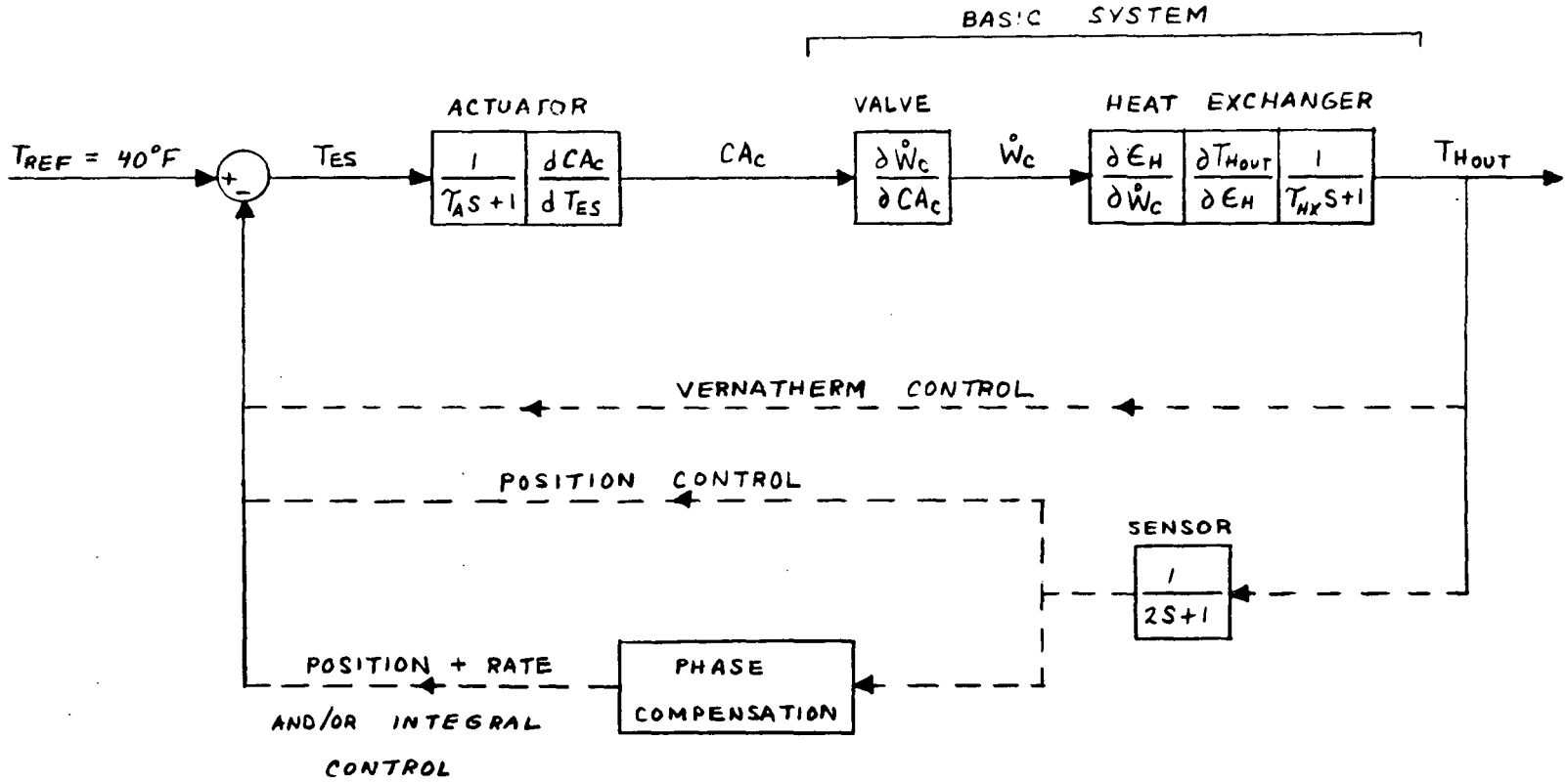

Figure C-1. Linear Heat Exchanger System Model

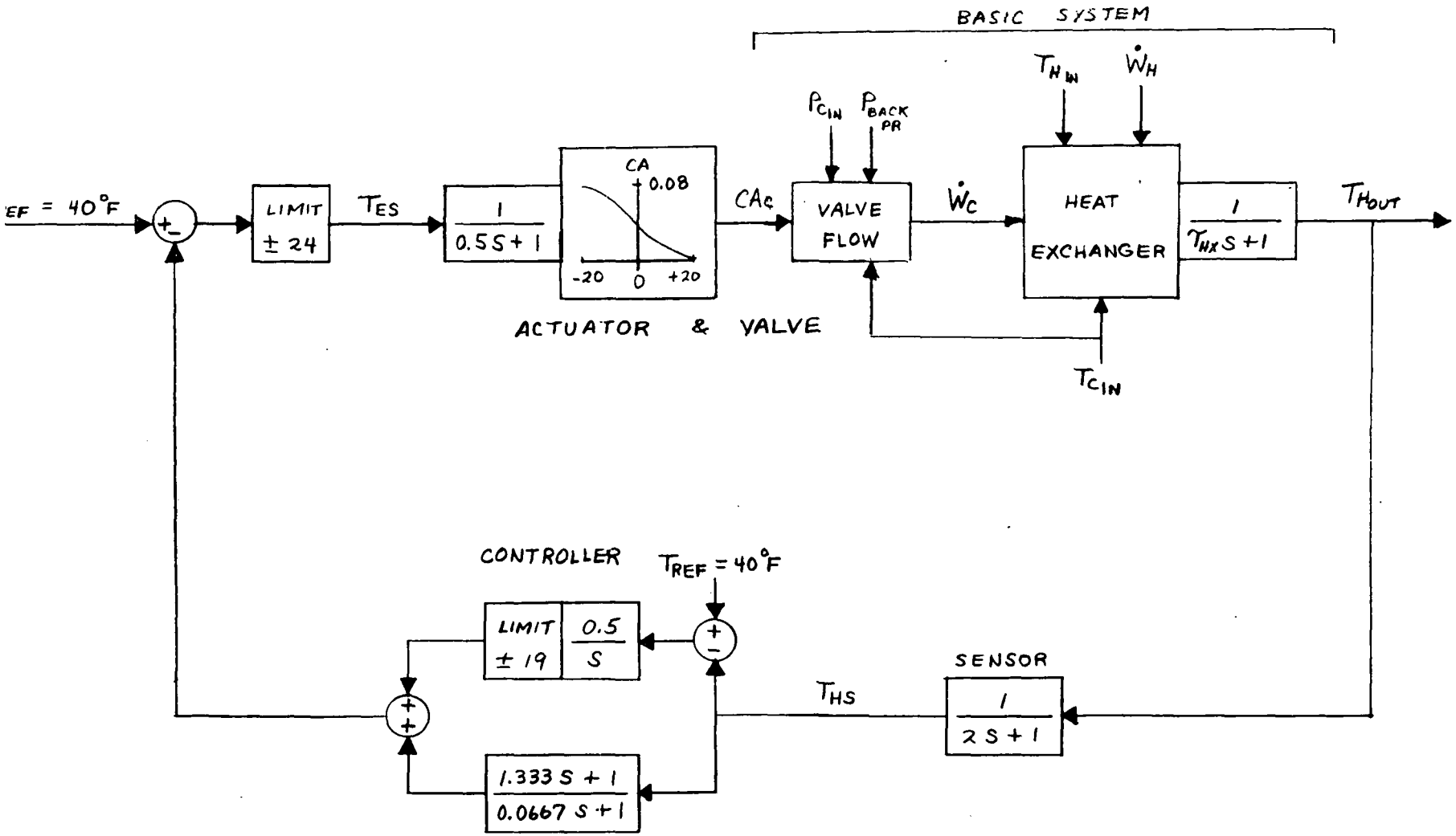

Figure C-2. Analog Computer Simulation Schematic for System with Position + Rate + Integral Control

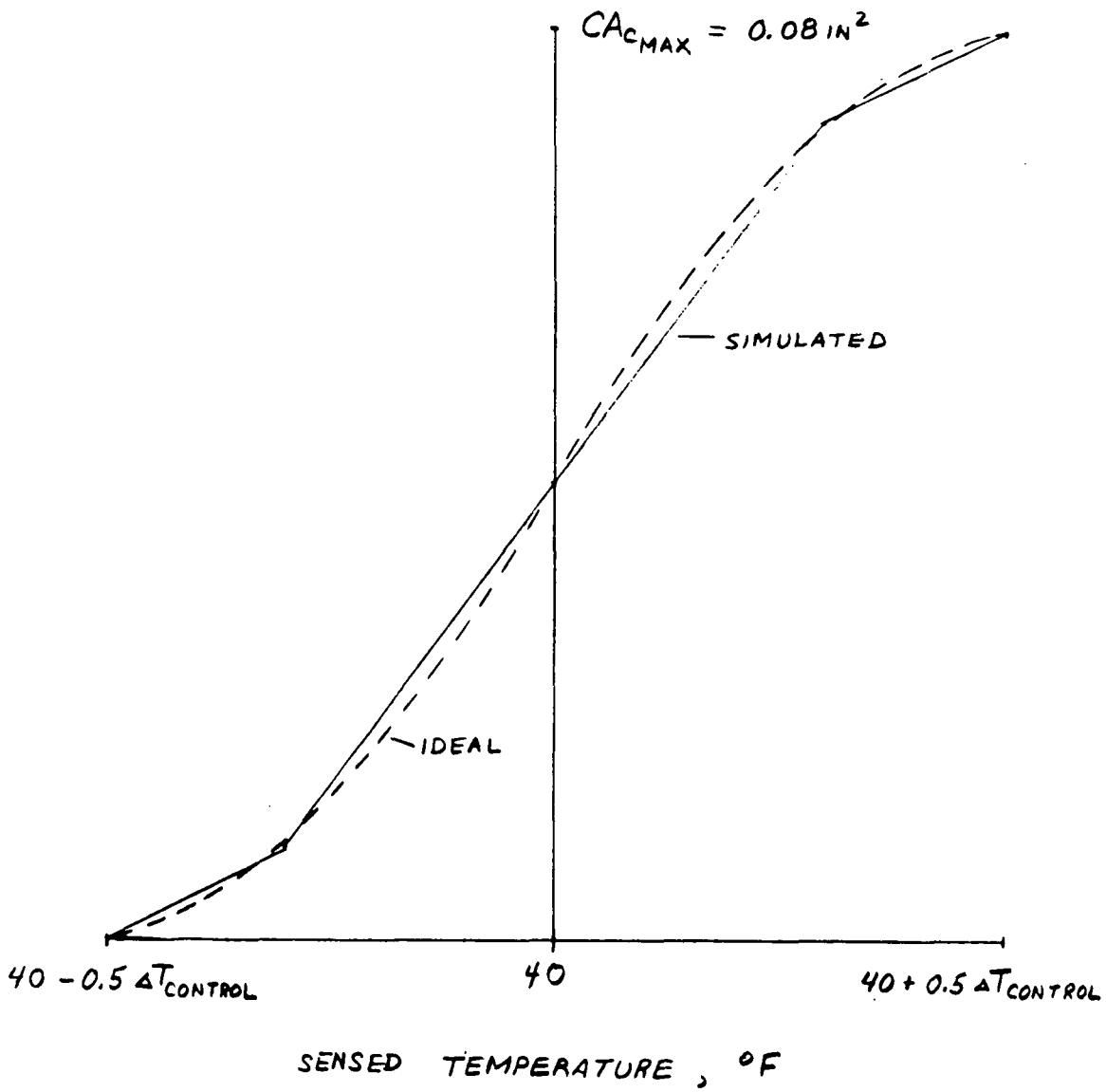

Figure C-3. Cryogen Valve CA_c Function

$T_{C\ IN} = -400^{0}F$

$T_{H\ IN} = 105^{0}F$ (maximum heat load condition)

$W_H = 69$ lb/min (constant for all conditions)

At this condition the system open loop gain is highest although it represents a low cryogen flow case where the valve is positioned on the low slope of the CA_c function of Figure C-3. For a control band of $\pm 10^{0}F$ the linear model gains become

$$\frac{dCA_c}{dT_{ES}} = 0.002\ \frac{in.^2}{^{0}F}$$

$$\frac{\partial W_c}{\partial CA_c} = \frac{60(0.5303)1(40)}{(60)^{1/2}} = 164.5\ \frac{lb/min}{in.^2}$$

$$\frac{\partial E_H}{\partial \overset{0}{W}_c} = 0.2033\ (lb/min)^{-1}$$

$$\frac{\partial T_{H\ out}}{\partial E_H} = 105.2 - (-400) = 505.2^{0}F$$

Open Loop Gain = 0.002 (164.5) 0.2033 (505.2)

= 33.75 (30.6 db)

CRYOGENIC FLOW VALVE

In terms of system stability and response, the location of the cryogen flow valve makes little difference. With the cryogen supply at 40 psia pressure the valve flow capacity with the valve location upstream of the heat exchanger is only decreased by the heat exchanger pressure drop (estimated at less than 5 psia) when the valve is located downstream of the heat exchanger. In both locations the cryogen flow is assumed to be gaseous in nature and essentially sonic through the valve. As a consequence, the valve can be sized for the maximum flow condition as follows:

heat load = 65,000 Btu/hr

$T_{H\ out} = 40^{0}F$

$Cp_H = 0.241$ Btu/lb ^{0}F

$W_H = 69$ lb/min

$T_{c\ in} = 0^{0}F$

$$T_{H\ in} = T_{H\ out} + \frac{\text{heat load}}{60\ \overset{o}{W}_H Cp_H} = 105^{o}F$$

$$E_H = \frac{T_{H\ in} - T_{H\ out}}{T_{H\ in} - T_{c\ in}}$$

$$= \frac{105.2 - 40}{105.2 - 0} = 0.62$$

From the E_H relationship with W_c

$$W_{c\ max} = 3.1\ lb/min$$

$$CA_{c\ max} = \frac{\overset{\rho}{W}_{c\ max} (T_{c\ ABS})^{1/2}}{60\ KN\ P_c}$$

$$= \frac{3.1\ (460)^{1/2}}{60(0.5303)1(40)}$$

$$= 0.0522\ in^2$$

In order to insure adequate cryogen flow capacity, a valve with a somewhat larger CA_c (0.08 in^2) is recommended.